Phosphate Use for Sequestration, Anti-Scaling, and Corrosion Control: Critical Review, Simultaneous Optimization of Polyphosphate Dosing, Sequestration Mechanisms, and Stabilization of Magnesium Silicate Scale

Christian Lytle

Dissertation Submitted to the faculty of the Virginia Polytechnic Institute and State university in partial fulfillment of the requirements for the degree of

Doctor of Philosophy
In
Civil Engineering

Marc Edwards, Chair
William Knocke
Jeffrey Parks
Madeline Schreiber

April 30th, 2024
Blacksburg, Virginia

Key words: Phosphates, Scale inhibition, Sequestration, Corrosion Control, Turbidity, Color

Phosphate Use for Sequestration, Anti-Scaling, and Corrosion Control: Critical Review, Simultaneous Optimization of Polyphosphate Dosing, Sequestration Mechanisms, and Stabilization of Magnesium Silicate Scale

Christian Lytle

ABSTRACT

Phosphates are used by drinking water utilities to 1) reduce iron/manganese aesthetic problems by sequestration, 2) inhibit calcium carbonate scale formation via threshold inhibition, and 3) reduce corrosion of pipes by forming protective pipe scales. Orthophosphates can control lead, copper and iron corrosion through the formation of durable, low solubility scale, but are widely believed ineffective for sequestration or anti-scaling. Conversely, polyphosphates are effective sequestrants and anti-scalants, but can increase corrosion of plumbing materials. Here, we first critically reviewed the current state of the science, operational guidance, and knowledge gaps related to use of orthophosphate and polyphosphates for all three objectives. Three major gaps in understanding were identified and then addressed in subsequent chapters: 1) use of phosphates to achieve both sequestration and anti-scaling 2) mechanisms of iron sequestration, and 3) stabilization of magnesium silicate scale linings in a distribution system.

In the critical review, we holistically conceptualize phosphate use as a three-dimensional (3-D) challenge of optimizing sequestration, anti-scaling and corrosion control. Despite nearly a century of widespread use, there is a poor scientific and practical understanding of how to use phosphates to achieve each of these key objectives, much less achieve synergies and avoid antagonistic effects. Many water systems are reliant on trial-and-error methods, or guidance from vendors of these proprietary chemicals, creating potential inefficiencies or even adverse unintended consequences. Effective sequestration of iron and manganese, to prevent formation of visible discoloration, can occur through four possible mechanisms which are undoubtedly dependent on the water chemistry (e.g., pH, hardness, redox). Anti-scaling of calcium carbonate occurs through threshold inhibition and crystal distortion, but sometimes phosphates can encourage scaling due to the precipitation of calcium phosphate. Corrosion control via orthophosphate is often effective, but polyphosphates can sometimes increase lead or copper levels in drinking water.

Despite their widespread use in scientific studies, it was discovered that standardized measurements of color and turbidity do not fully account for the range of subjective consumer observations regarding cloudy or discolored water. At a constant apparent color of 110 Pt-Co, testing illustrated that relatively non-offensive air bubbles had a high turbidity of 74 NTU compared to just 0.1 NTU for offensively orange fulvic acid. Additionally, factors such as background color, type of light source, and direction of light significantly influenced perception of discolored water. For instance, under typical laboratory lighting conditions (light from above) with a white background, colors caused by iron, manganese, and fulvic acid were very prominent, whereas white calcium carbonate and magnesium silicate particles were more challenging to see. But white particles became much more prominent when the light source was from below or there was a darker background.

A study of Fe sequestration was conducted to elucidate a mechanistic basis for the empirical trends revealed in the utility field study. As revealed in the literature review, polyphosphates could sequester Fe by inhibiting any step of the reaction sequence Fe^{2+} oxidation → precipitation of $Fe(OH)_3$ → particle agglomeration to visible sizes. Phosphates generally inhibited Fe^{2+} oxidation above about pH 7-8, dependent on chain length, and catalyzed oxidation at lower pHs. But in oxygenated waters above about pH 7, the dominant mechanism of sequestration was some combination of Fe^{3+} complexation and colloid stabilization at small particle sizes that were practically invisible. Increasing the phosphate chain length, phosphate concentration, and Si concentration caused more effective Fe sequestration, whereas Ca, Mg, and increased pH hindered its effectiveness. It was also discovered that orthophosphate can be an effective sequestrant under ideal conditions, polyphosphate can sequester more than 1 mg/L Fe despite some claims to the contrary, and Ca at very high doses can precipitate polyphosphates.

During this dissertation work, a novel, thick (~1 mm), glassy magnesium silicate (MgSi) scale was discovered covering much of the pipe surfaces in a large water distribution system. This MgSi lining was hypothesized to be an extremely effective means of corrosion control that was important to maintain in its present state, as dissolution could cause it to detach from pipes, whereas further precipitation could clog them. To better understand how to maintain the scale, factors affecting the formation and dissolution of the MgSi solid were examined. Phosphate corrosion inhibitors had little effect on MgSi solubility at pH 8.5 and 10, while

hexametaphosphate (HMP) and zinc orthophosphate slightly reduced Mg and Si dissolution rates at pH 7. Zinc orthophosphate reduced Mg dissolution by 50% and completely inhibited Si dissolution from the solid, while HMP decreased dissolution of Mg by 32% and Si by 63%. The magnesium silicate did not precipitate below pH 10 without the presence of a pre-existing seed solid. With a pre-existing seed scale, however, the MgSi further precipitated at a pH 8.5-9 in one source water and 7.5-8 in another. Below these pH levels, scale dissolution was shown to occur. Strategies were evaluated to help identify the equilibration pH for operation of a system with varying concentrations of silica, magnesium and pH.

The two-dimensional (2-D) interplay of polyphosphate use for sequestration and anti-scaling was investigated for nine small utilities who rely on groundwater in North Carolina. Bench-top testing methods were developed to determine the 'optimal phosphate doses,' defined here as the lowest level of polyphosphate that maintains visually clear water and acceptable levels of scale formation. One proprietary polyphosphate chemical had an optimal sequestrant dose that depends on the concentration of Fe, Mn, Ca, and Mg. The dose (in mg/L as P) is equal to 58.5[Fe] + 59.7[Mn] + 0.041[Ca + Mg] + 0.4669 (units mM). Interestingly, color was well correlated with particulate (> 0.45 μm) Mn ($R^2 = 0.79$) while turbidity was mostly correlated with particulate iron ($R^2 = 0.60$). Furthermore, neither color nor turbidity measurements were reliable predictors of discoloration detected by eye. In the three utilities with higher hardness (> 100 mg/L as $CaCO_3$), at least 3.6X more phosphate was needed for Fe and Mn sequestration than scale inhibition. But lab testing in very hard water with 300 mg/L as $CaCO_3$ demonstrated that achieving anti-scaling, will sometimes require more polyphosphate than that needed for control of sequestration.

Overall, this dissertation advances understanding of phosphate use in relation to important problems arising in water distribution or buildings. The innovative practical testing methods, improved practical understanding, and mechanistic insights can be applied to maximized the benefits of phosphates use while avoiding detriments. This is an important first step towards developing a rational holistic framework to guide utility decision-making regarding phosphate use.

Phosphate Use for Sequestration, Anti-Scaling, and Corrosion Control: Critical Review, Simultaneous Optimization of Polyphosphate Dosing, Sequestration Mechanisms, and Stabilization of Magnesium Silicate Scale

Christian Lytle

GENERAL AUDIENCE ABSTRACT

Phosphates are safe chemicals dosed to drinking water for a variety of objectives. Phosphates can prevent black water caused by manganese, red water caused by iron, clogging of pipes by precipitation of $CaCO_3$, and to control corrosion of lead, copper and iron pipes. The simplest and least expensive phosphate is orthophosphate. Several orthophosphate molecules can be joined together to form a chain of 2 phosphates (pyrophosphate), a chain of 3 phosphates (tripolyphosphates), and chains up to 100s of phosphates in length. Some utilities only use orthophosphate to control pipe corrosion, and orthophosphate is not believed to be very effective for sequestration or anti-scaling. Conversely, polyphosphates can reduce red and black water from iron/manganese discoloration, and also inhibit the formation of calcium carbonate scale, but they sometimes increase corrosion of plumbing materials.

Here, we review the current state of the science, operational guidance, and knowledge gaps related to use of ortho- and poly-phosphates. Three major gaps in understanding were identified and then addressed in subsequent chapters: 1) use of phosphates to achieve sequestration and anti-scaling simultaneously, 2) improve our understanding of how phosphates stop iron and red water (i.e., sequestration), and 3) stabilization of magnesium silicate scale linings in a distribution system.

In a critical review, the use of phosphate for sequestration, anti-scaling and corrosion control was comprehensively examined. Despite nearly a century of widespread use, there is little understanding of how to properly use phosphates to achieve each objective. For dosing, many water systems rely on trial-and-error methods or guidance from chemical vendors, which could lead to mistakes that cause harmful unintended consequences. This could include elevated lead and copper release at the consumer's tap, increased consumer complaints caused by aesthetically displeasing water, increased head loss in pipes, and staining of dishes and appliances.

Despite their widespread use in scientific literature, traditional measurements of color and turbidity are not always perfect measures of what is seen by eye. Additionally, factors such as background color, type of light source, and direction of light significantly influence the visual properties of water. For instance, under typical laboratory lighting conditions (light from above) with a white background, colors caused by iron, manganese, and fulvic acid were most noticeable, whereas white calcium carbonate and magnesium silicate particles were more challenging to see. In contrast, all particles became more observable when the light source was positioned below.

A study of iron sequestration was conducted to investigate the ability of different phosphates to reduce the formation of red-colored water. As revealed in the literature review, polyphosphates could sequester iron in 3 different ways, but experiments revealed only two would be important in waters with higher pH and oxygen. Increasing the phosphate chain length, phosphate concentration, and silica concentration caused less visual discoloration, whereas calcium, magnesium, and increased pH had the opposite effect. It was also discovered that, at very high doses of calcium, a calcium-polyphosphate solid can precipitate.

During this work, we also discovered a magnesium silicate (MgSi) scale covering much of the pipe surfaces in a large water distribution system. This MgSi lining is believed to protect underlying pipe materials from corrosion. To maintain the benefits of this protective scale, factors influencing its formation or dissolution were tested. The MgSi precipitated above pH 8.5-9 in one source water and 7.5-8 in another if a seed of the scale was present. Below this pH, the scale dissolved. The dosing of some phosphates slightly reduced the amount of scale which dissolved at a lower pH, but had no influence over the formation of more scale at higher pHs. Strategies were then evaluated to help the utility identify a good pH to operate the system, and to maintain the MgSi scale.

The use of polyphosphate for sequestration and anti-scaling was investigated for nine small groundwater utilities in North Carolina. Laboratory experiments were conducted to determine the lowest level of polyphosphate that maintains visually clear water and acceptable levels of scale formation. This ‘optimal polyphosphate dose’ could be predicted by the iron, manganese, magnesium, and calcium concentrations of the water, at least for the utilities tested. Even in the three utilities with highest hardness in the study, more phosphate was needed for

sequestration than inhibiting the formation of calcium carbonate scale. But lab testing in another very hard water with 300 mg/L as $CaCO_3$, did demonstrate anti-scaling will sometimes require more polyphosphate than that required for sequestration.

Overall, this dissertation advances understanding of phosphate use and abuse in relation to important problems arising in water distribution or buildings. The testing methods and improved practical understanding will help maximize the benefits of phosphates while avoiding detriments. This is an important first step towards developing a framework to guide utility decision-making regarding phosphate use for the benefit of consumers.

ACKNOWLEDGMENTS

First, I want to thank my advisor, Dr. Marc Edwards, for your support and guidance over the past five years. I am so grateful for the time you have dedicated to mentoring me and for always being available to answer my questions, edit my papers, and provide new ideas. You have pushed me to grow, and I am sincerely appreciative of the impact you have had on my life and academic journey.

I would also like to thank my committee members, Dr. Knocke, Dr. Schreiber, and Dr. Parks for your help and input on the direction of my dissertation. I want to give a special thanks to Dr. Parks. You were always there for me when I have had questions, needed my ICP samples analyzed, or just wanted to talk about sports. I will truly miss seeing you every day in lab.

Thank you to everyone in the Edwards Research Group for your support. I genuinely appreciate each of you for making my time in the lab so enjoyable. Getting to know all of you has been a privilege, and I feel fortunate to have had the opportunity to work alongside you.

I also want to thank the friends I have made throughout my time at Virginia Tech. Your friendship and support have meant the world to me and I am deeply grateful for the memories we made. Graduate school has truly been the best time of my life, and that is in large part due to you.

Lastly, I want to thank my parents, siblings, and fiancé, Emily, for standing by me throughout this journey. To my parents, your unwavering love and encouragement has made me the person I am today. I owe so much of my success to you. And to Emily, I am so fortunate to have met you in our Environmental Health class, and am grateful for your love and support during this process. I truly wouldn't be the same person without you by my side.

TABLE OF CONTENTS

ABSTRACT ix

GENERAL AUDIENCE ABSTRACT xii

LIST OF FIGURES xxi

CHAPTER 1 : RESEARCH OBJECTIVES, DISSERTATION OUTLINE, AND ATTRIBUTIONS 1

Research Objectives 1

Dissertation Outline and Attributions 1

CHAPTER 2 : PHOSPHATE CHEMICAL USE FOR SEQUESTRATION, SCALE INHIBITION, AND CORROSION CONTROL 3

Abstract 3

Introduction 3

Chemistry of Orthophosphate and Polyphosphate 4

Structure 4

Differences between Polyphosphates 5

Reversion 5

Soluble Complex Formation 6

Chelation of Soluble Metals 6

Particle Stabilization 6

Particle Bridging 7

Particle Destabilization 7

Some Practical Aspects of Phosphate Use 7

Dosing Considerations 7

Turbidity and Color 8

Measuring Phosphates 9

Proprietary Nature of Phosphates 10

Practical Overview of Single Purpose Use of Phosphates 10
Sequestration 12
Scale Inhibition (Anti-Scaling) 18
Corrosion Control 23
Conclusions 29
References 30
CHAPTER 3 : SEEING IS BELIEVING; COLOR, TURBIDITY, AND VISUAL OBSERVATIONS... 44
MEASURING CLOUDY AND DISCOLORED WATER 47
Objective Quantitative Measurements by Instrumentation. 47
Subjective Visual Observations by Human Eye. 49
Impact of lighting conditions and viewing backgrounds. 51
References 54
CHAPTER 4 : A MECHANISTIC STUDY OF IRON SEQUESTRATION BY PHOSPHATES 55
Abstract 56
Introduction 56
Experimental/Methods 59
Chemicals. 59
Simulated Sequestration Tests. 59
Apparent Particle Size Characterization 60
Ferrous Iron 60
Other Analytes. 60
Zeta Potential 60
Statistical Methods 60
Results and Discussion 61
Mechanisms of Sequestration 61
Effect of Phosphate, pH, and Calcium on Zeta Potential 65
Secondary Effects of Water Chemistry on Formation of Color 66
Chlorine 66

Very High Doses of Phosphate Cannot Stop All Problems with Iron Discoloration, and Can Sometimes Make Them Worse 69

References 72

APPENDIX A 76

CHAPTER 5 : STABILIZATION OF A MAGNESIUM SILICATE SCALE PROVIDING CORROSION CONTROL IN A POTABLE WATER DISTRIBUTION SYSTEM 86

Abstract 86

Introduction 87

Materials and Methods 89

OKC Source Water and Analysis of MgSi Solids 89

Harvested Magnesium Silicate Seed 90

Analytical Methods 91

Chemicals 91

Precipitation and Dissolution Experiments 92

Statistical Methods 92

Results and Discussion 92

Examining the Possible Origins of the MgSi Solids 92

Influencing MgSi Solubility by Silica Additions 96

Impact of Phosphate Inhibitors 96

Impact of Temperature on MgSi Solubility 97

Considering Approaches for Stabilizing MgSi Scales 98

Conclusion 100

References 102

APPENDIX B 105

Modeling MgSi Precipitation/Dissolution 110

CHAPTER 6 : SIMULTANEOUS USE OF POLYPHOSPHATE FOR SEQUESTRATION AND ANTI-SCALING 112

Abstract 112

Introduction 112

Background 114

Understanding Sequestration and Scale Inhibition 114

Literature Guidance for Dose Selection. 115

Competition between Hardness and Fe/Mn for Polyphosphate. 115

pH 116

Simulated Distribution System Testing 116

Experimental/Methods 117

System Selection 117

Systems Excluded from Data Analysis 117

Simulated Sequestration Test 118

Simulated Scaling Tests 119

Chemicals 120

Particle Size Characterization 121

Statistical Methods 121

Analytical Methods 121

Results and Discussion 123

Effectiveness of Sequestration at Each Utility 123

Difference between Iron and Manganese. 124

Chemical A vs Chemical B 125

Color and Turbidity 125

Understanding the relationship between phosphates and sequestration 127

Simultaneous Scale Inhibition and Sequestration 128

Anti-Scaling Can Control Optimal Polyphosphate Dose 129

Conclusion 130

References 132

APPENDIX C 137

CHAPTER 7 : CONCLUSIONS AND FUTURE WORK 140

Conclusions 140

Future Work 141

References 143

LIST OF FIGURES

Figure 2-1. Hypothetical illustration of some key issues in tap water as it is transported through a long distribution system with or without polyphosphate. The representative values at each point are for: N = number of particles in the glass, Radius = radius of each particle, $T_{settling}$ = time required for the iron oxide particles to settle about 15 cm at terminal velocity based on Stokes Law, and τ = turbidity. Particle density is assumed to be 1.1 g/cm^3 for these calculations. In parts of the distribution system with accumulations of settled particles, hydraulic disturbances can cause massive contamination of water, whereas in normal circumstances particle concentrations can be low. 9

Figure 2-2. Four steps by which polyphosphate might influence problems with Fe/Mn discoloration in potable water systems. 13

Figure 2-3. Increasing hardness reduces the % of total manganese complexation with 1 mg/L TPP as P. Total Mn = 0.1 mg/L and ionic strength = 0.1 M (assuming no calcite formation). The binding constants for Mn^{+2} and Ca^{+2} with TPP^{-5} are Log K_{Mn} = 7.15, Log K_{Ca} = 5.2, and H^+ binding with TPP^{-5} are Log K_1 = 8, Log K_2 = 5.5, Log K_3 = 2.6 (Smith & Martell, 1976). 17

Figure 2-4.Calcium carbonate scale forming on plumbing material and in the bulk water. 19

Figure 2-5. The three mechanisms for scale inhibition: threshold inhibition, crystal distortion, and dispersion. Yellow lines represent polyphosphate chains. 21

Figure 2-6. The importance and generalized effect of phosphates on each of the five main types of corrosion: Pitting, scale buildup, soluble metal release, particulate metal release, and galvanic corrosion. 24

Figure 2-7. The detrimental effect of polyphosphate (left) and the beneficial effects of orthophosphate (right) on lead pipe corrosion. 27

Figure 3-1. Sources of iron, treatments, and distribution phenomena. Different homes throughout the distribution system can have different levels of color and turbidity. Coagulation can be a

treatment to assist removal of iron and manganese, but dissolve iron and manganese in the chemical can also be a source of these constituents. 46

Figure 3-2. Diagram of turbidity, true color, and apparent color. 48

Figure 3-3. A lab test that began with addition of invisible 1 mg/L Fe^{3+} at low pH (< 3), then raising pH to allow precipitation and coagulation. A decline in turbidity and color only occurred after adding anionic polymer that created very large particles. 48

Figure 3-4. Color and turbidity were measured for laboratory solutions of DI water, fulvic acid, air bubbles, calcium carbonate, and ferric iron. Despite identical apparent color, the turbidity varied greatly. 50

Figure 3-5. Impact of particulate or dissolved species, background color, and lighting type/direction on visual discoloration and cloudiness. A color of 50 Pt-Co was chosen as it is about 3.3X more than the 15 Pt-Co SMCL. Those marked with a * were easily visible by eye compared to the control DI water condition. 53

Figure 4-1. A) Polyphosphate decreases the rate of iron oxidation from Fe^{2+} to Fe^{3+} at pH 7, B) Polyphosphate and orthophosphate decrease the rate of iron oxidation from Fe^{2+} to Fe^{3+} at pH 8, and C) at pH 6.5, HMP and orthophosphate resulted in quicker oxidation. Red-dashed lines denote 80 or 90% oxidation. 61

Figure 4-2. A) Nearly 100% of the 2 mg/L Orthophosphate and TPP passed through a 10K ultrafilter at pH 7, while 66% of the HMP was rejected. B) Almost all the HMP passed through the 10K filter when dosed with 200 mg/L $CaCO_3$. 62

Figure 4-3. Increasing phosphate concentration and chain length reduced particle size of 1 mg/L iron (Left), and increasing pH resulted in increased iron between 10K and 0.45µm in size. A ‘V’ denotes visible iron and an ‘I’ denotes invisible iron. 64

Figure 4-4. A) Increasing the concentration of orthophosphate and HMP resulted in more negative zeta potentials of ferric solids over a 1-day period (10 mg/L Fe^{3+}, 0, 2, 5, 10 mg/L P), and B) the addition of 200 mg/L $CaCO_3$ resulted in more neutral zeta potentials (after 10 minutes at 10 mg/L iron and 20 mg/L P). 66

Figure 4-5. Effect of silica on 1 mg/L iron size characterization at pH 7 and 8.5. 67

Figure 4-6. Effect of calcium on <10K iron concentration. Total iron = 1 mg/L, Total P = 2 mg/L. Note: trends for HMP have no simple interpretation, due to rejection of the polymers by 10 K ultrafilters. 68

Figure 4-7. Optimal TPP phosphate dose trends for a synthetic water at pH 7 with 100 mg/L $CaCO_3$ and 40 mg/L magnesium as $CaCO_3$. 69

Figure 4-8. The use of TPP for sequestration caused an increase in color and turbidity in an extreme use case (200 mg/L $CaCO_3$, pH 9, 2.5 mg/L Fe^{2+}). 70

Figure 5-1. Exemplary sequential Pb profile samples from a residential customer with a LSL on the utility side of the meter using an escalating flow rate protocol (Clark et al., 2014). Low flowrate sampling from the LSL (0.94 L/min) was conducted after a minimum 6-hour stagnation, followed immediately by a set of samples at a moderate flowrate (5.4 L/min), and then an atypical high scouring flow rate (7.5 L/min) with the faucet aerator removed. Pipes were lined with an approximately 1 mm thick coating, as shown by a harvested lead pipe. 86

Figure 5-2. Image of Seed A, Seed B, and Seed C after drying. 90

Figure 5-3. A MgSi solid can precipitate at elevated pH in a synthetic water comprised of 32 mg/L Mg and 3.5 mg/L Si to simulate water B. 93

Figure 5-4. Magnesium and silica tended to dissolve from the seed at lower pHs and precipitate from the bulk water at higher pHs. These samples were taken after 1-week to represent a reasonably old water age in the distribution system. Similar trends, but at lower magnitudes, were observed at 1, 8, and 72 hours. 94

Figure 5-5. Increased seed surface area increased the rate of precipitation and dissolution of magnesium and silica. 95

Figure 5-6. Effect of spiking 5 mg/L of silica on MgSi equilibrium in Water A and Water B. 96

Figure 5-7. Impact of phosphate inhibitors on MgSi precipitation and dissolution in Water A when dosed with a medium seed concentration. 97

Figure 5-8. Impact of temperature on dissolved Mg and Si concentrations in a synthetic water at pH 8.75 with 0.6 mg/L of soluble Si and 2.6 mg/L of soluble Mg. 98

Figure 6-1. Simulated (left) and synthetic (right) scaling test setups. 119

Figure 6-2. Size distribution of iron and manganese after 1 week using Chemical A. The 0, 25, 50, 75, and 100% represent the percentage of the max dose used. 123

Figure 6-3. Samples which did not completely eliminate color at the highest phosphate dose had high concentrations of particulates (only Chemical A shown). The 0, 25, 50, 75, and 100% represent the percentage of the max dose used. 124

Figure 6-4. Simple relationships provided strong correlations between color and particulate Fe/Mn. Slope = 0.877 ± 0.047, y-int = 4.52 ± 2.11 (left); Slope = 15.28 ± 0.084, y-int = 6.40 ± 2.08 (right). 126

Figure 6-5. Simple relationships between turbidity and Fe/Mn. Slope = 0.169 ± 0.015, y-int = 0.302 ± 0.135 (left); Slope = 0.174 ± 0.015, y-int = 0.302 ± 0.134 (right). 126

Figure 6-6. Relationship between the color and turbidity in systems A1, A2, B, C, D, E, F, G1, H1..... 127

Figure 6-7. This model accurately predicts the polyphosphate doses determined by experimentation. The orange line represents y = x. 128

Figure 6-8. Mass of calcium precipitated in 1.5 L bottles in the three systems with > 100 mg/L $CaCO_3$. 128

Figure 6-9. Mass of calcium precipitated in 1 L of water at 75˚C for 3 hours. Without phosphate, 136 mg/L $CaCO_3$ precipitation in the heating element setup..... 129

Figure 6-10. Conceptual phosphate dose and response for Ca scale inhibition and sequestration in system D. More polyphosphate is needed for sequestration than scale inhibition near 300 mg/L $CaCO_3$. 130

Figure C 1. Example of the visual discolored vs visually clear water conditions in Water D. ……..139

Figure C 2. Optimal dosing trends for systems that did reach an optimal dose. For Chemical A, Z = 1.02 and X = 0.0007, slope = 58.5 ± 9.5, y-int = 0.47 ± 0.10. For Chemical B, Z = 1.2 and X = 0.0012, slope = 49.61 ± 11.31, y-int = 0.37 ± 0.13. 139

LIST OF TABLES

Table 2-1. Broad overview of the three dimensions of phosphates use. 11

Table 5-1. Representative water quality of the two source waters, and SEM analysis of harvested MgSi solids (refered to as “seeds”) from different locations in the distribution system. 90

Table 5-2. Approximate solid metal concentrations found in each seed level, as measured by ICP-MS. 91

Table 5-3. Best fit X, equilibrium concentration, and rate constants over the 53-day period. 99

Table 5-4. Experimentally determined Ksp values for a hypothesized $MgSi_{0.4}(OH)_2$ and $MgSi_{0.7}(OH)_2$ solid in Water A and Water B. 100

Table 6-1. Water quality parameters for each water tested. Those labeled with a 1 and 2 represent systems which were resampled 117

Table C 1. Water quality parameters for each water tested. Those labeled with a 1 and 2 represent systems which were resampled……138

CHAPTER 1 : RESEARCH OBJECTIVES, DISSERTATION OUTLINE, AND ATTRIBUTIONS

Research Objectives

This dissertation will achieve the following objectives:

1. Summarize the current state of science, provide operational guidance, and identify knowledge gaps regarding the use of orthophosphate and polyphosphate in potable water distribution systems.
2. Examine the limitations of standardized, objective color and turbidity measurements, to characterize visual observations of discolored or cloudy water.
3. Evaluate the mechanisms, limitations and potential for iron sequestration by phosphates.
4. Investigate the nature of a novel magnesium silicate scale lining pipes in a water distribution system, and the role of phosphates in its maintenance.
5. Examine the optimization of polyphosphate dosing for simultaneous control of anti-scaling and discolored water from iron and manganese at nine groundwater utilities.

Each objective is addressed in a separate chapter.

Dissertation Outline and Attributions

In Chapter 2, we summarize existing practical and scientific understanding of phosphate use in potable water treatment through a state-of-the-art critical literature review. Phosphate chemistry, practical considerations of phosphate use, and single objective optimization strategies for sequestration, anti-scaling, and corrosion control are summarized. The need to holistically consider impacts for all three objectives simultaneously is then emphasized. This review was published in *Environmental Science and Technology Water* in 2023 (10.1021/acsestwater.2c00570), and is co-authored by Dr. Marc Edwards (funding source, advising, review and editing).

In Chapter 3, bench-top experiments are utilized to describe the limitations to color and turbidity measurements. We examine the impact of particle size, particle type, lighting, and background color on visual observations of discoloration and cloudiness. This research article

will be submitted to *Opflow*, and is co-authored by Dr. Marc Edwards (methodology, advising, review and editing, funding source).

In Chapter 4, a mechanistic understanding of ortho- and poly-phosphate use for iron sequestration was explored. The effects of different phosphate inhibitors, calcium, magnesium, silica, pH, ionic strength, and temperature on sequestration are examined. This research article will be submitted to *Environmental Science and Technology Water*, and is co-authored by Dr. Marc Edwards (methodology, advising, review and editing, funding source).

In Chapter 5, a magnesium silicate scale formed in the Oklahoma City water distribution system that is believed to be providing very effective corrosion control is described. To maintain this scale, we investigate its solubility under a range of pHs, phosphate inhibitor doses, and temperatures. Since formation of this scale was not described by simple solubility models, a magnesium silicate "Marble Test" is proposed to guide selection of pH to prevent scale destabilization. This research article will be submitted to *Environmental Science and Technology Water* and is co-authored by Dr. Marc Edwards (funding acquisition, methodology, advising, review and editing), Luke Snell (funding source, coordinating with the water utility, review and editing), and Rebecca Poole (funding source, coordinating with the water utility, review and editing).

In Chapter 6, simulated sequestration and anti-scaling tests were used to investigate the impact of phosphates at nine small groundwater utilities in North Carolina. A procedure for optimizing polyphosphate dosing was developed, along with empirical trends relating that dose to levels of Fe, Mn, Ca, and Mg in the water. This research article was published in *Environmental Science and Technology Water* in 2023 (10.1021/acsestwater.3c00553), and is co-authored by Dr. Marc Edwards (methodology, advising, review and editing) with Aqua America as a funding source.

In Chapter 7, the conclusions are presented along with future research needs.

CHAPTER 2 : PHOSPHATE CHEMICAL USE FOR SEQUESTRATION, SCALE INHIBITION, AND CORROSION CONTROL

Christian J. Lytle, Marc A. Edwards

Reprinted (adapted) with permission from Lytle, C. J., & Edwards, M. A. (2023). Phosphate Chemical Use for Sequestration, Scale Inhibition, and Corrosion Control. *ACS ES&T Water*, *3*(4), 893-907.

Abstract

Water utilities commonly dose phosphates to potable water to (1) reduce aesthetic problems by sequestration, (2) inhibit calcium carbonate scale formation via threshold inhibition, and (3) reduce corrosion of lead or copper plumbing materials by forming protective pipe scales. Despite widespread use and increasing importance of phosphates, significant gaps in fundamental understanding still exist. This is partly due to the proprietary nature of some phosphate chemicals, causing experimental data and acquired knowledge for public water supplies to be considered trade secrets. Here, we summarize the current state of science, provide operational guidance, and identify knowledge gaps regarding the use of ortho- and poly-phosphate. The goal is to empower water scientists to improve phosphate chemical performance and to avoid unintended adverse consequences.

Introduction

Water utilities dose phosphates (i.e., polyphosphate, orthophosphate or blends thereof) to control iron (Fe) and manganese (Mn), scaling, or corrosion. Phosphates can reduce aesthetic problems with Fe/Mn including red, black, or brown water through a process known as sequestration. Systems experiencing calcium carbonate precipitation problems dose phosphates as an anti-scalant. Phosphates are also frequently dosed to inhibit corrosion damage to pipe infrastructure and reduce iron, lead, or copper contamination of drinking water. These objectives are collectively referred to as the three dimensions (3-D) of phosphate use in potable water.

The use of polyphosphates in potable water treatment dates back to at least 1929 when it was used as a sequestrant for Fe/Mn and to prevent formation of $CaCO_3$ scale in water heaters (Carus

Corporation, 2017; Carus Water, 2012). Their complementary use in household soap to prevent formation of soap scum increased markedly post-World War II (Folsom & Oliver, 1980). Phosphate use in soap started to decrease in the 1970s in an effort to reduce eutrophication of lakes and waterways (Gilbert & DeJong, 1977).

The use of phosphates in boiler corrosion control began in the 1930s (Schwartz & Munter, 1942), and the first use of zinc orthophosphate to control corrosion of potable water pipelines was in 1950 (Hill & Giani, 2011). The use of phosphates to control corrosion in the U.S. has since increased markedly following the 1991 Environmental Protection Agency (EPA) Lead and Copper Rule (McNeill & Edwards, 2002). In the intervening three decades, there has been an increasing switch from polyphosphate to orthophosphate (Arnold et al., 2020; McNeill & Edwards, 2002).

The use of phosphates for sequestration, scale inhibition, and corrosion control is increasing in importance today due to the (1) increase in focus on the consequences of using polyphosphate for sequestering Fe/Mn on corrosion, (2) increase in calcium carbonate scaling concerns in drinking water caused by climate change and the need for higher water temperature in hot water systems (Richards et al., 2018), and (3) revisions to the lead and copper rule that emphasize higher dosing of phosphate for corrosion control (United States Environmental Protection Agency, 2019). Unfortunately, profound gaps in fundamental scientific understanding still exist for each of these three 1-Dimensional objectives. Lessons learned from case studies are infrequently shared or generalized, and much of the expert knowledge and experimental results remain trade secrets. Failure to understand each objective may result in unsafe drinking water, consumer complaints, and other distribution system-related issues. Thus, this critical review will summarize the current knowledge of centralized phosphate dosing by addressing phosphate science, operational guidance, and current gaps in knowledge.

Chemistry of Orthophosphate and Polyphosphate

Structure

The molecules of phosphates dosed to potable water have a wide range of lengths, charges, and structures, all of which largely influence their overall performance. Orthophosphate is a monomer present in water as phosphoric acid H_3PO_4, $H_2PO_4^{-1}$, HPO_4^{-2}, or PO_4^{-3}. The predominance of these orthophosphate species is controlled by pH and can be predicted by

appropriate acidity constants (i.e. at an ionic strength (*I*) of 0.5 M, Log K_1 = 11.74, Log K_2 = 5.72, Log K_3 = 2.0) (Smith & Martell, 1976).

Monomeric (PO_4^{-3}) and trimeric ($P_3O_{10}^{-5}$) phosphate molecules are available for consumer purchase in cleaning products such as trisodium phosphate (TSP) or sodium tripolyphosphate (TPP). Larger polymers come in a heterogeneous collection of shapes and sizes including linear chains, rings, and branched structures. The chain length of polyphosphates dosed to potable water is inherently heterogeneous and varies with each proprietary vender formulation, but is often between four to eighteen (n= 4-18) phosphorus atoms long, and may reach extreme lengths of up to n=3000 (Rashchi & Finch, 2000).

Differences between Polyphosphates

There are many proprietary formulations of orthophosphate, polyphosphate, and blended phosphate products available for purchase. Orthophosphates are the raw material and the least expensive. Polyphosphates are created by appropriate manipulation of the cation and heating processes (Sper Chemical Corporation, n.d.-a). For instance, pyrophosphate is formed by heating sodium phosphate to 300-400°F, whereas heating to 1200°F or higher can produce hexametaphosphate and other n= 6-14 chain lengths. Each polyphosphate blend or product may differ in chain length, shape, and other chemical additives such as zinc. All polyphosphates will inevitably contain a range of chain lengths and at least some orthophosphate. Polyphosphates break down into smaller sizes over time through a process known as reversion. Thus, all polyphosphate formulations are somewhat different at creation, and continuously change with time. These differences and changes sometimes impact practical performance.

Reversion

All polyphosphate in drinking water distribution systems is thermodynamically destined to hydrolyze or "revert" back to stable orthophosphate over time (Goldberg & Nuttall, 1998; Holm & Edwards, 2003). Polymer degradation follows complex first-order kinetics and can occur by clipping one unit from the end of the chain or separation of trimetaphosphate rings (Holm & Edwards, 2003). Breaking a molecule mid-chain may also occur, although little evidence supports this mechanism (Griffith & Buxton, 1967).

The reversion rate increases at higher chain lengths (Fuchs & Lutz, 1969), higher temperatures (Shekhar, 2007; Thilo, 1965), longer water age, and lower alkalinities (Holm &

Edwards, 2003). In addition, the presence of divalent cations and certain pipe materials (Holm & Edwards, 2003), biological growth, and pH may also increase reversion rates. Phosphate can be a nutrient for microbes (Park et al., 2008), therefore the presence of biofilm may increase hydrolysis. The effect of pH is less understood; some reports show that lower pH around 7 causes higher reversion rate (Griffith & Buxton, 1967; Holm & Edwards, 2003), whereas others showed the opposite trend (Fuchs & Lutz, 1969; Shekhar, 2007).

Soluble Complex Formation

Polyphosphates form strong soluble complexes with metal ions such as Fe^{2+}, Mn^{2+}, or Ca^{2+} via covalent or ionic bonds. Each phosphate polymer has a unique binding strength and forms complexes at different rates (Bailey et al., 2002). Both kinetic (De Jager & Heyns, 1998; Hamilton et al., 2017) and diffusion limitations can play a role in complex formation.

Orthophosphates often form relatively insoluble precipitated solids with many metals and weak soluble complexes that are generally of insignificant concentration. For instance, published complexation constants for cupric and ferric iron (at pH 7) predict less than 1% complexation of 1 mg/L Cu^{2+} and Fe^{3+} in the presence of 1 mg/L orthophosphate as PO_4^{3-}P (Kodama, 1974; Smith & Martell, 1976). Soluble complexes between orthophosphate and Fe^{2+}, Mg^{2+}, Ca^{2+}, Pb^{2+}, and Zn^{2+} are also practically insignificant. However, precipitated orthophosphate solids can form with many metals including lead, copper, calcium, magnesium, aluminum, and iron.

Chelation of Soluble Metals

Each molecule of polyphosphate has characteristic numbers of available binding sites, acid dissociation constants, and binding strengths for specific metals. Some large polymers can complex a metal with two or more bonds through a process termed chelation. This allows for long polyphosphates with highly negative electric charges to form very strong soluble complexes. This ring formation is particularly important for strong binding of Ca^{2+} and Mg^{2+} (Bailey et al., 2002; Rulliere et al., 2012). Orthophosphate cannot chelate metals, whereas 5–6-member polymer rings are thought to cause the strongest binding (Bailey et al., 2002).

Particle Stabilization

Particle agglomeration (i.e., particle aggregation/flocculation) is the process by which smaller particles collide and gradually grow into larger particles. Neutral or weakly charged particles readily collide and coagulate to form large agglomerations. Effective collisions between particles

can be hindered by repulsive forces between like charged surfaces that are either too negative or too positive. If repulsive forces are present, colloids are considered "stabilized" because they do not grow appreciably in size. This phenomenon is known as dispersion.

In centralized water treatment, the magnitude of the particle surface charge is purposefully reduced by careful dosing of coagulants. At some point, repulsive forces are below a critical value allowing particles to spontaneously coagulate and grow so they can be removed by sedimentation or filtration. Sequestration achieves the opposite effect as it seeks to coat particles with a sufficiently negative surface charge to prevent effective collisions and coagulation. A sufficiently high dose of phosphates can also stabilize colloidal particles by physically blocking collisions between surfaces by steric forces (Piacenza et al., 2018). A lower dose of phosphate that does not achieve a sufficient negative surface charge can still allow rapid particle agglomeration to occur.

Particle Bridging

If long polymer chains simultaneously attach to surfaces of two or more different particles, a larger agglomerate can be formed without direct collision between particles via a process known as bridging (Stumm & Morgan, 1995). A chain length exceeding the characteristic thickness of the repulsive double layer between particles is necessary for bridging. To our knowledge, bridging of particles has not been definitely reported for polyphosphates sequestration of Fe/Mn.

Particle Destabilization

While phosphates can stabilize particles when dosed appropriately, they can also destabilize particles if dosed at low levels via bridging (Bonet Avalos et al., 1994; Rossi & Pincus, 1989), or via a patch effect between the negatively charged areas of adsorbed polymer and positively charged areas of oxide surfaces (Hierrezuelo et al., 2010; Hogg, 2012; Ye et al., 2007).

Some Practical Aspects of Phosphate Use

Dosing Considerations

There is significant variability in the type of phosphate and the characteristic dose range used to achieve each objective. For corrosion control, orthophosphate is often dosed from 0.33 to 1 mg/L as P (EPA, 2016). More than 50% of utilities surveyed in 2020 dosed between 0.3 and 0.5 mg/L as P, while just over 10% had doses over 0.5 mg/L (Arnold et al., 2020). The Lead and Copper

Rule Revision (LCRR) requires utilities to consider dosing up to 1 mg/L ortho-P (United States Environmental Protection Agency, 2019). For sequestration, approximately 2 mg/L of polyphosphate is thought to sequester 1 mg/L of either Fe and/or Mn (Volpe, 2012). Manufacturers often claim about 0.66-1.33 mg/L of polyphosphate as P is sufficient (Pure water Products, n.d.; The phosphate Forum of the Americas, n.d.). For scale inhibition, manufacturers claim approximately 2-4 mg/L of hexametaphosphate will inhibit scaling from 200 mg/L of hardness (as $CaCO_3$) (The phosphate Forum of the Americas, n.d.). However, as little as 0.1 mg/L polyphosphate-P can reduce scaling by 75-95%, and 0.1 mg/L orthophosphate-P can reduce scaling by 50% (Y. P. Lin & Singer, 2005; F. Wang et al., 2017).

Turbidity and Color

Color and turbidity measurements are important tools for characterizing consumer observations of iron and manganese precipitation in potable water distribution. Turbidity, measured in nephelometric turbidity units (NTU), is a measurement of light scattering in water. Color, commonly measured using the platinum cobalt color test (units of Pt-Co) (Thermoscientific, n.d.), is determined from the absorbance of light at a particular wavelength. The human eye detects some combination of light scattering and absorbance.

Turbidity, color, and consumer perception of color are all strong functions of particle size (e.g., He & Nan)(He & Nan, 2012). Little or no turbidity is measured for dissolved or very small particles with a fixed mass of metal such as Fe^{2+}. At the other extreme, if the same mass of iron was concentrated into a few very large particles of iron oxide, it may be perceived as an errant particle and not turbidity or color, and it could settle quickly in a consumer's glass or in a cuvette before color or turbidity could be measured.

Consider a hypothetical example of a water with $3x10^{12}$ $Fe(OH)_3$ particles per liter of 100 nm (0.1 μm) diameter and specific gravity of 1.1. According to Stokes law, it would take about 8.6 years to settle about 15 cm to the bottom of a glass. The same mass of iron agglomerated into just three 0.1 mm diameter particles would settle 15 cm in about 3 seconds and might not appear as turbidity (Figure *2-1*). Because particles of ~0.1 μm are believed to create the most intense turbidity per unit mass of iron, the worst aesthetic issues may be associated with this size range (P. L. Dawson & Acton, 2018).

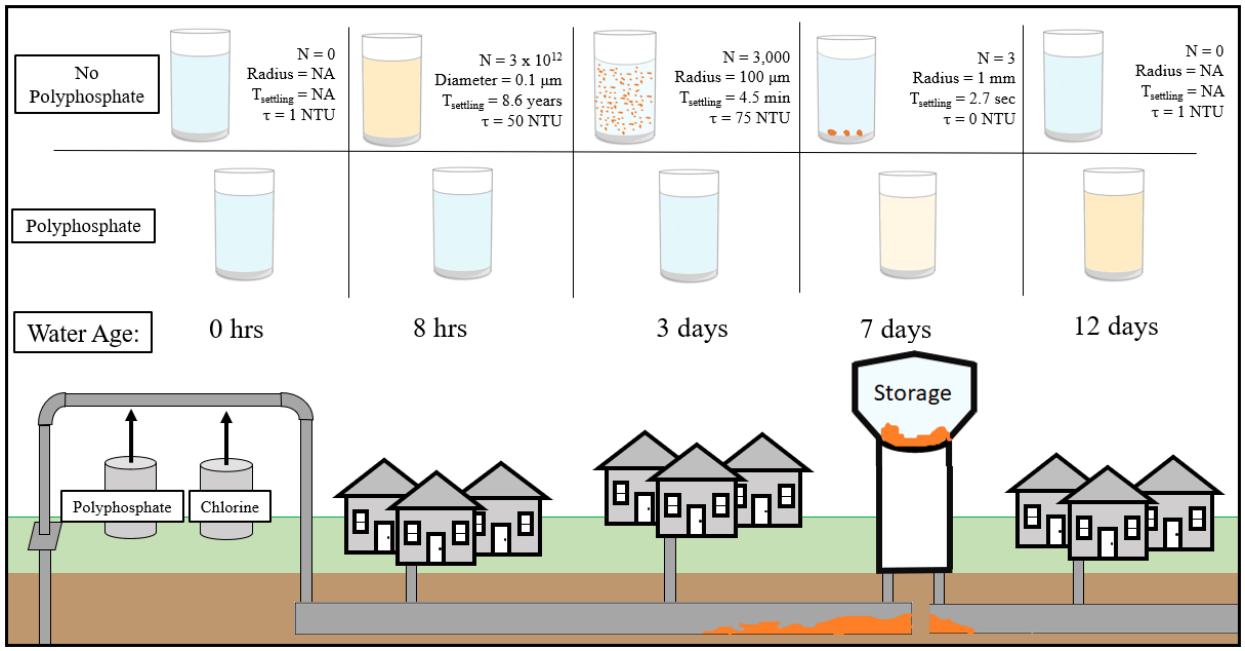

Figure 2-1. Hypothetical illustration of some key issues in tap water as it is transported through a long distribution system with or without polyphosphate. The representative values at each point are for: N = number of particles in the glass, Radius = radius of each particle, $T_{settling}$ = time required for the iron oxide particles to settle about 15 cm at terminal velocity based on Stokes Law, and τ = turbidity. Particle density is assumed to be 1.1 g/cm^3 for these calculations. In parts of the distribution system with accumulations of settled particles, hydraulic disturbances can cause massive contamination of water, whereas in normal circumstances particle concentrations can be low.

Measuring Phosphates

Phosphates in a water sample can be present in particles such as $Cu_3(PO_4)_2$ or $FePO_4$, or dissolved as orthophosphate, polyphosphate or phosphate-metal complexes. The summation of all components is termed the total phosphate in a sample. Techniques and standardized procedures are available to operationally quantify each fraction using filtration to remove particulate phosphate, or via colorimetric reagents that only react with dissolved orthophosphate and not particulates or polyphosphates (Dabkowski & White, 2013). The exact type of polyphosphate polymers present in samples cannot be determined in potable water due to the low concentrations that are present and a lack of reference standards. Hence, the measurement of "total polyphosphate" includes all chain lengths of n=2 or higher.

Proprietary Nature of Phosphates

While a practical working understanding of phosphate use to control lead and copper corrosion has been developed over the last few decades, some utilities are still reliant on the advice of chemical vendors with proprietary interests to meet their needs. In fact, many water utilities have selected their dose and type of polyphosphate through vendor recommendations without generating their own independent data to confirm performance (McNeill & Edwards, 2002). Proprietary test data generated for these systems may be lost if it ever existed in the first place. Therefore, it is virtually certain that many utilities are either underdosing or overdosing phosphate to their finished water, or might even be better served by using a different type of phosphate. At present, there are no accepted protocols to improve on the existing situation. This is because each dimension of phosphate performance is so poorly understood, which will be discussed in the following sections.

Practical Overview of Single Purpose Use of Phosphates

As of 2001, about 56% of all large water systems used phosphates (McNeill & Edwards, 2002). A follow-up 2019 survey showed approximately 69% of small, medium, and large systems with lead service lines used phosphate inhibitors, compared to 45% of those without lead service lines (Arnold et al., 2020). Some systems only dose phosphate to address their most important problem, while the impacts on other dimensions are either ignored or considered incidental. Others are fortunate to have a combination of naturally non-corrosive water, no lead pipes, and/or relatively low calcium and Fe/Mn, so only one dimensions of performance need to be considered (McNeill & Edwards, 2002). Generally speaking, polyphosphate is best used for inhibiting scale formation and sequestering Fe/Mn, while it is often detrimental or has no benefit for corrosion control. On the other hand, orthophosphate is often beneficial for corrosion control, but has much less or no benefit on sequestration and scale inhibition (Table *2-1*).

Table 2-1. Broad overview of the three dimensions of phosphates use.

	Lower Level Problem	Moderate Problem	More Serious Problem
Iron and Manganese Control			
Fe/Mn Level	Fe < 0.100 mg/L and Mn < 0.025 mg/L	0.1 < Fe < 0.3mg/L or 0.025 mg/L < Mn < 0.05 mg/L	Fe > 0.3 mg/L or Mn > 0.05 mg/L
Effect of Polyphosphate	Can be very effective	Often effective	Unlikely to be effective in all parts of system
Effect of Orthophosphate	Might slightly reduce problems	Generally ineffective	
Options for Centralized Treatments	Some systems decide to live with aesthetic Fe/Mn problems. If action is taken, generally speaking, removal of Mn/Fe from water by treatment is increasingly desirable at the higher levels while sequestration is more cost effective at lower levels. The ten state standards assert that polyphosphate shall not be used it if the Fe + Mn concentration exceeds 1.0 mg/L (Great Lakes-Upper Mississippi River Board, 2012).		
Options for Consumer Treatments	Consumers can mitigate these problems by purchasing whole house and POU filters for cooking or drinking, or dose polyphosphate on-site		
Calcium Carbonate Scaling			
Calcium Level (Widder & Baechler, 2013) **(as $CaCO_3$)**	< 60 mg/L	61 < $CaCO_3$ < 180	> 180 mg/L
Effect of Polyphosphate	Highly effective or not necessary	Effective	Variable effectiveness
Effect of Orthophosphate	Moderately effective or not necessary	Slightly effective	Not effective
Options for Centralized Treatments	No action needed.	Use of phosphates, softening	Centralized softening is necessary in severe cases
Options for Consumer Treatments	No action needed.	Antiscalant devices, home softeners. Sometimes it is only necessary to treat hot water.	
Corrosion Control			
Level	Depends on chemistry, types of materials in distribution system, types of materials in consumers specific home		
Effect of Polyphosphate	With few exceptions higher poly-P is thought to worsen or have no effect on corrosion		
Effect of Orthophosphate	Orthophosphate often has benefits for metallic corrosion		
Options for Centralized Treatments	Phosphates, or pH/alkalinity corrosion control		
Options for Consumer Treatments	POU filters to remove lead, copper and whole house filters to remove Fe/Mn		

Sequestration

Groundwaters and surface waters can occasionally have high levels of iron and manganese. The EPA has no maximum contaminant level (MCL) for iron or manganese as they do not pose a direct human health concern. However, iron and manganese can cause aesthetic problems for consumers including taste, odor, and visual issues, as well as staining of clothes, appliances, porcelain, toilets, baths, and sinks. The EPA has set secondary maximum contaminant levels (SMCL) of 0.3 mg/L iron and 0.05 mg/L manganese in recognition of the greater likelihood of aesthetic problems with higher concentrations of these metals.

The SMCL is not enforceable, although some states do have their own guidelines limiting concentration (Great Lakes-Upper Mississippi River Board, 2012). Many private well owners and small water systems choose to tolerate very serious aesthetic problems rather than pay to control the problems, while others address the problem using whole house or point of use filters. Large utilities often install relatively expensive treatments such as oxidation and filtration to remove Fe/Mn from water to very low levels and virtually eliminate the problems for all consumers. Yet another strategy is to add polyphosphates to water that can "sequester" the Fe/Mn to reduce the likelihood of consumer complaints.

Dosing polyphosphate may not eliminate all aesthetic problems, but it can be a very cost-effective approach to reducing them. To illustrate, the capital cost for a small Fe/Mn removal plant serving 200 people is around $500,000, whereas the setup cost to dose polyphosphate is as little as $1,400 per well (AmeriWest Water Services Inc, n.d.). Furthermore, conventional Fe/Mn removal plants require more supervision and expertise to operate and maintain than the simple dosing of polyphosphate.

The use of phosphates for sequestration can be very complicated due to the long water transport times to distant homes. Consider two scenarios for a hypothetical utility with high iron choosing whether to dose polyphosphate or do nothing. In a case without polyphosphate, the iron may oxidize, agglomerate, and partly settle in the system as it travels to homes (Figure 2-1). Depending on their location, some homes in this system may have serious problems while other homes may have none. The addition of polyphosphate can slow all of these reactions, but some consumers in the system may still have relatively pleasing water while others' is displeasing.

Moreover, the location in the system with the good or bad water might shift with the addition of polyphosphate.

While sequestration can be a useful tool for reducing water discoloration, it can also introduce new challenges for utilities wanting to achieve optimized dosing. In the following paragraphs, we review existing knowledge regarding control of Fe/Mn problems.

Mechanism

Soluble iron and manganese are virtually invisible, but large particles of iron or manganese oxides are easily detected by eye. Aesthetic problems arise from a three step process (Figure 2-2) in which: (1) soluble Mn(II) or Fe(II) ions are oxidized to relatively insoluble Fe(III) or Mn(IV) ions, (2) $Fe(OH)_3$ or MnO_2 colloids precipitate, and (3) small colloids agglomerate into larger particles that cause light scattering. In practice, the term "sequestration" by polyphosphate could refer to interference with any or all of these steps. It is also hypothetically possible that polyphosphates could sometimes reverse formation of the visible particles by a process of dissolving solids or converting large particles into smaller particles (i.e., deagglomeration).

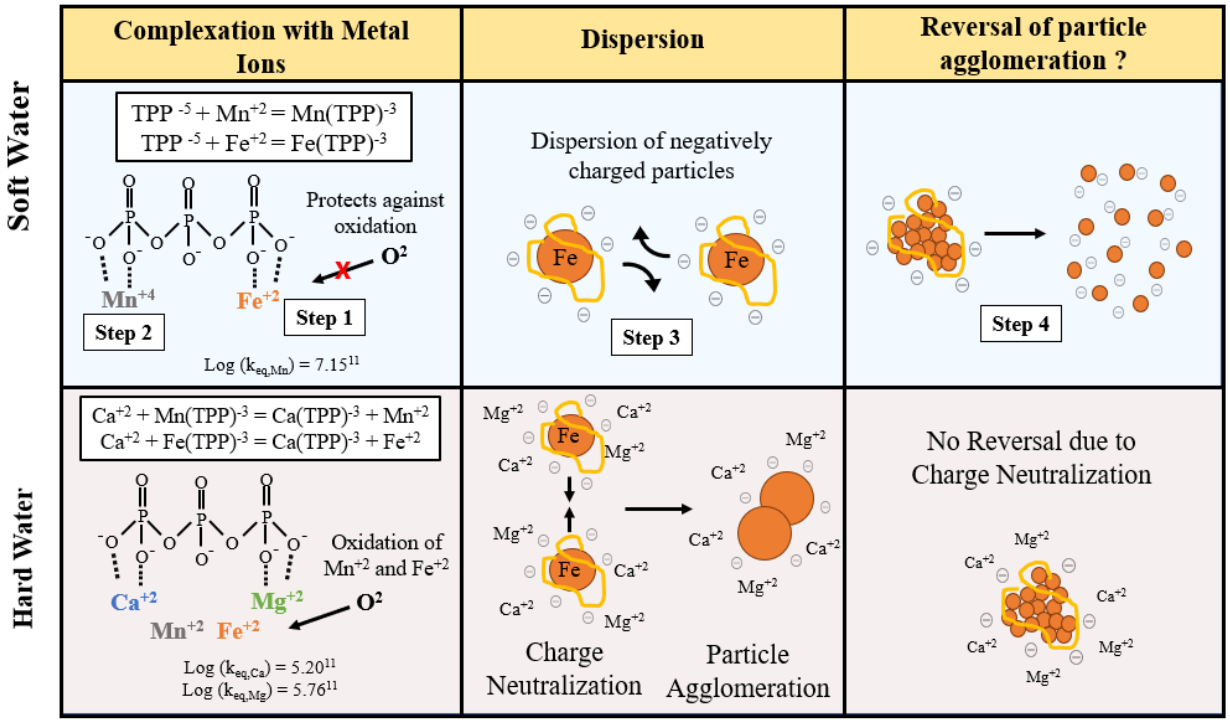

Figure 2-2. Four steps by which polyphosphate might influence problems with Fe/Mn discoloration in potable water systems.

Step 1: Preventing Fe(II), Mn(II) Oxidation. The binding of dissolved iron and manganese by polyphosphate can hinder their oxidation by oxygen or chlorine, helping to maintain ions in solution in their invisible soluble form (Robinson et al., 1990). There is no evidence orthophosphate can hinder Fe/Mn oxidation, likely due to the lower strength complexes.

Polyphosphate complex formation has often been attributed to reductions in visual color/turbidity of Fe^{2+} and/or Mn^{2+} (Bull & Craun, 1977; Rashchi & Finch, 2000; Ting et al., 2008; Volpe, 2012). There is more data in the literature describing the formation of manganese complexes than for iron. For example, equilibrium complexation constants have been published for Mn^{2+} with triphosphate (Log K = 7.15, I = 0.1 M), trimetaphosphate (Log K = 3.57, I = 0 M),, and tetrametaphosphate (Log K = 5.74, I = 0 M), raising the expectation of a very significant role for polyphosphate in Mn(II) complexation (Smith & Martell, 1976). There are no such published complexation constants for Fe(II). To best hinder oxidation, the polyphosphate should be added before the chlorine injection point (Klueh & Robinson, 1988; Volpe, 2012) to allow complexation before the oxidant is introduced. This will also tend to increase the chlorine residual in the water for a given dose throughout a distributions system.

Step 2: Complexation of Fe^{3+}, Mn^{4+} or Hindering Formation of $Fe(OH)_3$ or $Mn(OH)_4$ Solids. To the extent Step 1 oxidation is not inhibited, polyphosphates might bind the very insoluble Fe(III) and Mn(IV) ions that form.

Orthophosphate has been reported to form a binuclear (bidentate) complex with two Fe^{3+} ions (Atkinson et al., 1974; Lente et al., 2000; Parfitt et al., 1975) and a mononuclear (unidentate) complex with one singular Fe^{3+} (Galal-Gorchev & Stumm, 1963). It is reasonable to believe that polyphosphate can form much stronger complexes with these ions than Fe(II) or Mn(II), although no data available in the literature.

To the extent that the newly formed Fe(III) and Mn(IV) are not complexed, the polyphosphate could also hinder nucleation of the Fe^{3+} and Mn^{4+} colloids through a process known as “crystal poisoning.” This phenomenon is well understood for polyphosphate inhibition of calcium carbonate precipitation (Vidic et al., 2015), but little research has examined the analogous reaction for iron and manganese.

Step 3: Dispersion of Colloids and Particles. To the extent that $Mn(OH)_4$ or $Fe(OH)_3$ are formed, polyphosphate could hinder overall agglomeration into larger particles. A decrease in surface charge from coatings of anionic polyphosphate can create a high repulsive charge between particles.

The ability of phosphates to make a particle surface charge more negative are thought to increase with higher molecular weight of the polyphosphate as demonstrated on iron (D. A. Lytle & Snoeyink, 2002). Pyro, tri, and long-chained polyphosphate all tended to reduce particle size, make zeta potential highly negative, and reduce apparent color and turbidity. Orthophosphate had a much lesser effect (D. A. Lytle & Snoeyink, 2002) as expected, given its lower anionic charge per molecule sorbing to the surface.

It has been suggested that polyphosphate interference with step 3 is the dominant mechanism for sequestration, while its hindrance of steps 1 and 2 was a relatively minor contributor (Illig, 1960; Klueh & Robinson, 1988). However, mechanistic studies proving this are lacking in the literature.

Step 4: Reversal of Agglomeration. Polyphosphates are advertised as being capable of reversing particle agglomeration (or deflocculating particles) in some cases. Multiple chemical manufactures have mentioned ‘cleaning’ of pipes as a benefit (APEC Water, n.d.; Carus Water, 2012; The Honest Water Filter Company, n.d.; Town of Newmarket New Hampshire, 2016). In these cases, polyphosphate is reported to deflocculate and detach calcium and/or magnesium adhered to pipe walls. The city of Sutherlin, Oregon reportedly used polyphosphate to clean scale and corrosion buildup on cast iron pipes (Dollar, 1992), however we can find no supporting documentation in the literature backing this mechanism. This issue is deserving of future research.

Effect of Hard Water on Sequestration Effectiveness

Ions other than Fe/Mn can compete for individual polyphosphate complexing sites (Figure 2-2). Most notably in potable water, dissolved calcium and magnesium can bind the polyphosphate, and reduce its ability to prevent discoloration caused by iron and manganese. Hardness can therefore interfere with sequestration by polyphosphate (Figure 2-2) or require much higher doses of polyphosphate to achieve the same level of effectiveness relative to soft waters.

Step 1, 2: Effect of Hardness on Sequestration of Metal Ions. Calcium and magnesium form complexes with phosphates. While polyphosphate binds to Mn/Fe more strongly than for hardness ions Mg^{2+} and Ca^{2+}, the concentrations of magnesium or calcium are often more than three orders of magnitude higher.

This effect can be illustrated using complexation constants for the simple polymer TPP binding of Mn^{2+}. The equilibrium binding constants for manganese are 2-3 orders of magnitude higher than either calcium and magnesium (7.15 compared to 5.2 and 5.76 respectively) (Smith & Martell, 1976). While kinetic and diffusion limitations may play a role in real-world situations, modeling of this equilibrium for TPP as a function of calcium predicts a very significant effect (Figure 2-3). With no calcium in the water, virtually all (97-99.7%) of the manganese is expected to be complexed by the TPP. As the concentration of calcium increases from 0 to 100 mg/L, the amount of Mn^{2+} that is not complexed, and is available for oxidation and precipitation, increases at all pH values. The predicted increase is about 0.0003 mg/L to 0.03 mg/L, or about 100X, comparing high to no hardness at pH 10. Assuming uncomplexed Mn^{2+} is the primary reactant with oxidants, the rate of creating aesthetic problems would also be increased proportionately. At pH 7, the same increase in calcium raises the uncomplexed Mn^{2+} concentration by a lesser, but still significant, factor of 10X (0.003 to 0.03 mg/L).

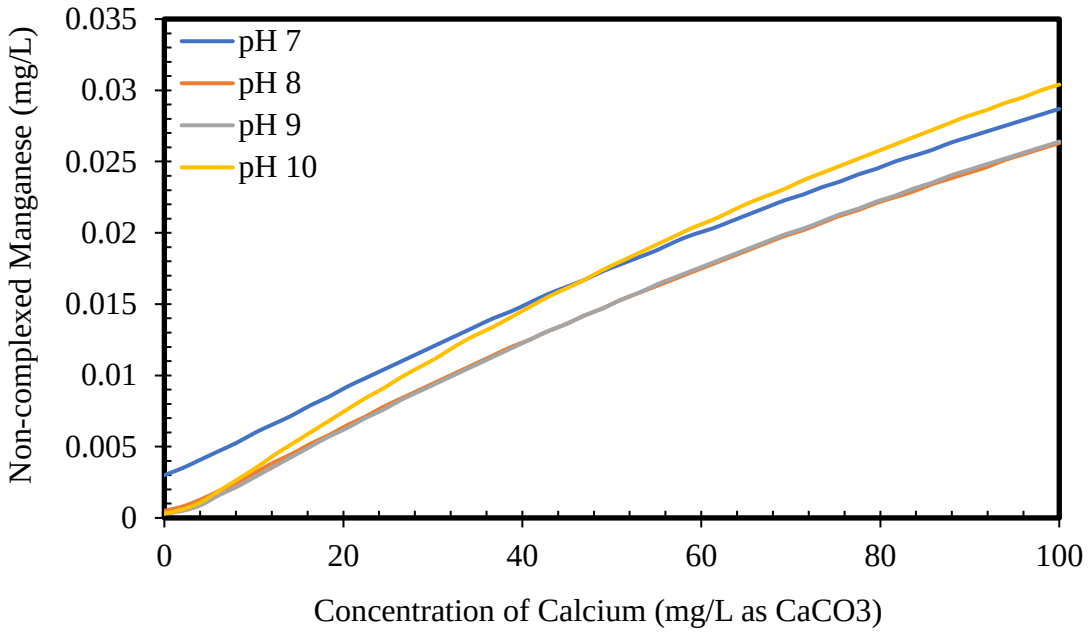

Figure 2-3. Increasing hardness reduces the % of total manganese complexation with 1 mg/L TPP as P. Total Mn = 0.1 mg/L and ionic strength = 0.1 M (assuming no calcite formation). The binding constants for Mn^{+2} and Ca^{+2} with TPP^{-5} are Log K_{Mn} = 7.15, Log K_{Ca} = 5.2, and H^{+} binding with TPP^{-5} are Log K_1 = 8, Log K_2 = 5.5, Log K_3 = 2.6 (Smith & Martell, 1976).

Step 3: Effect of Hardness on Sequestration of Particles. The presence of high levels of Ca^{2+} and Mg^{2+} can decrease particle stability and encourage agglomeration even in the absence of polyphosphate by double layer compression and charge neutralization (Zeta-Meter, 1993). Moreover, binding of calcium and magnesium by polyphosphate reduces the negative surface charge of the polymer and can prevent it from sorbing to the surface of solid particles. The net result of all three effects is that much higher doses of polyphosphate may be required to achieve a given result in a hard water versus a soft water, and in some cases, polyphosphate may not be able to prevent aesthetic problems.

Step 4: Effect of Hardness on Reversal of Particle Agglomeration. If polyphosphate can indeed reverse particle agglomeration, the presence of hardness would tend to reduce that effect by the same reasoning as described for stabilization of particles.

Differences between Iron and Manganese

Iron and manganese react differently with phosphates and are oxidized, precipitated, and agglomerated at different rates. Hypothetically, an effective polyphosphate dose for iron may be different than for the same molar concentration of manganese. Iron has been hypothesized to be better sequestered than manganese when there was no calcium or magnesium present (Ting et al., 2008), Water characteristics such as pH, temperature, secondary disinfectant, polyphosphate geometry, and others are also likely involved in controlling the relative efficacy of iron and manganese sequestration.

Effect of pH

Iron and manganese are generally reported to be more effectively sequestered at lower pH conditions (Henry, 1950; Rashchi & Finch, 2000; Rowe, 2013; Sullivan, 2007; Ting et al., 2008; Volpe, 2012), although research has shown that pH made no difference in other circumstances (D. A. Lytle & Snoeyink, 2002). A chemical explanation for this discrepancy has not yet been proposed, however, increased oxidation rate at higher pHs (Mamadou et al., 2021; Volpe, 2012; Zinati & Shuai, 2005) could play a role.

Chemical manufacturers will sometimes recommend products based on pH. For example, Sper Chemical manufacturer recommends one product if the pH is between 6.0 and 7.5, and a different product if the pH is between 7.0 and 9.0 (Sper Chemical Corporation, n.d.-b). The exact reasons behind these recommendations are not clear.

Dosing Limitations

The effectiveness of dosing higher levels of polyphosphates tends to plateau or reach a point of diminishing return (Volpe, 2012). The precise point of diminishing return is expected to vary with water chemistry.

<u>Scale Inhibition (Anti-Scaling)</u>

Calcium carbonate precipitation is a major problem for many water systems. In the distribution system, scale formation reduces water velocity and pressure by clogging, increases operational costs, and reduces flow capacity. In homes, calcium carbonate can block drains and destroy appliances, stain dishes, sinks, toilets, inhibit heat transfer in water heaters, increase soap demand, and cause pipe leaks (Figure 2-4) (Devine et al., 2021). There are no federal health

regulations that require control of scaling, but the above consequences can be so devastating that some kind of treatment is necessary.

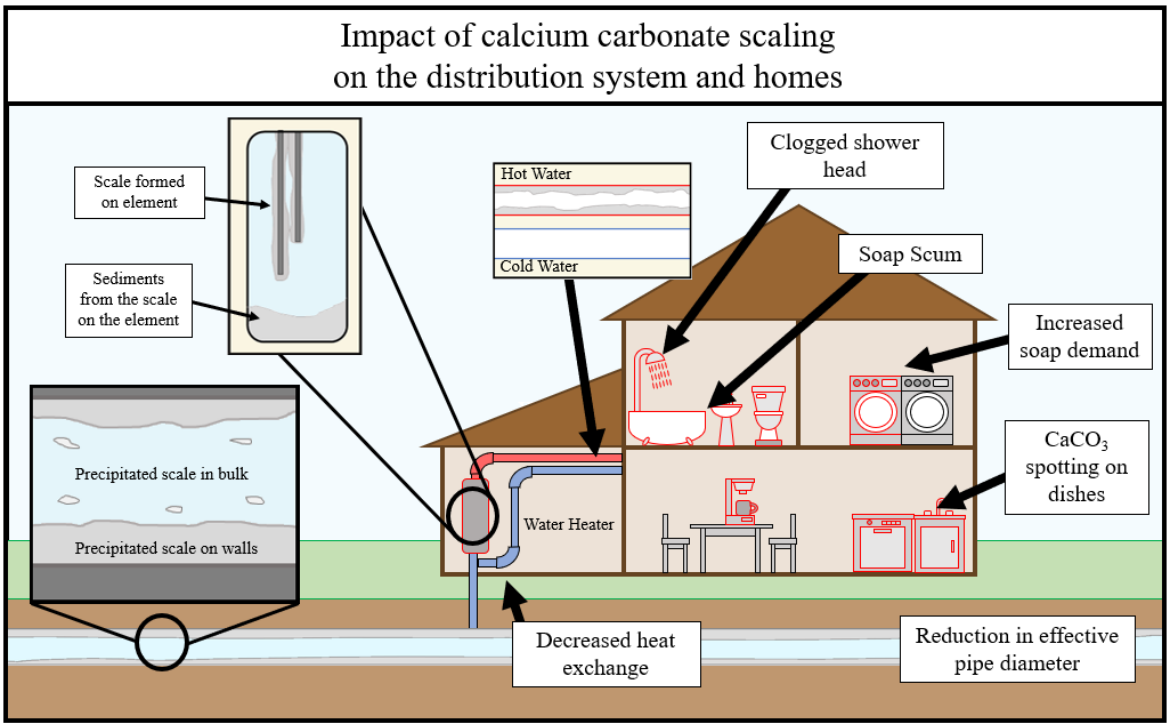

Figure 2-4.Calcium carbonate scale forming on plumbing material and in the bulk water.

Consumers may choose to remove calcium in their own building by installing in-home water softeners or large systems can choose to soften all treated water at high pH (i.e., addition of lime or soda ash) followed by sedimentation and filtration. Ideally, water utilities and consumers would work together to determine the best overall approach of centralized and consumer treatments for their system. There are certainly cases in which centralized treatment is much more cost effective, however other situations favor in-building treatments. This work will focus on the situation in which polyphosphate is dosed at a central treatment plant to prevent scaling at lower cost.

For calcium carbonate to precipitate, the water must be supersaturated relative to its solubility. Factors such as temperature, pH, and ionic strength can affect the degree of supersaturation along with the concentration of carbonate and hardness. Supersaturation can be reasonably predicted through popular indices including Langelier and Ryznar (Langelier, 1936; Ryznar, 1944) even though temperature effects are not very predictable with existing knowledge.

Precipitation of calcium carbonate can occur in the bulk water as well as on pre-existing scale on the walls of pipes (Figure 2-4). Existing calcium carbonate scale decreases the induction time for precipitation by a process known as seeding (Spanos & Koutsoukos, 1998); spontaneous precipitation requires a much greater degree of supersaturation to occur in bulk water. Precipitation that mostly occurs in bulk water tends to pose a lesser risk of pipe clogging.

Mechanism

Calcium carbonate scale formation is inhibited in three ways: threshold inhibition, crystal distortion, and dispersion (Amjad & Koutsoukos, 2015; Mpelwa & Tang, 2019; Vidic et al., 2015). These mechanisms involve "poisoning" the two steps of crystal formation: nucleation and crystal growth. Nucleation occurs first and includes initial crystal development and formation of a deposit on a surface. Primary nucleation occurs in a system with no pre-formed calcite crystals (or "seed") while secondary nucleation occurs in systems with pre-existing calcite present (Botsaris, 1976; Mullin, 2001). In primary nucleation, supersaturated calcium ions form clusters of a large enough size that a crystalline phase and additional growth sites are formed (Jančić & Grootscholten, 1984). In secondary nucleation, pre-formed scale molecules become sites for additional crystals grow (Vidic et al., 2015). The precipitates increase in size over time as more calcium deposits.

Threshold Inhibition (Nucleation Modification). Threshold inhibition is widely reported as a major contributing mechanism for calcium inhibition (Rashchi & Finch, 2000; Rice & Hatch, 1939; Rice & Partridge, 1939; Sorbie & Laing, 2004; Tomson et al., 2002; Vidic et al., 2015). The general idea is that phosphate can dissolve or prevent further formation of calcium carbonate nuclei (Sorbie & Laing, 2004; Tomson et al., 2002; Vidic et al., 2015). The primary nucleation stage can be inhibited so no new crystal lattices can form, or the polyphosphate binds to the small clusters of calcium ions before initial nucleation occurs, thereby "deagglomerating" the calcium before a crystal structure is created.

Crystal Distortion. Very small amounts of polyphosphate can bind to an existing crystal causing formation of a higher solubility amorphous phase (Benton et al., 1993; Sorbie & Laing, 2004; Tomson et al., 2002; Vidic et al., 2015; Yuan et al., 1998). These particles are believed to have difficulty agglomerating with other particles or scale due to increased internal stress caused by the structure (Chauhan et al., 2015; Mehta et al., 2015). This can lead to the deagglomeration of

larger particles into smaller ones that tend to remain suspended in solution (Figure 2-5). This decrystallization and deagglomeration is often cited by polyphosphate manufactures as a means of removing calcite that is already coating the interior of pipes (APEC Water, n.d.; Carus Water, 2012; The Honest Water Filter Company, n.d.; Town of Newmarket New Hampshire, 2016).

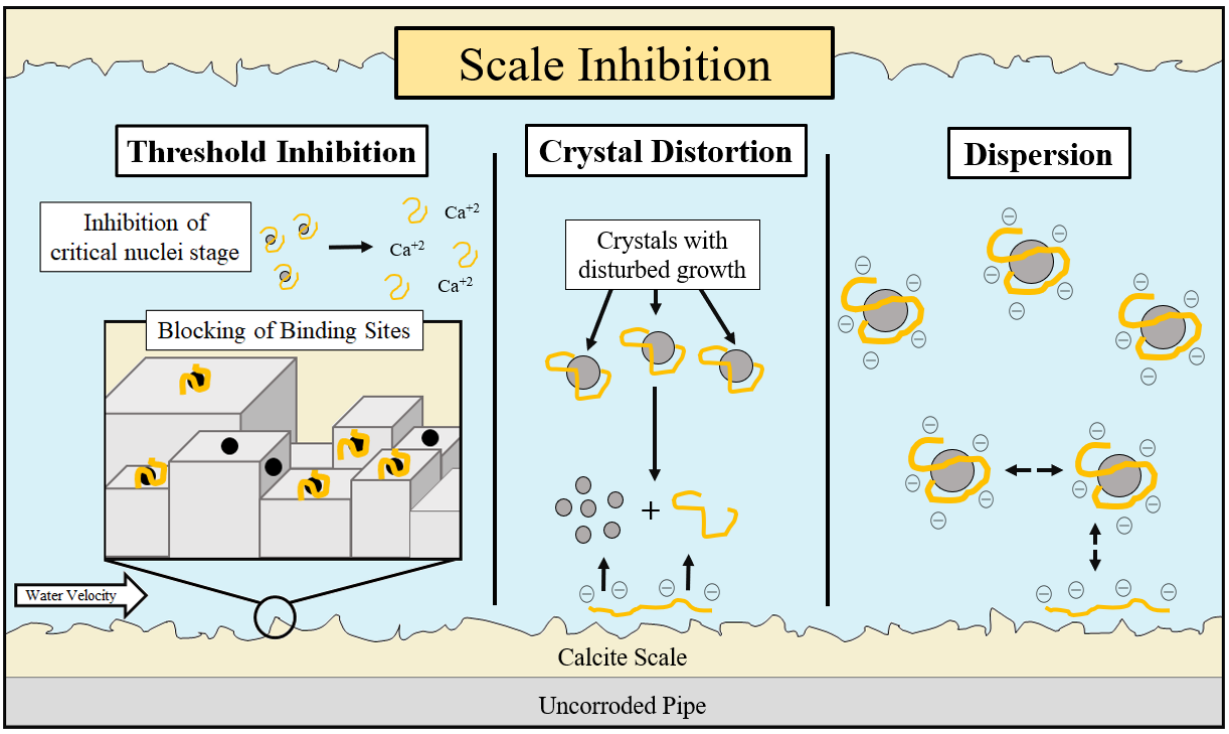

Figure 2-5. The three mechanisms for scale inhibition: threshold inhibition, crystal distortion, and dispersion. Yellow lines represent polyphosphate chains.

Dispersion. Similar to Fe/Mn, inhibition of calcite scale formation by dispersion can occur (Chauhan et al., 2015; Mehta et al., 2015; Vidic et al., 2015). Negatively charged polyphosphate chains complex with colloidal calcium to produce particles with high negative charge which discourages agglomeration (as explained in the "sequestration" section). Particles that are not complexed by polyphosphate will not be held in solution through dispersion.

Effect of pH

As pH increases, carbonic acid (H_2CO_3) and bicarbonate (HCO_3^{-1}) (pKa = 6.35) increasingly form carbonate (CO_3^{-2}) (pKa = 10.25) that is free to form precipitates. Therefore, calcium carbonate is more likely to precipitate at higher pH (D. M. Dawson, 1990; Irani & Callis, 1962; Ketrane et al., 2009). There is a saturation pH (pH_{sat}) below which calcium carbonate cannot

form. In general, a pH of 7.5 or lower is less likely to have issues with calcium carbonate precipitation (University of California, n.d.), at least up to a calcium hardness and alkalinity of about 120 mg/L as $CaCO_3$ in cold water. Thus, polyphosphate is generally only required at a pH above 7.5 to combat calcium carbonate scaling (Irani & Callis, 1962; Ketrane et al., 2009; University of California, n.d.). Other variables, such as temperature, however, may widen this range (Richards et al., 2018). The literature suggests that scale inhibition is effective over a fairly wide range, although this is not proven in all cases.

Effect of Temperature

Solubility of calcium carbonate decreases markedly at higher temperatures (Cowan & Weintritt, 1976; Ketrane et al., 2009; Richards et al., 2018) and the rate of precipitation increases (Wu et al., 2010). Consequently, calcium carbonate can pose problems in some hot water systems even when it poses no problem in cold water. Scale formation can inhibit heat transfer in these devices, increasing energy costs and causing heater failure (Brazeau & Edwards, 2011; Water Quality Research Foundation, 2011).

If polyphosphate is used to prevent hot water scaling, it is important to consider water age because reversion rates also increase with higher temperature (see "Reversion" section). Thus, the effectiveness of scale inhibition at high temperatures may decrease at high water age. While this is likely not an issue for systems with very high polyphosphate doses, systems with trace doses could experience a strong effect.

Heater Type

Water heater temperature set-points can vary greatly depending on the circumstance and consumer preference. Lower water heater temperatures are often used to save money in heating costs and reduce scaling while high temperatures are often targeted to discourage opportunistic pathogen growth. Calcium carbonate precipitation may increasingly become an issue with the use of higher temperatures to control emerging problems with *Legionella* (Devine, 2021).

The type of heater can also be important (Brazeau & Edwards, 2011). While no water heaters are immune to problems with scaling, on-demand water heaters tend to be the most susceptible to precipitation due to the increased watt density and decreased diameter of tubes in the water heater (Devine et al., 2021; Devine & Edwards, 2022). In fact, on-demand water heaters can be rendered useless in a matter of months in some hard waters (Brazeau & Edwards,

2011; Thomas et al., 2006). Tank heaters have similar but less severe problems due to the lower watt density. Scale forms on the bottom of gas water heaters, or on electric heating elements where it can be self-cleaned by spalling due to expansion and contraction of the heating element (Devine & Edwards, 2022). Large quantities of scale can accumulate at the bottom of a tank before flow is blocked. Electric heaters can be cleaned with vinegar or other acids, but this requires specialized, intensive labor by consumers.

In all of these situations, polyphosphate can be a useful tool for increasing operational life and decreasing electric costs.

Inhibition of Non-Calcium Carbonate Scales by Polyphosphate

Polyphosphate could be used to inhibit precipitation of solids other than calcium carbonate. For example, polyphosphate may inhibit the formation of calcium sulphate scale commonly formed from brackish waters in reverse osmosis desalination plants (Rahman, 2013; The Honest Water Filter Company, n.d.; Van Driessche et al., 2019). It is assumed that similar mechanisms to calcium carbonate inhibition apply for calcium sulphate. Likewise, other types of scale including calcium phosphate, aluminum phosphate, and magnesium silicate are sometimes important in potable water systems. However, it is unknown what effect polyphosphate may have on the precipitation of these solids. More work is needed to better understand inhibition of these scales.

Corrosion Control

There are at least five distinct types of corrosion that are important in potable water systems: pitting, scale buildup, soluble metal release, particulate metal release, and galvanic corrosion (Figure 2-6). Erosion and microbial induced corrosion can also likely play a role (Douterelo et al., 2020; Roy et al., 2018). While pitting corrosion and erosion corrosion scale buildup can have devastating economic and operational impacts, the effects of ortho and polyphosphate on these issues is relatively poorly understood. This review will focus on soluble and particulate metal release, as these involve both primary (i.e., Pb/Cu) and secondary (i.e., Fe/Mn) drinking water regulations and are better understood.

	Pitting	Scale Buildup	Soluble Metal Release	Particulate Metal Release	Galvanic Corrosion
Types of Corrosion:	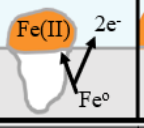		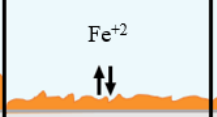		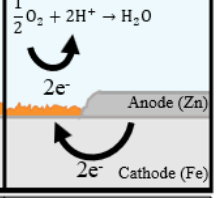
Importance:	Pinhole Leaks and associated problems are expensive to repair (nearly $1 billion annual cost)[100]	Increased scale buildup causes head, decreased water flow, high pumping cost, and sites for bacterial growth[105]	Increased metal concentration in drinking water	Increased metal concentration in drinking water	Increased metal release from the anode while the cathode is protected
Metal Types:	• Iron • Copper • Stainless Steel • Galvanized Iron • Brass	• Iron • Galvanized iron	• Lead • Copper • Iron • Brass	• Lead • Copper • Iron • Brass	• Copper + Lead (Solder, pipe, brass) • Copper + Iron • Copper + Galvanized Iron • Steel water tank + Sacrificial Anode (Mg / Al)
Effect of Orthophosphate:	May help reduce Pitting of copper in some circumstances	Often negative, however very little literature present	Often beneficial to reducing soluble Cu, Pb	Often beneficial to reducing particulate Cu, Pb release	Unclear for most metals. Most research focuses on copper + lead solder, however little is unknown
Effect of Polyphosphate:	May help reduce pitting of copper in some circumstances	Often negative, however very little literature present	Often detrimental to reducing soluble Cu, Pb	Often detrimental to reducing particulate Cu, Pb release	Unclear
References:	(Edwards et al., 2004; Lattyak, 2007; Lytle & White, 2014; Sarver & Edwards, 2012)	(McNeill & Edwards, 2000, 2001)	See *Iron Pipe, Copper Pipe, and Lead Pipe* sections	See *Iron Pipe, Copper Pipe, and Lead Pipe* sections	(Bradley, 2018; Gregory, 1990; Nguyen et al., 2010; Oliphant, 1967)

Figure 2-6. The importance and generalized effect of phosphates on each of the five main types of corrosion: Pitting, scale buildup, soluble metal release, particulate metal release, and galvanic corrosion.

With some noteworthy exceptions, the conventional wisdom is that orthophosphate tends to inhibit all types of metallic corrosion, whereas polyphosphate either has no effect on or can increase corrosion. Benefits of orthophosphate are generally attributed to formation of insoluble and protective orthophosphate scale layers on the surface of pipes, whereas complexation by polyphosphate is thought to hinder passivation. As a result, the concept of ortho:poly ratio can be important in the context of corrosion, as it can determine when the "good" effects of orthophosphate may outweigh the "bad" effects of polyphosphate. This is an oversimplification, but the concept is nonetheless useful. Moreover, in practice, all polyphosphate contains at least some orthophosphate even when freshly made, and the percentage of orthophosphate increases to some extent during water distribution.

Iron Pipe

Orthophosphate. Orthophosphate is generally reported to be beneficial for reducing iron leaching (Koudelka et al., 1982; D. A. Lytle et al., 2005; McNeill & Edwards, 2000; Mi et al., 2013; Sarin et al., 2003; Tang et al., 2018). For reasons that are not clear, there are exceptional circumstances in which orthophosphate has performed worse than polyphosphate, had no effect, or been harmful compared to a condition with no inhibitor (McNeill & Edwards, 2000; Mi et al., 2013). Therefore, identification of the correct product and dose for iron would require a long-term trial-and-error process that can be financially impractical.

Overall, relatively little literature is available relating to the mechanisms of orthophosphate and polyphosphate inhibition of iron pipe corrosion. The formation of a durable iron phosphate scale (D. A. Lytle et al., 2005) or sorption of orthophosphate to the iron surface is possible. If an iron phosphate was to form, vivianite [$Fe_3(PO_4)•8H_2O$] is one representative solid. X-ray diffraction has shown the presence of vivianite in drinking water pipe scales but its extent is unclear (Tavanpour et al., 2016). More work is needed to quantify its formation and impact in distribution systems.

The second potential mechanism involves the sorption of orthophosphate to the iron surface. One study hypothesized that the orthophosphate is absorbed on iron cathodic sites and inhibits oxidation, but this mechanism is speculative (Andrzejaczek, 1979).

Polyphosphate*.* In general, the use of polyphosphate for iron corrosion control is considered risky. In a few cases it was believed to be superior to orthophosphate (Koudelka et al., 1982; Maddison et al., 2001; Mi et al., 2013), although reversion and use of blended chemicals means it is always possible that the benefits were due to the presence of orthophosphate. Other studies showed polyphosphate was nearly always worse than no inhibitor (McNeill & Edwards, 2000) or beneficial at lower and detrimental at higher concentrations compared to no phosphate (Facey & Smith, 1995; Koudelka et al., 1982). Even with such data, the short-term effect can be different than the long-term effect; a result obtained after 3 months was the complete opposite of that obtained after 4 years in one study (McNeill & Edwards, 2000).

The beneficial or detrimental effect of polyphosphate is likely to depend on water chemistry, however it is not well understood. One theory is that polyphosphate sorbs to the iron surface such that iron oxidation is inhibited. Likewise, the released particulate iron could

increase through a decrease in scale stability while soluble iron release may be increased through ligand promoted dissolution (C. F. Lin & Benjamin, 1990; McNeill & Edwards, 2001).

Copper Pipe

Orthophosphate. The effect of orthophosphate on copper corrosion depends on the type of composition of the existing scale. Generally, only newer pipes experience positive effects of orthophosphate additions (Cantor et al., 2003; Dartmann et al., 2010; Edwards et al., 2002; Schock & Sandvig, 2009). As explained by the cupric hydroxide model, scale on new pipes in the absence of phosphates consists of relatively soluble copper hydroxide [$Cu(OH)_2(s)$] (Edwards et al., 2001; Schock et al., 1995; Schock & Sandvig, 2009). Over time, more stable and thermodynamically favorable malachite [$Cu_2CO_3(OH)_2$] or tenorite [CuO(s)] form (Edwards et al., 2002; Hidmi & Edwards, 1999; Schock & Sandvig, 2009) as a function of pH (Schock & Sandvig, 2009). While they take time to form, malachite and tenorite formation ultimately has lower solubility than cupric phosphate scales. Thus, high copper release may be experienced without phosphate in the short term, but a significant reduction in copper corrosion may sometimes be observed over time. In some waters this natural decrease of copper release with aging does not occur and orthophosphate dosing is necessary.

Polyphosphate. The literature on polyphosphates is relatively limited. On one hand, polyphosphate-based inhibitors have been reported to increase copper release to water (Cantor et al., 2000; Lee et al., 2012; McNeill & Edwards, 2004). In other circumstances, that was not the case. In fact, experiments have shown polyphosphates to be more effective at reducing copper release than orthophosphate but worse than no inhibitor (Edwards et al., 2002), beneficial to copper release at low concentrations (Facey & Smith, 1995), and overall unclear if it was beneficial or detrimental (Dodrill & Edwards, 1995). As mentioned previously, a major contributor to the disparate results could be the inevitable reversion of polyphosphates to orthophosphates making it difficult to determine its relative importance. In one study, the increased copper release caused by polyphosphate, while accounting for reversion, found that the increase in copper due to polyphosphate followed a simplified equation of the form:

$$\text{Excess Soluble Cu} = \frac{K\,[Total\ Poly{-}P]}{[PO_4^{-3}]^{0.66}} \text{ (Edwards et al., 2002)} \qquad (1)$$

This equation captures the fact that increasing orthophosphate often decreases copper solubility while polyphosphate increases soluble copper. The net effect on solubility is dependent on which effect is dominant.

Lead Pipe

Orthophosphate. Orthophosphate can dramatically reduce soluble lead release and sometimes increase scale durability in drinking water by forming lead phosphate scales (Figure 2-7). Multiple lead phosphate scales can form depending on the water conditions, including hydroxypyromorphite ($Pb_5(PO_4)_3OH$), chloropyromorphite ($Pb_5(PO_4)_3Cl$), and ($Pb_3(PO_4)_2$) (D. A. Lytle et al., 2009; Ng et al., 2012; Trueman et al., 2018), while other complex amorphous layers can also form (Wasserstrom et al., 2017), as confirmed by surface measurement techniques including SEM, TEM, and XANES (D. A. Lytle et al., 2009; Ng et al., 2012).These scales are often thought to be more durable and less soluble than scales formed in absence of phosphate (i.e., cerrusite, hydrocerrusite). Orthophosphate can also beneficially affect lead release without forming a lead phosphate scale by reducing the kinetics of dissolution and other factors. For instance, dissolution of lead scale can involve the reduction of Pb^{4+} in PbO_2 and release of Pb^{2+}, and orthophosphate can block Pb^{2+} binding sites and slow or inhibit the reduction of lead (Noel et al., 2014; Xie, 2010).

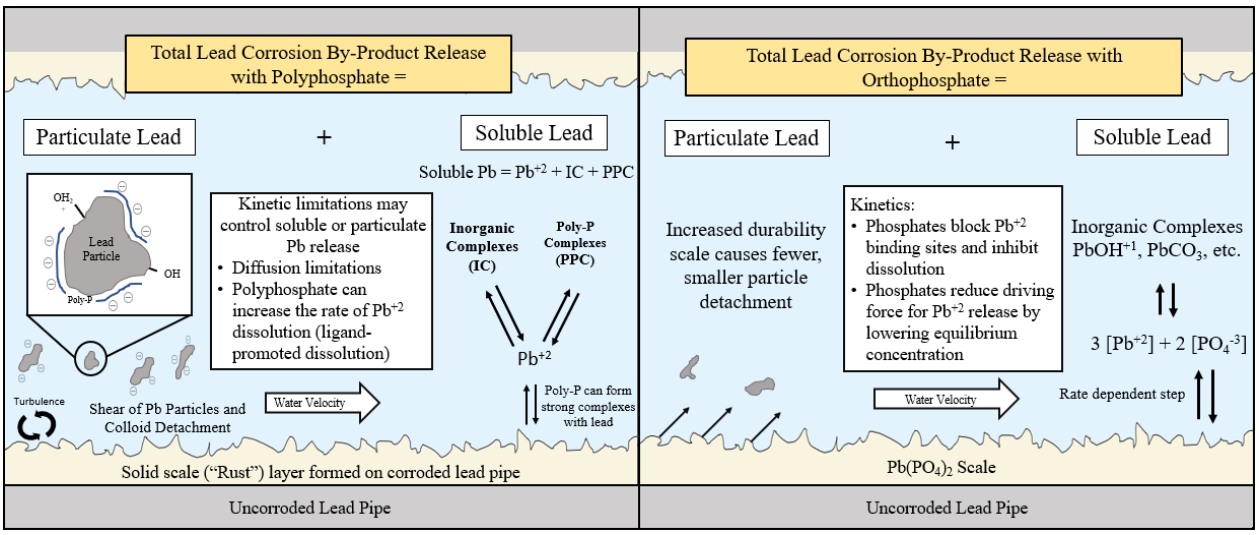

Figure 2-7. The detrimental effect of polyphosphate (left) and the beneficial effects of orthophosphate (right) on lead pipe corrosion.

The use of orthophosphate can cause transient issues that might temporarily increase lead release to drinking water. If not incorporated into the scale, orthophosphate can react with soluble lead producing nanoparticles in certain water conditions (i.e. low hardness) (D. A. Lytle, Formal, et al., 2020). Particles of this size have shown to be difficult to filter out (Doré et al., 2021), as was experienced in Newark, NJ, resulting in more than 10 µg/L of lead passing through faucet and pitcher filters (D. A. Lytle, Schock, et al., 2020; Pan et al., 2021; Purchase et al., 2021). The formation of the stable nanoparticles appeared to be due to a highly negative surface charge that was countered by hardness ions (Zhao et al., 2018, 2022). If this proposed mechanism is accurate, polyphosphate would be even more likely to cause this problem.

Polyphosphate. Polyphosphate can increase soluble lead release in two ways. First, polyphosphate facilitates ligand-promoted dissolution. Holm and Schock first hypothesized this as a potential mechanism for lead release (Holm & Schock, 1991). This mechanism is relatively well studied for iron (C. F. Lin & Benjamin, 1990; Z. Wang et al., 2017), however, it is not as well documented for lead. Secondly, polyphosphate binds free Pb^{2+} in solution, thereby increasing the soluble lead at equilibrium (Figure 2-7) (Edwards & McNeill, 2002; Holm & Schock, 1991; Locsin et al., 2022). In long term experiments at pH 7.2, 7.8, and 9.5 and alkalinity ranges of 15-300 mg/L, the addition of 1 mg/L of hexametaphosphate caused 1.6 mg/L of additional soluble lead release after 72 hours (Edwards & McNeill, 2002).

For orthophosphate corrosion control, a sufficient concentration of orthophosphate is required to form a protective scale. Reversion of polyphosphate to orthophosphate, or the use of blended phosphates, may provide a sufficient amount of orthophosphate to form such a scale. At some point, the detriments of polyphosphate are believed to outweigh the benefits of orthophosphate.

Polyphosphate may also increase particulate lead release through the destabilization of scale particles. Similar to particle agglomeration with iron and manganese, polyphosphate can coat lead particles and colloids (Edwards & McNeill, 2002). At some point, the surface can become sufficiently negatively charged that repulsive forces might cause agglomerates to break apart (Hubbe, 1984; Sharma et al., 1992; Shen et al., 2012; Zeta-Meter, 1993).

Conclusions

Phosphates can often provide an inexpensive means of reducing aesthetic Fe/Mn problems, reducing scaling, and controlling corrosion. Improved understanding of phosphate type and dose selection is needed to meet new regulatory requirements and address increased propensities for scaling at higher hot water system temperatures. Existing trial and error methodologies are inadequate, especially in situations where the short-term effect might be different than the long-term effect. The proprietary nature of these products and a lack of publicly available research have impeded improvements in understanding the use of phosphates.

Approaching optimization through a one-dimensional lens is the simplest approach, but it virtually guarantees unanticipated benefits and detriments because phosphate effects are so wide-ranging. Future work should consider how to holistically optimize dosing in situations where 2-D (i.e., when two objectives must be met) and even 3-D benefits must be realized. An improved understanding of 1-D optimization is a pre-requisite for that higher-level understanding.

Major knowledge gaps include a lack of understanding of sequestration mechanisms, and an inability to account for practical effects of water parameters (i.e., pH, hardness, temperature, alkalinity, chlorine, ionic strength, etc.) on each dimension of performance. Furthermore, fundamental understanding of phosphate chemicals is limited and requires more research. This includes better understanding of orthophosphate vs zinc orthophosphate, and appropriate use of blended phosphates. It is also important to understand if deagglomeration or “cleaning” of calcium carbonate and other pipe scale occurs as claimed, especially since this mechanism might explain destabilization of scale and water discoloration events. Finally, since pilot or full-scale testing can be expensive and impractical, the creation of a simple, cheap bench test that can predict performance would be highly desirable.

References

1. Carus Water. Phosphates in Drinking Water FAQ's. 2012. https://www.battlecreekmi.gov/DocumentCenter/View/7614/Phosphate-FAQs
2. Carus Corporation. The Use of Phosphates in Water Treatment for Corrosion Control & Sequestration. 2017. https://mwua.org/wp-content/uploads/2017/08/Lead-Copper-Control-with-Phosphates_20170413.pdf
3. Folsom JM, Oliver LE. Economic Analysis of Phosphate Control: Detergent Phosphate Limitations vs. Wastewater Treatment. Glassman-Oliver Economic Consultants; 1980.
4. Gilbert PA, DeJong AL. The use of phosphate in detergents and possible replacements for phosphate. *Ciba Found Symp*. 1977;(57):253-268. doi:10.1002/9780470720387.ch14
5. Schwartz C, Munter CJ. Phosphates in Water Conditioning. *Ind Eng Chem*. 1942;34(1):32-40. doi:10.1021/ie50385a007
6. Hill CP, Giani R. Water Quality Monitoring and Assessment of Internal Corrosion and Increased Metals Concentrations. In: *Internal Corrosion Control in Water Distribution Systems*. AWWA; 2011:31-60.
7. McNeill LS, Edwards M. Phosphate inhibitor use at US utilities. *J / Am Water Work Assoc*. 2002;94(7):57-63. doi:10.1002/j.1551-8833.2002.tb09506.x
8. Arnold RB, Rosenfeldt B, Rhoades J, Owen C, Becker W. Evolving Utility Practices and Experiences With Corrosion Control. J AWWA. 2020;112(7):26-40. doi:10.1002/awwa.1534
9. Richards CS, Wang F, Becker WC, Edwards M. A 21st-Century Perspective on Calcium Carbonate Formation in Potable Water Systems. *Environ Eng Sci*. 2018;35(3):143-158. doi:10.1089/ees.2017.0115
10. United States Environmental Protection Agency. National Primary Drinking Water Regulations: Lead and Copper Rule Revisions. 2019. https://www.regulations.gov/document/EPA-HQ-OW-2017-0300-0001
11. Smith RM, Martell AE. *Critical Stability Constants*. Vol 4: Inorgan. Springer US; 1976.

doi:10.1007/978-1-4757-5506-0

12. Rashchi F, Finch JA. Polyphosphates: A review. Their chemistry and application with particular reference to mineral processing. *Miner Eng*. 2000;13(10):1019-1035. doi:10.1016/S0892-6875(00)00087-X

13. Sper Chemical Corporation. Phosphates and Polyphosphates – Effective Corrosion Control and Sequestering Compounds for Potable and Irrigation Water Systems. Accessed December 16, 2021. https://www.sperchemical.com/polyphosphate-orthophosphate/

14. Goldberg MM, Nuttall DT. Development of an Analytical Methodology to Identify Species in Phosphate-based Corrosion Inhibitors. *AWWA*. 1998.

15. Holm TR, Edwards M. Metaphosphate reversion in laboratory and pipe-rig experiments. *J / Am Water Work Assoc*. 2003;95(4):172-178. doi:10.1002/j.1551-8833.2003.tb10343.x

16. Griffith EJ, Buxton RL. The preparation and properties of Tetra-, Penta-, Hexa-, Hepta-, and Octaphosphate. *J Chem Soc*. 1967;89(12):2884-2890. doi:10.1039/jr9270002477

17. Fuchs RJ, Lutz CW. Effect of chain length on storage stability and hydrolytic reversion of sodium polyphosphate glasses. *Can J Chem*. 1969;47(16):3081-3084. doi:10.1139/v69-509

18. Shekhar A. Reversion of Poly-Phosphates To Ortho-Phosphates in Water Distribution Systems. Masters of Science Thesis, University of Central Floride, Orlando, Floride. 2007. http://purl.fcla.edu/fcla/etd/CFE0001832

19. Thilo E. The structural Chemistry of Condensed Inorganic Phosphates. *Angew Chem Internat*. 1965;4(12):1061-1071. doi:10.1039/qr9651900303

20. Park S-K, Kim Y-K, Choi S-C. Response of microbial growth to orthophosphate and organic carbon influx in copper and plastic based plumbing water systems. *Chemosphere*. 2008;72(7):1027-1034. doi:10.1016/j.chemosphere.2008.04.006

21. Bailey RA, Clark HM, Ferris JP, Krause S, Strong RL. *Chemistry of the Environment*. Elsevier Science & Technology Books; 2002.

22. Hamilton JG, Hilger D, Peak D. Mechanisms of tripolyphosphate adsorption and hydrolysis on goethite. *J Colloid Interface Sci*. 2017;491:190-198.

doi:10.1016/j.jcis.2016.12.036

23. De Jager HJ, Heyns AM. Kinetics of acid-catalyzed hydrolysis of a polyphosphate in water. *J Phys Chem A*. 1998;102(17):2838-2841. doi:10.1021/jp9730252

24. Kodama T. Formation of Iron Orthophosphate Colloids and Anodic Films on Iron in Phosphate Solutions. Corros Eng. 1974;23(11):545-551. doi:10.3323/jcorr1974.23.11_545.

25. Rulliere C, Perenes L, Senocq D, Dodi A, Marchesseau S. Heat treatment effect on polyphosphate chain length in aqueous and calcium solutions. *Food Chem*. 2012;134(2):712-716. doi:10.1016/j.foodchem.2012.02.164

26. Piacenza E, Presentato A, Turner RJ. Stability of biogenic metal(loid) nanomaterials related to the colloidal stabilization theory of chemical nanostructures. *Crit Rev Biotechnol*. 2018;38(8):1137-1156. doi:10.1080/07388551.2018.1440525

27. Stumm W, Morgan JJ. *Aquatic Chemistry: Chemical Equilbria and Rates in Natural Waters*. John Wiley & Sons, INC; 1995. doi:10.16309/j.cnki.issn.1007-1776.2003.03.004

28. Rossi G, Pincus PA. Properties of Polymer Layers Adsorbed on Surfaces under Nonequilibrium Conditions. *Macromolecules*. 1989;22(1):276-283. doi:10.1021/ma00191a051

29. Bonet Avalos J, Johner A, Joanny JF. Bridging by adsorbed polymers between two surfaces. *J Chem Phys*. 1994;101(10):9181-9194. doi:10.1063/1.468448

30. Hierrezuelo J, Sadeghpour A, Szilagyi I, Vaccaro A, Borkovec M. Electrostatic stabilization of charged colloidal particles with adsorbed polyelectrolytes of opposite charge. *Langmuir*. 2010;26(19):15109-15111. doi:10.1021/la102912u

31. Ye C, Wang D, Shi B, et al. Alkalinity effect of coagulation with polyaluminum chlorides: Role of electrostatic patch. *Colloids Surfaces A Physicochem Eng Asp*. 2007;294(1-3):163-173. doi:10.1016/j.colsurfa.2006.08.005

32. Hogg R. Bridging flocculation by polymers. *KONA Powder Part J*. 2012;30(30):3-14. doi:10.14356/kona.2013005

33. EPA. Optimal Corrosion Control Treatment Evaluation Technical Recommendations for

Primacy Agencies and Public Water Systems. 2016;6:140. https://www.epa.gov/sites/production/files/2016-03/documents/occtmarch2016.pdf

34. Volpe D. Assessment of iron and manganese sequestration. *Am Water Work Assoc Annu Conf Expo 2012, ACE 2012*. 2012. doi:10.7275/HA5A-GG93

35. The phosphate Forum of the Americas. The Use of Phosphates For Potable Water Treatment. n.d.:1-6. https://phosphatesfacts.org/wp-content/uploads/2015/09/The-Use-of-Phosphates-For-Potable-Water-Treatment.pdf

36. Pure water Products L. Feeding Polyphosphate to Sequester Iron and Manganese. Accessed November 1, 2022. https://www.purewaterproducts.com/articles/feeding-polyphosphate

37. Lin YP, Singer PC. Inhibition of calcite crystal growth by polyphosphates. *Water Res*. 2005;39(19):4835-4843. doi:10.1016/j.watres.2005.10.003

38. Wang F, Devine C, Edwards MA. Effect of Corrosion Inhibitors on in Situ Leak Repair by Precipitation of Calcium Carbonate in Potable Water Pipelines. *Environ Sci Technol*. 2017;51(15):8561-8568. doi:10.1021/acs.est.7b01380

39. Thermoscientific. Color measurement. Accessed February 7, 2022. https://assets.thermofisher.com/TFS-Assets/LPD/Application-Notes/an_034_tip_color_measurement_1120.pdf

40. He W, Nan J. Study on the impact of particle size distribution on turbidity in water. *Desalin Water Treat*. 2012;41(1-3):26-34. doi:10.1080/19443994.2012.664675

41. Dawson PL, Acton JC. Impact of proteins on food color. In: *Proteins in Food Processing;* Yada R. Y. Elsevier; 2018:599-638. doi:10.1016/B978-0-08-100722-8.00023-1.

42. Dabkowski B, White M. Understanding the Different Phosphorus Tests. Water Analysis Handbook, 8th Edition, Hach, Loveland, CO. 2013.

43. Great Lakes-Upper Mississippi River Board of State and Provinical Public Health and Environmental Managers. Recommended Standards for Water Works. *Health Educ*. 2012.

44. Widder S, Baechler M. Impacts of Water Quality on Residential Water Heating Equipment. *Pacific Northwest Natl Lab*. 2013;(November):46.

http://www.pnnl.gov/main/publications/external/technical_reports/PNNL-22921.pdf

45. AmeriWest Water Services Inc. Frequently Asked Questions. Accessed January 26, 2022. https://www.ameriwestwater.com/faq

46. Robinson RB. Sequestering methods of iron and manganese treatment. American Water Works Association; 1990.

47. Ting A, Coelho JM, Kucher KM. Polyphosphate Sequestration of Manganese (II). Degree of Bachelor of Science Qualifying Project Report. 2008. https://digitalcommons.wpi.edu/mqp-all/591%0AThis

48. Bull RJ, Craun GF. Health Effects Associated With Manganese in Drinking Water. *Water Technol*. 1977;31(2):386-408. doi:10.1097/EDE.0b013e3181

49. Klueh KG, Robinson RB. Sequestration of iron in ground water by polyphosphates. *J Environ Eng (United States)*. 1988;116(5):1002. doi:10.1061/(ASCE)0733-9372(1990)116:5(1002.2)

50. Lente G, Elizabeth M, Magalhães A, Fábián I. Kinetics and mechanism of complex formation reactions in the iron(III)-phosphate ion system at large iron(III) excess. Formation of a tetranuclear complex. *Inorg Chem*. 2000;39(9):1950-1954. doi:10.1021/ic991017p

51. Parfitt RL, Atkinson RJ, Smart RSC. The Mechanism of Phosphate Fixation by Iron Oxides. *Soil Sci Soc Am J*. 1975;39(5):837-841. doi:10.2136/sssaj1975.03615995003900050017x

52. Atkinson RJ, Parfitt RL, Smart RSC. Infra-red study of phosphate adsorption on goethite. *J Chem Soc Faraday Trans 1 Phys Chem Condens Phases*. 1974;70:1472. doi:10.1039/f19747001472

53. Galal-Gorchev H, Stumm W. The reaction of ferric iron with ortho-phosphate. *J Inorg Nucl Chem*. 1963;25(5):567-574. doi:10.1016/0022-1902(63)80243-2

54. Vidic RD, Liu W, Li H, He C. 72In: *Mineral Scales and Deposits;* Amjad, Z., Demadis, K. D.; Elsevier 2015:169-192.

55. Lytle DA, Snoeyink VL. Effect of ortho- and polyphosphates on the properties of iron

particles and suspensions. *J / Am Water Work Assoc*. 2002;94(10):87-99. doi:10.1002/j.1551-8833.2002.tb09560.x

56. Illig GL. Use of Sodium Hexametaphosphate in Manganese Stabilization. *J Am Water Works Assoc*. 1960;52(7):867-874. doi:10.1002/j.1551-8833.1960.tb00565.x

57. Town of Newmarket New Hampshire. Polyphosphate Added to Water. 2016. Accessed October 20, 2021https://www.newmarketnh.gov/water-wastewater/news/polyphosphates-added-to-water

58. The Honest Water Filter Company. Polyphosphates... What you need to know. Accessed December 10, 2021. https://honestwaterfilter.com/polyphosphates/

59. APEC Water. Sequestration- Polyphosphate Treatment. Accessed December 10, 2021. https://www.freedrinkingwater.com/water_quality/chemical/sequestration-page2.htm

60. Dollar F. Polyphosphates Eliminate Rusty Water Complaints. *Opflow*. 1992;18(6):1-5. doi:10.1002/j.1551-8701.1992.tb00291.x

61. Ravina L, Moramarco N. Everything you want to know about Coagulation & Flocculation. Zeta-Meter, Inc. 1993:1-37.

62. Henry CR. Prevention of the Settlement of Iron. *Am Water Work Assoc*. 1950;42(9):887-896.

63. Rowe J. Out With Fe and Mn. Published 2013. Accessed February 11, 2021. https://www.tpomag.com/editorial/2013/03/out_with_fe_and_mn_wso

64. Sullivan R. Treatment of Manganese in West Boylston Drinking Water. Degree of Bachelor of Science Qualifying Project Report. Worcester Polytechnic Institute. 2007. https://digital.wpi.edu/downloads/pc289k323

65. Zinati G, Shuai X. Management of iron in irrigation water. Fact sheet FS516. Rutgers Cooperative Research & Extension, the State University of new Jersey. 2005. https://njaes.rutgers.edu/fs516/

66. Mamadou F, Mbacké SF, Moussa DEH, Ousmane TA, Aminata MF, Guèye DMC. Iron in Water: Study of Iron Removal Kinetics in Chemically Reconstituted Waters: Application to Groundwater of South Pout (PS2 Site). *Open J Met*. 2021;11(01):1-10.

doi:10.4236/ojmetal.2021.111001

67. Sper Chemical Corporation. The Function of Sequestering Mineral Ions Iron, Manganese, & Calcium/Magnesium –. Accessed November 9, 2021. https://www.sperchemical.com/sequestering-iron-manganese/

68. Devine C, Wang F, Edwards M. A Standardized Test Protocol for Evaluation of Scale Reduction Technologies. *Environ Eng Sci*. 2021;38(12):1109-1119. doi:10.1089/ees.2021.0047

69. Langelier WF. The Analytical Control of Anti-Corrosion Water Treatment. 1936;28(10):1500-1521.

70. Ryznar JW. A New Index for Determining Amount of Calcium Carbonate Scale Formed by a Water. *AWWA*. 1944;36(4):472-483.

71. Spanos N, Koutsoukos PG. Kinetics of precipitation of calcium carbonate in alkaline pH at constant supersaturation. Spontaneous and seeded growth. *J Phys Chem B*. 1998;102(34):6679-6684. doi:10.1021/jp981171h

72. Mpelwa M, Tang SF. State of the art of synthetic threshold scale inhibitors for mineral scaling in the petroleum industry: a review. *Pet Sci*. 2019;16(4):830-849. doi:10.1007/s12182-019-0299-5

73. Amjad Z, Koutsoukos PG. *Mineral Scales and Deposits;* Elsevier 2015. doi: 10.1016/C2012-0-07278-X

74. Mullin JW. *Crystallization*. Fourth. Reed Educational and Professional Publishing LTD; 2001.

75. Botsaris GD. Secondary Nucleation — A Review. In: *Industrial Crystallization*. Springer US; 1976:3-22. doi:10.1007/978-1-4615-7258-9_1

76. Jančić SJ, Grootscholten PAM. *Industrial Crystallization*. Delft, Holland; 1984.

77. Sorbie KS, Laing N. How Scale Inhibitors Work: Mechanisms of Selected Barium Sulphate Scale inhibitors Across a Wide Temperature Range. In: *All Days*. SPE; 2004. doi:10.2118/87470-MS

78. Tomson MB, Fu G, Watson MA, Kan AT. Mechanisms Of Mineral Scale Inhibition. In: *All*

Days. SPE; 2002. doi:10.2118/74656-MS

79. Rice O, Hatch GB. Threshold Treatment of Municipal Water Supplies : Use of Sodium Hexametaphosphate. *Am Water Work Assoc*. 1939;31(7):1171-1185.

80. Rice O, Partridge EP. Threshold treatment: Elimination of Calcium Carbonate Deposits from Industrial Waters. *Ind Eng Chem*. 1939;31(1):58-63. doi:10.1021/ie50349a013

81. Yuan, M.D., Jamieson, E., and Paul Hammonds. Investigation of Scaling and Inhibition Mechanisms and the Influencing Factors in Static and Dynamic Inhibition Tests. Paper presented at the CORROSION 98, San Diego, California, March 1998.

82. Benton WJ, Collins IR, Grimsey IM, Parkinson GM, Rodger SA. Nucleation, growth and inhibition of barium sulfate-controlled modification with organic and inorganic additives. *Faraday Discuss*. 1993;95:281-297. doi:10.1039/FD9939500281

83. Chauhan K, Sharma P, Chauhan GS. Removal/Dissolution of Mineral Scale Deposits. In: *Mineral Scales and Deposits;* Amjad, Z., Demadis, K. D.; Elsevier 2015:701-720.

84. Mehta S, Shulman J, Dufour A. Scaling Problems in Home Care Applications. In: *Mineral Scales and Deposits;* Amjad, Z., Demadis, K. D.; Elsevier 2015:323-352.

85. Ketrane R, Saidani B, Gil O, Leleyter L, Baraud F. Efficiency of five scale inhibitors on calcium carbonate precipitation from hard water: Effect of temperature and concentration. *Desalination*. 2009;249(3):1397-1404. doi:10.1016/j.desal.2009.06.013

86. Irani RD, Callis CF. Calcium and magnesium sequestration by sodium and potassium polyphosphates. *J Am Oil Chem Soc*. 1962;39(3):156-159. doi:10.1007/BF02632750

87. Dawson DM. COLLOID-A-TRON: a non-chemical water treatment system. *Corros Prev Control*. 1990;37(3).

88. University of California. Maintenance of Microirrigation Systems; Lime (calcium carbonate). Accessed November 9, 2021. https://micromaintain.ucanr.edu/Solutions/know/Chemical_precipitation/Treatments_to_Minimize_Clogging_182/Lime_calcium_carbonate/

89. Cowan JC, Weintritt DJ. *Water-Formed Scale Deposits*. Gulf Publishing Company; 1976.

90. Wu Z, Davidson JH, Francis LF. Effect of water chemistry on calcium carbonate

deposition on metal and polymer surfaces. *J Colloid Interface Sci*. 2010;343(1):176-187. doi:10.1016/j.jcis.2009.11.031

91. Water Quality Association. Softened Water Benefits Study: Energy Savings and Detergent Savings. Water Quality Research Foundation. 2010.

92. Brazeau RH, Edwards M. A review of the sustainability of residential hot water infrastructure: Public health, environmental impacts, and consumer drivers. *J Green Build*. 2011;6(4):77-95. doi:10.3992/jgb.6.4.77

93. Devine C. Effects of Scale Reduction Technologies and Chemical Inhibitors on Calcium Precipitation in Premise Plumbing Systems. Ph.D. Dissertation. Virginia Polytechnic Institute and State University, Blacksburg, VA. 2021. http://hdl.handle.net/10919/112095

94. Devine C, Edwards M. Bench-Scale Prediction of Scaling in Water Heaters. 2022.

95. Thomas M, Hayden ACS, MacKenzie D. Reducing GHG emissions through efficient water heating technologies. *2006 IEEE EIC Clim Chang Technol Conf EICCCC 2006*. 2006;1-9. doi:10.1109/EICCCC.2006.277277

96. Rahman F. Calcium sulfate precipitation studies with scale inhibitors for reverse osmosis desalination. *Desalination*. 2013;319:79-84. doi:10.1016/j.desal.2013.03.027

97. Van Driessche AES, Stawski TM, Kellermeier M. Calcium sulfate precipitation pathways in natural and engineered environments. *Chem Geol*. 2019;530(August):119274. doi:10.1016/j.chemgeo.2019.119274

98. Roy S, Coyne JM, Novak JA, Edwards MA. Flow-induced failure mechanisms of copper pipe in potable water systems. *Corros Rev*. 2018;36(5):449-481. doi:10.1515/corrrev-2017-0120

99. Douterelo I, Dutilh BE, Calero C, Rosales E, Martin K, Husband S. Impact of phosphate dosing on the microbial ecology of drinking water distribution systems: Fieldwork studies in chlorinated networks. *Water Res*. 2020;187:116416. doi:10.1016/j.watres.2020.116416

100. Tang M, Schock MR, Buse HY, et al. Understanding Copper Pitting in Drinking Water Pipes. *Opflow*. 2021;47(8):20-22. doi:10.1002/opfl.1589

101. Edwards M, Rushing JC, Kvech S, Reiber S. Assessing copper pinhole leaks in residential

plumbing. *Water Sci Technol*. 2004;49(2):83-90. doi:10.2166/wst.2004.0094

102. Lytle DA, White CP. The effect of phosphate on the properties of copper drinking water pipes experiencing localized corrosion. *J Fail Anal Prev*. 2014;14(2):203-219. doi:10.1007/s11668-014-9786-6

103. Lattyak R. Non-Uniform Copper Corrosion in Potable Water: Theory and Practice. Masters Thesis, Virginia Tech, Blacksburg, VA, 2007. http://hdl.handle.net/10919/42820

104. Sarver E, Edwards M. Inhibition of copper pitting corrosion in aggressive potable waters. *Int J Corros*. 2012;2012. doi:10.1155/2012/857823

105. McNeill LS, Edwards M. Phosphate Inhibitors and Red Water in Stagnant Iron Pipes. *J Environ Eng*. 2000;126(12):1096-1102. doi:10.1061/(ASCE)0733-9372(2000)126:12(1096)

106. McNeill LS, Edwards M. Iron pipe corrosion in distribution systems. *J / Am Water Work Assoc*. 2001;93(7):88-100. doi:10.1002/j.1551-8833.2001.tb09246.x

107. Bradley TN. Evaluation of Zinc Orthophosphate to Control Lead Solder Corrosion in Waters With High Chloride to Sulfate Mass Ratio. Masters Thesis. Virginia Polytechnic Institute and State University, Blacksburg, VA. 2018. http://hdl.handle.net/10919/93931

108. Gregory R. Galvanic Corrosion of Lead Solder in Copper Pipework. *Water Environ J*. 1990;4(2):112-118. doi:10.1111/j.1747-6593.1990.tb01566.x

109. Oliphant RJ. Contamination of Potable Water by Corrosion of Tin-Lead Soldered Joints. Ph.D. Dissertation, University of Surrey, 1967.

110. Nguyen CK, Stone KR, Dudi A, Edwards M. Corrosive microenvironments at lead solder surfaces arising from galvanic corrosion with copper pipe. *Environ Sci Technol*. 2010;44(18):7076-7081. doi:10.1021/es1015185

111. Koudelka M, Sanchez J, Augustynski J. On the Nature of Surface Films Formed on Iron in Aggressive and Inhibiting Polyphosphate Solutions. *J Electrochem Soc*. 1982;129(6):1186. doi:10.1149/1.2124084

112. Lytle DA, Sarin P, Snoeyink VL. The effect of chloride and orthophosphate on the release of iron from a cast iron pipe section. *J Water Supply Res Technol - AQUA*.

2005;54(5):267-281. doi:10.2166/aqua.2005.0026

113. Mi Z, Zhang X, Wu H. Effects of Adding Phosphates on Iron Release Control in Drinking Water Pipelines. In: *ICPTT 2013*. American Society of Civil Engineers; 2013:1237-1250. doi:10.1061/9780784413142.129

114. Sarin P, Clement JA, Snoeyink VL, Kriven WM. Iron Release from corroded, unlined cast-iron pipe. *AWWA*. 2003;95(11). http://www.jstor.org/stable/41311260.

115. Tang M, Pieper K, Parks J, et al. The Relationship Between Discolored Water from Corrosion of Old Iron Pipe and Source Water Conditions. *Environ Eng Sci*. 2018;35(9):943-952. doi:10.1089/ees.2017.0435

116. Tavanpour N, Noshadi M, Tavanpour N. Scale Formation and Corrosion of Drinking Water Pipes: A Case Study of Drinking Water Distribution System of Shiraz City. *Mod Appl Sci*. 2016;10(3). doi:10.5539/mas.v10n3p166

117. Andrzejaczek BJ. Mechanism of Action of Acidified Sodium Phosphate Solution as a Corrosion Inhibitor of Iron in Tap Water. *Br Corros J*. 1979;14(3):176-178. doi:10.1179/000705979798275690

118. Maddison LA, Gagnon GA, Eisnor JD. Corrosion control strategies for the Halifax regional distribution system. *Can J Civ Eng*. 2001;28(2):305-313. doi:10.1139/l00-114

119. Facey RM, Smith DW. Soft, Low-Temperature Water-Distribution Corrosion: Yellowknife, NWT. *J Cold Reg Eng*. 1995;9(1):23-40. doi:10.1061/(ASCE)0887-381X(1995)9:1(23)

120. Lin CF, Benjamin MM. Dissolution Kinetics of Minerals in the Presence of Sorbing and Complexing Ligands. *Environ Sci Technol*. 1990;24(1):126-134. doi:10.1021/es00071a016

121. McNeill LS, Edwards M. Review of iron pipe corrosion in drinking water distribution systems. *J Awwa*. 2001;93(7):88-100.

122. Dartmann J, Sadlowsky B, Dorsch T, Johannsen K. Copper corrosion in drinking water systems - Effect of pH and phosphate-dosage. *Mater Corros*. 2010;61(3):189-198. doi:10.1002/maco.200905241

123. Schock MR, Sandvig AM. Long-term effects of orthophosphate treatment on copper concentration. *J / Am Water Work Assoc*. 2009;101(7):71-82. doi:10.1002/j.1551-8833.2009.tb09925.x

124. Cantor AF, Park JK, Vaiyavatjamai P. Effect of chlorine on corrosion in drinking water systems. *J / Am Water Work Assoc*. 2003;95(5):112-122. doi:10.1002/j.1551-8833.2003.tb10366.x

125. Edwards M, Hidmi L, Gladwell D. Phosphate inhibition of soluble copper corrosion by-product release. *Corros Sci*. 2002;44(5):1057-1071. doi:10.1016/S0010-938X(01)00112-3

126. Schock MR, Lytle DA, Clement JA. Effect of pH, DIC, orthophosphate and sulfate on drinking water cuprosolvency. National Risk Management Research Lab., Cincinnati, OH (United States); 1995 Jun 1.

127. Edwards M, Powers K, Hidmi L, Schock MR. The role of pipe ageing in copper corrosion by-product release. *Water Sci Technol Water Supply*. 2001;1(3):25-32. doi:10.2166/ws.2001.0050

128. Hidmi L, Edwards M. Role of temperature and pH in Cu(OH)2 solubility. *Environ Sci Technol*. 1999;33(15):2607-2610. doi:10.1021/es981121q

129. Lee JE, Lee HD, Kim GE. The effect of corrosion inhibitor on corrosion control of copper pipe and green water problem. *Environ Eng Res*. 2012;17(1):17-25. doi:10.4491/eer.2012.17.1.017

130. McNeill LS, Edwards M. Importance of Pb and Cu particulate species for corrosion control. *J Environ Eng*. 2004;130(2):136-144. doi:10.1061/(ASCE)0733-9372(2004)130:2(136)

131. Cantor AF, Denig-Chakroff D, Vela RR, Pfeinik MG, Lynch DL. Use of polyphosphate in corrosion control. *J / Am Water Work Assoc*. 2000;92(2):85-102. doi:10.1002/j.1551-8833.2000.tb08820.x

132. Dodrill DM, Edwards M. Corrosion control on the basis of utility experience. *J Am Water Works Assoc*. 1995;87(7):74-85. doi:10.1002/j.1551-8833.1995.tb06395.x

133. Lytle DA, Schock MR, Scheckel K. The inhibition of Pb(IV) oxide formation in chlorinated water by orthophosphate. *Environ Sci Technol*. 2009;43(17):6624-6631.

doi:10.1021/es900399m

134. Ng DQ, Strathmann TJ, Lin YP. Role of orthophosphate as a corrosion inhibitor in chloraminated solutions containing tetravalent lead corrosion product PbO2. *Environ Sci Technol*. 2012;46(20):11062-11069. doi:10.1021/es302220t

135. Trueman BF, Krkošek WH, Gagnon GA. Effects of ortho- and polyphosphates on lead speciation in drinking water. *Environ Sci Water Res Technol*. 2018;4(4):505-512. doi:10.1039/c7ew00521k

136. Wasserstrom LW, Miller SA, Triantafyllidou S, Desantis MK, Schock MR. Scale Formation Under Blended Phosphate Treatment for a Utility With Lead Pipes. *J Am Water Works Assoc*. 2017;109(11):E464-E478. doi:10.5942/jawwa.2017.109.0121

137. Xie Y. Dissolution, Formation, and Transformation of the Lead Corrosion Product PbO2: Rates and Mechanisms of Reactions that Control Lead Release in Drinking Water Distribution Systems. Ph.D. Dissertation. Washing University in St. Louis, St. Louis, MI. 2010. http://dx.doi.org/10.7936/K7736NZ4

138. Noel JD, Wang Y, Giammar DE. Effect of water chemistry on the dissolution rate ofthe lead corrosion product hydrocerussite. *Water Res*. 2014;54:237-246. doi:10.1016/j.watres.2014.02.004

139. Lytle DA, Formal C, Doré E, et al. Synthesis and characterization of stable lead (II) orthophosphate nanoparticle suspensions. *J Environ Sci Heal - Part A Toxic/Hazardous Subst Environ Eng*. 2020;55(13):1504-1512. doi:10.1080/10934529.2020.1810498

140. Doré E, Formal C, Muhlen C, et al. Effectiveness of point-of-use and pitcher filters at removing lead phosphate nanoparticles from drinking water. *Water Res*. 2021;201:0-11. doi:10.1016/j.watres.2021.117285

141. Lytle DA, Schock MR, Formal C, et al. Lead Particle Size Fractionation and Identification in Newark, New Jersey's Drinking Water. *Environ Sci Technol*. 2020;54(21):13672-13679. doi:10.1021/acs.est.0c03797

142. Pan W, Johnson ER, Giammar DE. Lead Phosphate Particles in Tap Water: Challenges for Point-of-Use Filters. *Environ Sci Technol Lett*. 2021;8(3):244-249. doi:10.1021/acs.estlett.1c00055

143. Purchase JM, Rouillier R, Pieper KJ, Edwards M. Understanding Failure Modes of NSF/ANSI 53 Lead-Certified Point-of-Use Pitcher and Faucet Filters. *Environ Sci Technol Lett*. 2021;8(2):155-160. doi:10.1021/acs.estlett.0c00709

144. Zhao J, Giammar DE, Pasteris JD, Dai C, Bae Y, Hu Y. Formation and Aggregation of Lead Phosphate Particles: Implications for Lead Immobilization in Water Supply Systems. *Environ Sci Technol*. 2018;52(21):12612-12623. doi:10.1021/acs.est.8b02788

145. Zhao J, Mowla M, Pan Z, et al. Lead phosphate deposition in porous media and implications for lead remediation. *Water Res*. 2022;214(February):118200. doi:10.1016/j.watres.2022.118200

146. Holm TR, Schock MR. Potential effects of polyphosphate products on lead solubility in plumbing systems. *J / Am Water Work Assoc*. 1991;83(7):76-82. doi:10.1002/j.1551-8833.1991.tb07182.x

147. Wang Z, Fu H, Zhang L, Song W, Chen J. Ligand-Promoted Photoreductive Dissolution of Goethite by Atmospheric Low-Molecular Dicarboxylates. *J Phys Chem A*. 2017;121(8):1647-1656. doi:10.1021/acs.jpca.6b09160

148. Edwards M, McNeill LS. Effect of phosphate inhibitors on lead release from pipes. *J / Am Water Work Assoc*. 2002;94(3):79-90. doi:10.1002/j.1551-8833.2002.tb09383.x

149. Locsin JA, Trueman BF, Doré E, Bleasdale-Pollowy A, Gagnon GA. Impacts of orthophosphate–polyphosphate blends on the dissolution and transformation of lead (II) carbonate. *Sci Rep*. 2022;12(1):17885. doi:10.1038/s41598-022-22683-2

150. Hubbe MA. Theory of detachment of colloidal particles from flat surfaces exposed to flow. *Colloids and Surfaces*. 1984;12(C):151-178. doi:10.1016/0166-6622(84)80096-7

151. Shen C, Wang L-P, Li B, Huang Y, Jin Y. Role of Surface Roughness in Chemical Detachment of Colloids Deposited at Primary Energy Minima. *Vadose Zo J*. 2012;11(1). doi:10.2136/vzj2011.0057

152. Sharma MM, Chamoun H, Sarma DSHSR, Schechter RS. Factors controlling the hydrodynamic detachment of particles from surfaces. *J Colloid Interface Sci*. 1992;149(1):121-134. doi:10.1016/0021-9797(92)90398-6

CHAPTER 3 : SEEING IS BELIEVING; COLOR, TURBIDITY, AND VISUAL OBSERVATIONS.

Christian Lytle and Marc Edwards

Discolored water is major cause of consumer complaints (AWWA, 2020). Discoloration can be caused by minerals, dirt, rust, scale, bubbles and dissolved chromophores such as natural organic matter, that can originate at any point of the journey from source water to the consumers' tap.

Consider iron and manganese as an exemplary cause of discoloration (Figure 3-1). Iron exceeded the 0.3 mg/L aesthetic-based Secondary Maximum Contaminant Level (SMCL) in 19% of 2100 domestic wells tested, whereas manganese surpassed the 0.05 mg/L SMCL in 21% of wells. (DeSimone et al., 2009). Dissolved Fe(II) and Mg(II) can oxidize and precipitate, eventually settling or resuspending as insoluble particles within the distribution system (Figure 3-1). The iron and manganese can also originate as contaminants from coagulant chemicals, as well as from corrosion of unlined ductile iron, steel, stainless steel and galvanized iron in mains, service lines, home plumbing and water tanks (e.g., Edwards et al., 1997; Schwartz, 2002). Many public and private systems choose to lessen the risk of visual aesthetic issues by removing sources of discoloration from their source water, minimizing metal release to water from pipes by corrosion control, dosing of phosphate sequestrants or flushing of pipes but this is not a requirement. Other public utilities leave the problems of discolored water to consumers, who can choose to tolerate the problems or treat the water with in-home devices such as filters (Figure 3-1).

Likewise, other sources of discoloration including magnesium hydroxide, calcium carbonate, magnesium silicate, calcium phosphate, aluminum phosphate, and iron phosphate all have a range of characteristic origins and often baffling patterns of occurrence in consumer homes. This makes detection and diagnosis of problems a challenge. Standardized color and turbidity measurements are objective, but in our experience, they do not always explain the range of subjective consumer visual observations of cloudy or discolored water. Here we highlight the

factors influencing how humans detect discoloration from dissolved or particulate material, and some of the strengths and limitations of objective measurements in quantifying discoloration.

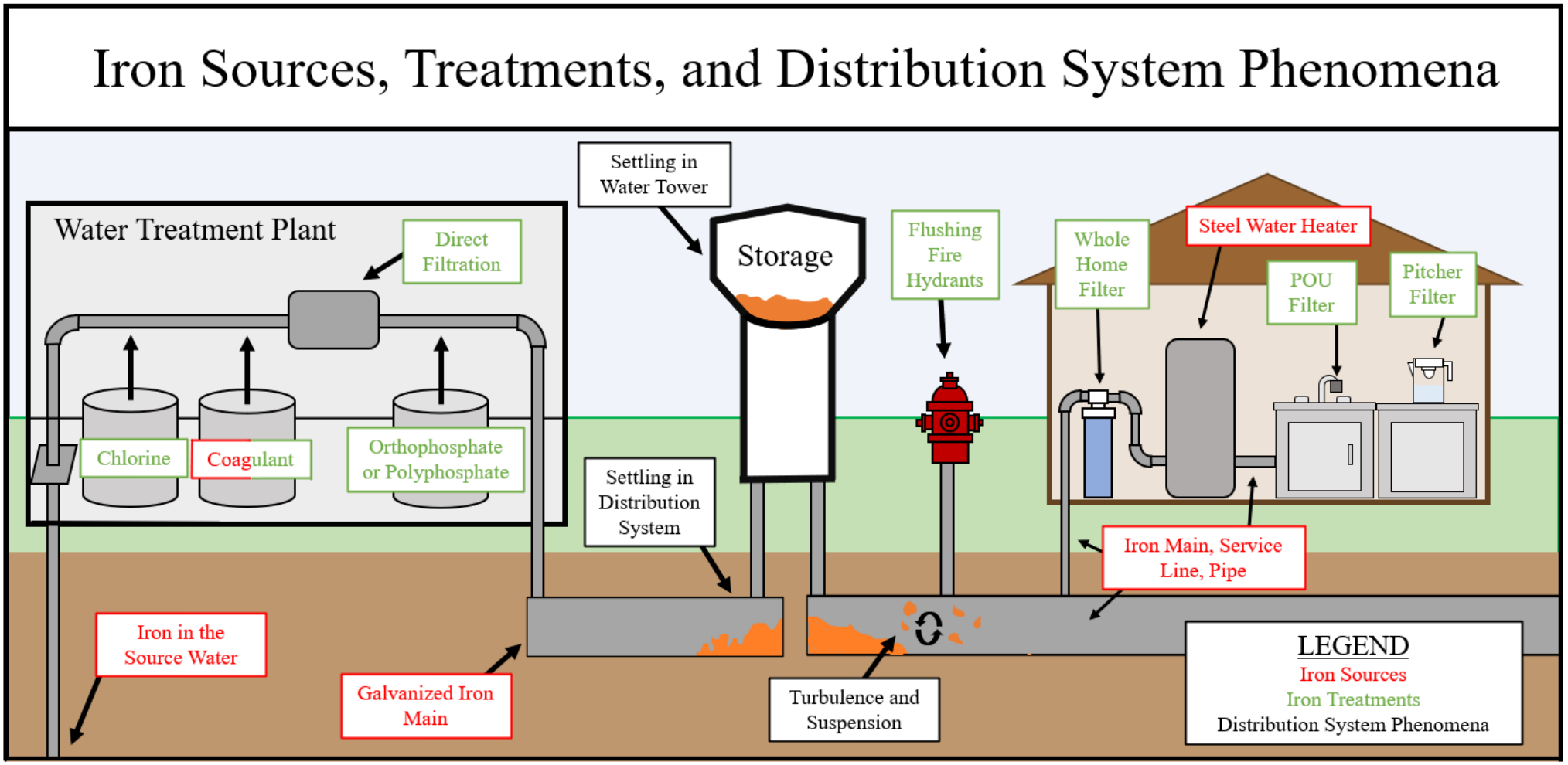

Figure 3-1. Sources of iron, treatments, and distribution phenomena. Different homes throughout the distribution system can have different levels of color and turbidity. Coagulation can be a treatment to assist removal of iron and manganese, but it can also occasionally be a source of Fe(II) and Mn(II) .

MEASURING CLOUDY AND DISCOLORED WATER

Objective Quantitative Measurements by Instrumentation.

Cloudy and discolored drinking water can be objectively measured using two different standard methods: color (i.e. Colorimetric-Platinum-Cobalt) (EPA-NERL, 1971) and turbidity (Figure 3-2). Turbidity has a health-based Maximum Contaminant Level (MCL) because it is a surrogate that tracks removal of disease-causing microbes. For systems using surface water, or groundwater influenced by surface water, the MCL is 1 NTU (and < 0.3 NTU in 95 percent of samples) if conventional or direct filtration is used and 5 NTU when any other type of filtration is used. Color has an SMCL of 15 Pt-Co (United States Environmental Protection Agency, 2022, 2024).

*Turbidity, measured in Nephelometric Turbidity Units (NTUs), is a measure of light scattering by reflection, refraction, and diffraction, which is often detected at a 90-degree angle from the incident light (*Figure 3-2

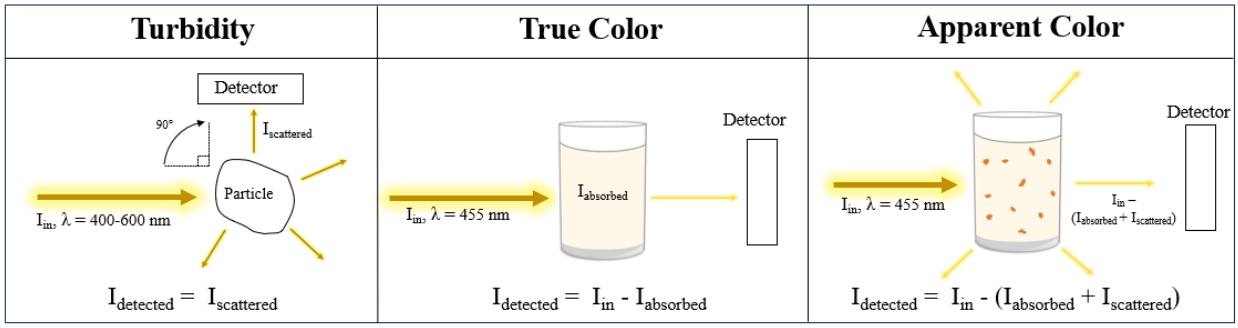

Figure *3-2*). The degree of light scattering is a function of particle concentration, size, shape, scattering angle, wavelength of light, and the difference in refractive index between the particle and medium (Huber & Frost, 1998).

Color, commonly measured on the Platinum-Cobalt (Pt-Co) scale at a wavelength of 455 nm corresponding to blue/violet light, is a measure of light absorption from dissolved species (true color), plus any light absorption from dissolved species, or light scattering and absorption from suspended species (also known as apparent color). If water is filtered before analysis the measurement is termed “true color.” Historically, color was measured by semiquantitative comparison to standardized Pt-Co solutions, but spectrophotometers are now used for more precise determination of color differences.

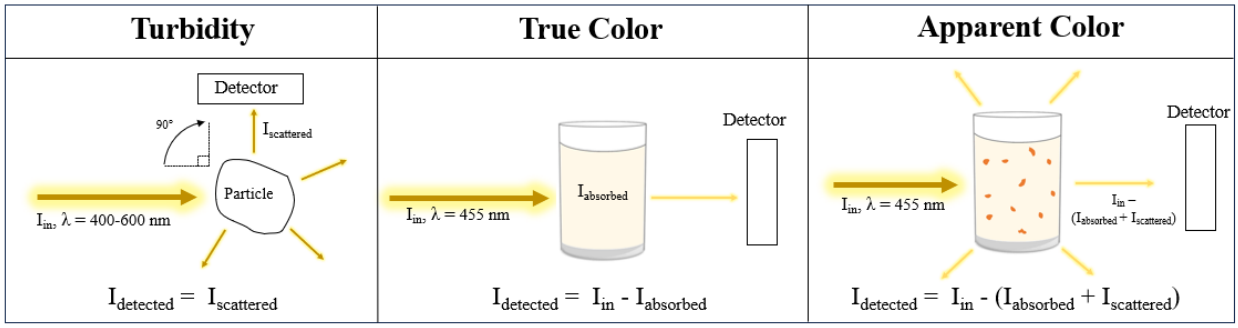

Figure 3-2. Diagram of turbidity, true color, and apparent color.

Light scattering of spherical particles of different sizes is described by Rayleigh, Mie, and geometric optic theory. Rayleigh scattering applies to particles between 2-75 nm in size which are smaller than the wavelength of the incident light (Kitchener et al., 2017). Mie scattering applies to particles between 20 nm -765 µm, which is in the range of the visible light wavelengths, whereas geometric optics describes particles > 200 µm, or larger than the size of visible light (Kitchener et al., 2017). In theory light scattering caused by a fixed mass of particles, increases with the diameter (d) cubed in the Rayleigh region, passes a maximum at a diameter of 0.3 µm, and

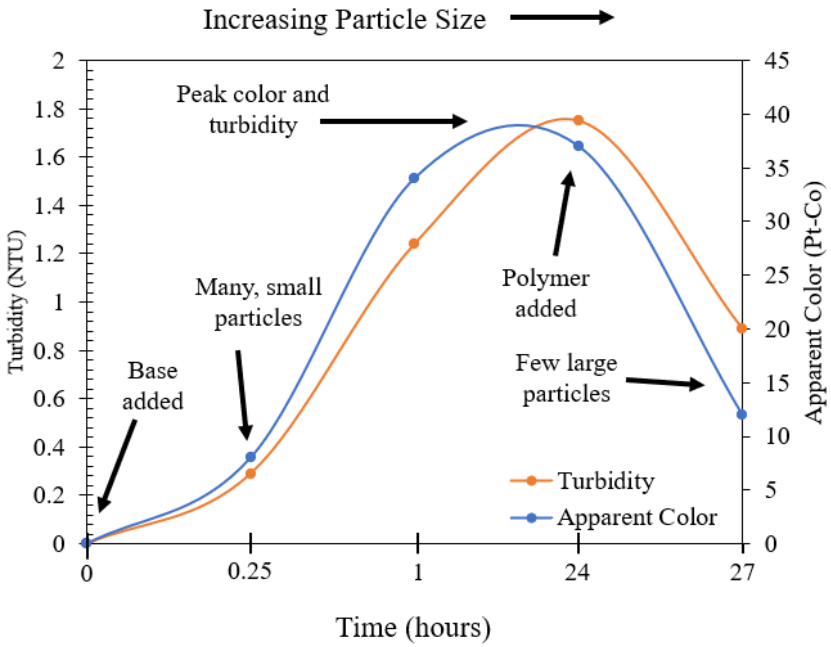

Figure 3-3. A lab test that began with addition of invisible 1 mg/L Fe^{3+} at low pH (< 3), then raising pH to allow precipitation and coagulation. A decline in turbidity and color only occurred after adding anionic polymer that created very large particles.

then decreases by 1/d as large particles become much fewer in number (Huber & Frost, 1998). The net result is that for a fixed mass of a contaminant, very small particles tend to be nearly invisible to the eye, while a few large particles are perceived as anomalies in water that appears visually clear, and the most intense discoloration occurs at intermediate particle sizes.

By adding 1 mg/L of invisible dissolved ferric iron at pH 3.0, and then raising pH to make measurements of rising turbidity and color after precipitation and coagulation, we recreated the expected rise in turbidity and color to a peak of about 1.75 NTU and 39 Pt-Co units (Figure 3-3). Using these fresh iron particles, we could only observe a peak in turbidity and color, after adding polymers that collected fine particles into very large agglomerates ≈1 mm diameter (Figure 3-3). In this particular experiment the objective measures of color and turbidity were well correlated with $R^2 = 0.9$, and the objective measures also agreed with what we subjectively observed by eye. That is not always the case.

Subjective Visual Observations by Human Eye.

Objective color and turbidity measurements are understandably emphasized in scientific research where precision and reproducibility are paramount, but these measures occasionally have little or no correlation to what consumers see by eye. Consequently, in Standard Methods (APHA, 2012), recording the subjective "appearance" of a water sample "by the unaided eye," occurs before any objective measurements of turbidity and color . It is relatively well understood that this can help in diagnosing consumer problems that can change dramatically during storage or transport to the laboratory. For instance, suspended milky white bubbles caused by depressurization of water supersaturated with gas, do not leave any trace that is detectable by objective measurements within seconds to minutes after collection. Conversely, dissolved invisible ferrous iron in a freshly collected water sample, can become disturbingly orange after collection due to oxidation, precipitation and coagulation. Very large particles in a sample can also settle before they are measured by an instrument, causing an objective measurement to falsely indicate there is no discoloration.

While color and turbidity measurements can give objective measures of light scattering and absorption, these measurements are also not always a reliable indicator of discoloration observed by the consumer. The human eye detects some combination of color and turbidity, that

vary dependent on lighting, background and viewing angle. This is another reason that utilizing only objective measures can be misleading when attempting to understand consumer concerns.

Consider an extreme comparison illustrated by drawings of actual laboratory suspensions prepared of fulvic acid, air bubbles, white calcium carbonate particles, and red iron particles (Figure 3-4). At a constant apparent color (~110 Pt-Co), each of these conditions produced noteworthy differences in turbidity measurements. At one extreme, despite being non-offensive or even considered pleasing to some consumers, effervescent air bubbles had the highest turbidity of 74 NTU. Conversely, fulvic acid at the same level of color, was offensively dark orange, despite having a nearly undetectable turbidity of 0.1 NTU. Similarly, relatively non-offensive white calcium carbonate particles, had more than 4 times the turbidity of relatively offensive fresh ferric particles. The point is that every particulate and dissolved species has its own unique size and color characteristics, causing it to be perceived differently by a consumer than the objective measure of either color or turbidity by instrumentation.

	No Scattering or Absorption	Complete Light Absorption	Complete Light Scattering	Light Scattering and Absorption	
	DI Water 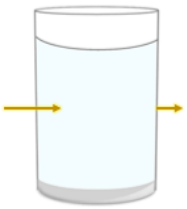	Fulvic Acid 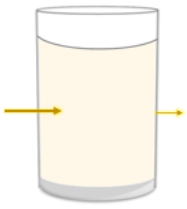	Air Bubbles 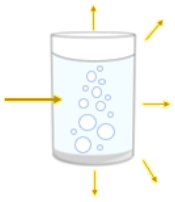	Calcium Carbonate Particles 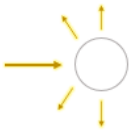	Fresh Ferric Particles 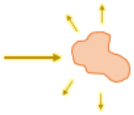
Visual	Clear	Discolored	Cloudy	Cloudy	Discolored + Cloudy
Apparent Color	0	110	109	109	110
Turbidity	0	0.1	74.0	12.28	2.97

Figure 3-4. Color and turbidity were measured for laboratory solutions of DI water, fulvic acid, air bubbles, calcium carbonate, and ferric iron. Despite identical apparent color, the turbidity varied greatly.

Impact of lighting conditions and viewing backgrounds.

The lighting conditions under which visual observations are taking place can contribute to the consumers perception of discoloration or cloudiness. In homes and other buildings, the light source can be from natural sunlight, or fluorescent, incandescent or LED artificial lighting of differing intensity and wavelength. The direction of the light source can be from ceiling lights above, or from floor or table lamps from a side, or light reflecting off the floor below, and combination of all three. Furthermore, the viewing background can greatly influence perception of discoloration. Extremes of all of these factors were explored to illustrate these concepts using suspensions at 50 Pt-Co units color which are 3.3 times the SMCL (Figure 3-5).

Light source from above with a white background

The presence of color (from dissolved or particulate species) was very evident in a bright laboratory with lighting coming from above in a room with a white background. In this situation the orange or brown discoloration of iron, manganese, and fulvic acid could be easily captured by both eye and photographs (Figure 3-5). However, white magnesium silicate and calcium carbonate particles at the exact same level of color, were not obvious or unpleasant looking, and might not trigger any consumer concern. For this condition the solutions ranked from worst to best in the order: iron ≈ fulvic acid > manganese > magnesium silicate ≈calcium carbonate.

Light source from below with a white background

With bright lighting from below in a darkened room, perceived color was less visible to the unaided eye, and the fulvic acid solution did not appear much more discolored than the DI water. But perceived haziness became much more apparent. As the observer is 90 degrees from the lighting source, perceived haziness seemed to be better correlated to the objective measurement of turbidity. The net result is that the suspensions of iron, manganese, magnesium silicate, and calcium carbonate became cloudy and less colored when compared to the situation with the general light source came from above (Figure 3-5). Similarly, the large number of particles in the calcium carbonate and magnesium silicate conditions became more visible. When each condition was ranked from worst to best under these conditions the ranking changed to magnesium silicate > iron ≈ calcium carbonate > manganese > fulvic acid.

Impact of an orange background

When the light source was from above, changing the background color to orange resulted in less detectable color from iron, manganese, and fulvic acid due to an expected chameleon effect. Somewhat surprisingly, it was also difficult to see the white particles, and only the magnesium silicate condition was observable by eye. Shifting the light source from above to below with the orange background, increased the haziness. The ranking of the worst-looking conditions followed the same trend as with the white background when the light was from below.

Impact of a black background

It was expected that a black background would tend to mask the darker particles and enhance the visibility of the whiter particles. Instead, if the light came from below, the black background maximized perception of color and haziness, although it did change the rank order from the situation with a white background. From cloudiest to clearest the ranked was: magnesium silicate > iron > calcium carbonate ≈ manganese > fulvic acid.

Color and turbidity

The measured apparent color for each condition was constant at about 50 Pt-Co, but as mentioned previously the measured turbidity varied markedly (Figure 3-5, column 1). Calcium carbonate (5.55 NTU) and magnesium silicate (8.03 NTU) had between 3.75X – 6.7X higher turbidity measurements than iron (1.2 NTU) and manganese (1.48 NTU) despite minimal visual discoloration or cloudiness. Therefore, visual observations may be more important considerations than color and/or turbidity, when determining if water is discolored or cloudy.

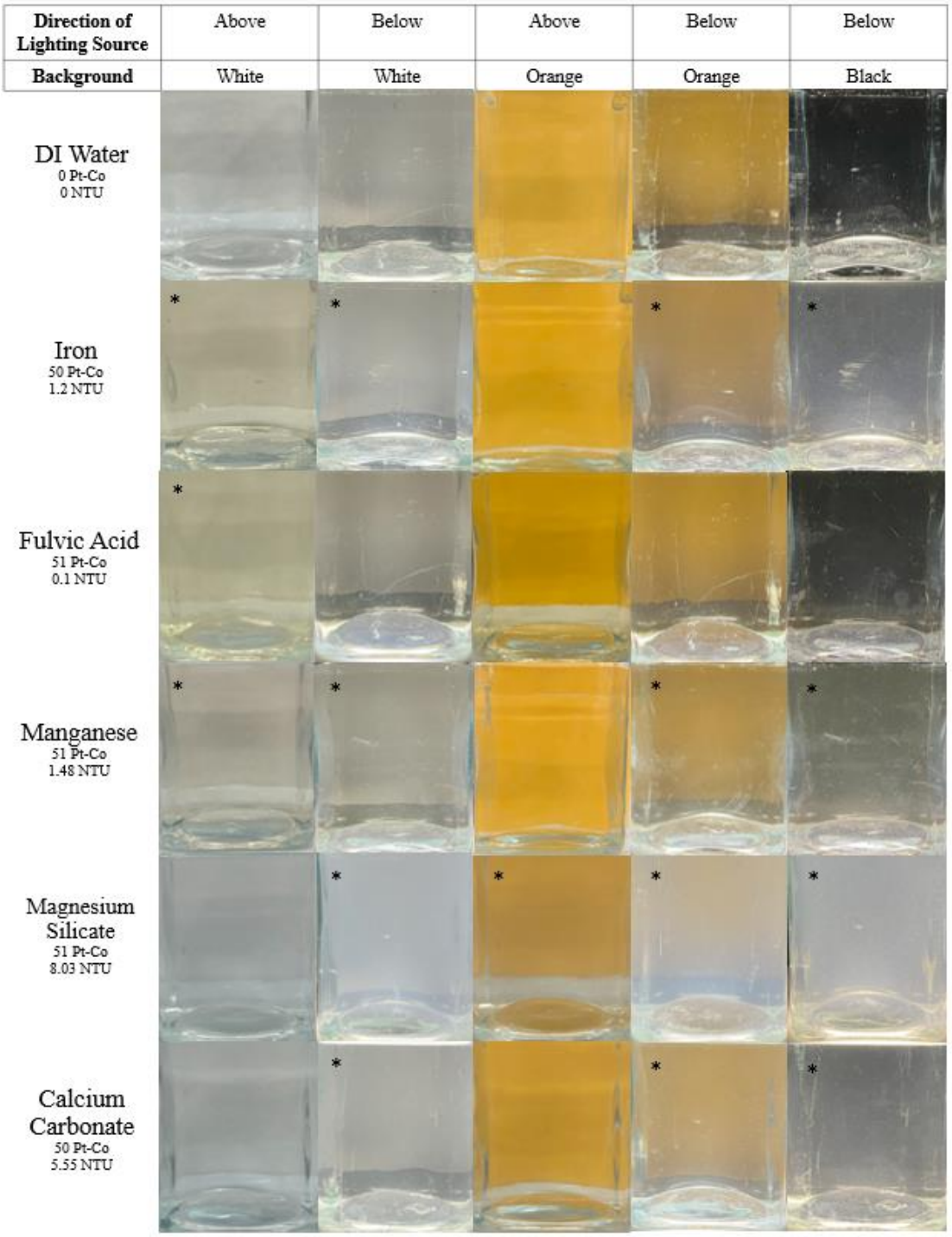

Figure 3-5. Impact of particulate or dissolved species, background color, and lighting type/direction on visual discoloration and cloudiness. A color of 50 Pt-Co was chosen as it is about 3.3X more than the 15 Pt-Co SMCL. Those marked with a * were easily visible by eye compared to the control DI water condition.

References

1. American public health association, American water works association, & Water environment federation (Eds.). (2012). *Standard methods for the examination of water and wastewater* (22nd ed). American public health association.

2. AWWA. (2020). *Public Perceptions of Tap Water*.

3. DeSimone, L. A., Hamilton, P. A., & Gilliom, R. J. (2009). Quality of water from domestic wells in principal aquifers of the United States, 1991–2004—Overview of major findings. In *Water: Vol. Circular 1*.

4. Edwards, M., Courtney, B., Heppler, P. S., & Hernandez, M. (1997). Beneficial Discharge of Iron Coagulation Sludge to Sewers. *Journal of Environmental Engineering*, *123*(10), 1027–1032. https://doi.org/10.1061/(ASCE)0733-9372(1997)123:10(1027)

5. EPA-NERL. (1971). Method #110.2: Color (Colorimetric-Platinum-Cobalt). In *Methods*.

6. Huber, E., & Frost, M. (1998). Light scattering by small particles. *Journal of Water Supply: Research and Technology - AQUA*, *47*(2), 87–94. https://doi.org/10.1046/j.1365-2087.1998.00086.x

7. Kitchener, B. G. B., Wainwright, J., & Parsons, A. J. (2017). A review of the principles of turbidity measurement. *Progress in Physical Geography*, *41*(5), 620–642. https://doi.org/10.1177/0309133317726540

8. Schwartz, M. (2002). *Encyclopedia of Materials, Parts and Finishes*. CRC Press. https://doi.org/10.1201/9781420017168

9. United States Environmental Protection Agency. (2022). *Secondary Drinking Water Standards: Guidance for Nuisance Chemicals*. https://www.epa.gov/sdwa/secondary-drinking-water-standards-guidance-nuisance-chemicals

10. United States Environmental Protection Agency. (2024). *National Primary Drinking Water Regulations*. https://www.epa.gov/ground-water-and-drinking-water/national-primary-drinking-water-regulations#three

CHAPTER 4 : A MECHANISTIC STUDY OF IRON SEQUESTRATION BY PHOSPHATES

Christian Lytle and Marc Edwards

Abstract

Iron sequestration by phosphate was examined from the perspective of mechanisms, water chemistry impacts, and limitations to its use. Phosphates did slow Fe^{2+} oxidation above about pH 7-8, but some combination of ferric complexation and colloid stabilization caused iron to remain invisible. Orthophosphate was a weak sequestrant, but at low pH and hardness it could be effective. Increased phosphate chain length, phosphate concentration, and silica concentration caused more effective sequestration, whereas calcium, magnesium, and increased pH could make it ineffective. In conditions dosed with polyphosphate, the % iron less than 10 kilodaltons in size decreased linearly by about 10% for every 100 mg/L increase in $CaCO_3$. Furthermore, up to 4X more tripolyphosphate was needed to effectively sequester iron at pH 9 versus pH 7. Contrary to some guidelines, above 1 mg/L of iron could sometimes be sequestered effectively at high doses of polyphosphate, but at some point higher chemical costs or precipitation of calcium phosphates or iron phosphates could be limiting.

Introduction

Elevated iron (Fe) is a serious concern for consumers in many water systems across the United States. There is no health-based Environmental Protection Agency (EPA) maximum contaminant level (MCL) for iron, but the EPA has set a secondary maximum contaminant level (SMCL) of 0.3 mg/L in recognition of aesthetic problems of taste, odor, and color and staining (US EPA, 2015). The SMCL is not enforceable and iron concentrations in potable water can be 10 mg/L or more in extreme cases (*Iron in Drinking Water*, n.d.). Iron can originate from the source water, coagulant carryover, or from corrosion of unlined iron water mains.

Community water systems deal with iron problems using a wide variety of approaches. Some systems decide to put the onus for iron control on homeowners, who can install filters to treat all or part of their home water supply. Other systems choose to eliminate all aesthetic concerns from iron in the source water, by removing the iron through treatment (i.e. oxidation/filtration) at the water source. Although it is usually more cost effective than installing treatment systems in every consumer home, such centralized treatment can be expensive. It was estimated that a ferrous iron removal plant serving 200 residents could cost upwards of $500,000

(AmeriWest Water Services Inc, n.d.). Removing iron from the source water does not stop problems arising from corrosion of water mains.

Sequestration is a chemical method of reducing iron aesthetic problems, from all sources of iron, at costs that are sometimes orders of magnitude lower than iron removal. A chemical such as polyphosphate, dosed to water to achieve this objective, is termed a sequestrant. Sequestration reduces human perception of visual discoloration, which is a complex function of light absorption (i.e, color), light scattering (i.e., turbidity), lighting and other factors. The intensity of color and turbidity is reduced as the amount and size of iron particles decrease. For instance, dissolved iron has neither color nor turbidity and is invisible to the eye. Light scattering intensity also decreases with particle diameter cubed (d^3) up to about 0.3 μm (Huber & Frost, 1998). Effective sequestration is achieved by maintaining iron as soluble ferrous, soluble ferric, or very small particles.

Phosphates can reduce the concentration of larger iron particles through four possible mechanisms including: 1) complexation of soluble Fe^{2+} to prevent its oxidation to relatively insoluble Fe^{3+}, 2) complexation of insoluble Fe^{3+} to inhibit precipitation of $Fe(OH)_3$ particles, 3) stabilizing $Fe(OH)_3$ or other particles by creating a strong negative surface charge that prevents agglomeration into larger particles (i.e. dispersion), and 4) destroying large particles by dissolution or de-agglomeration (Lytle & Edwards, 2023a). Prior research has not elucidated the importance of each step as a function of water chemistry or the type of phosphate.

Orthophosphate (PO_4^{-3}) is the simplest and least expensive form of phosphate. Longer chains of two or more phosphate units are termed polyphosphates. Increasing the chain length results in a more negatively charged molecule, that may form stronger complexes with dissolved metals and surfaces (Van Wazer & Callis, 1958), albeit with a possible reduction in the maximum binding capacity (D. A. Lytle & Snoeyink, 2002). Polyphosphates of known chain length include pyrophosphate ($P_2O_7^{-4}$), tripolyphosphate ($P_3O_7^{-5}$), hexametaphosphate ($P_6O_{18}^{-6}$), but in water treatment they are almost always a mixture of much longer chained polyphosphates. Polyphosphates also hydrolyze to smaller chains and orthophosphate over time (Holm & Edwards, 2003) through a process known as reversion. Hence, polyphosphates are almost infinitely variable chemically, even if they tend to have similar practical effects.

Source water composition is another possible factor influencing the successful sequestration of iron. Water quality parameters known to impact iron sequestration include

calcium (Ca) and magnesium (Mg) (Klueh & Robinson, 1988; C. J. Lytle & Edwards, 2023a, 2023b; Rashchi & Finch, 2000; Van Wazer & Callis, 1958; Volpe, 2012), pH (Irani & Morgenthaler, 1963; D. A. Lytle & Snoeyink, 2002; Robinson et al., 1990), chlorine (Klueh & Robinson, 1988; Robinson et al., 1990; Volpe, 2012), ionic strength (Bailey et al., 2002; Zeta-Meter, 1993), and silica (Davis et al., 2002; Robinson et al., 1992). The magnitude of the impact of these parameters on sequestration is not well understood.

Most utilities presently use trial-and-error methods to optimize dosing, or they rely on dosing recommendations from private chemical vendors. Underdosing can leave consumers more vulnerable to iron aesthetic concerns, whereas overdosing of polyphosphates is costly, and there is fear it can sometimes increase levels of lead and copper in water (Edwards & McNeill, 2002; Holm & Schock, 1991; Locsin et al., 2022). The use of polyphosphates for sequestration is viewed negatively by many, due to these concerns about higher lead and copper release, even though only a hand-full of studies have documented such problems (C. J. Lytle & Edwards, 2023a).

One recent 2023 study (Lytle & Edwards, 2023b) attempted to empirically characterize the effect of source water on the minimum dose of polyphosphate required to effectively sequester iron and/or manganese in nine groundwater sources. The optimal polyphosphate dose was approximately equal to 58.5[Fe] + 59.7[Mn] + 0.041[Ca + Mg] + 0.4669 (unit mM) for one proprietary polyphosphate chemical and similar trends were observed for another. It is unclear how accurate and representative such equations would be in predicting optimal dosing in a wider range of waters, or whether such linear relationships have a mechanistic chemical basis.

These important gaps in understanding are concerning because polyphosphate is reportedly used at more than 30 % of public water utilities (Arnold et al., 2020; Dodrill & Edwards, 1995). Many utilities are required to reconsider optimization of phosphate dosing as a result of the 2024 revised Lead and Copper Rule. Here we address this knowledge gap for phosphates by 1) evaluating the mechanisms of iron sequestration, 2) demonstrating the impact of water quality and phosphate type on the effectiveness of iron sequestration, and 3) identifying important limitations on sequestration for controlling iron aesthetic problems.

Experimental/Methods

Chemicals.

All stock solutions were prepared using laboratory-grade chemicals dissolved in deionized (DI) water. All stock solutions were stored in the dark at 6°C and replaced periodically. Ferrous sulfate solutions in 2% sulfuric acid were prepared weekly. Calcium chloride and magnesium chloride stock solutions were prepared at pH < 4 and replaced every few weeks. Sodium metasilicate pentahydrate, sodium hypochlorite, and sodium chloride were prepared just prior to the experiment. Fresh polyphosphate solutions including sodium hexametaphosphate crystals ($Na_{n+2}P_nO_{3n+1}$ where $n \approx 6$, Sigma-Aldrich), sodium pyrophosphate decahydrate ($P_2O_7 \bullet 10H_2O \bullet 4Na$, Acros Organics), and sodium tripolyphosphate ($Na_5O_{10}P_3$, Sigma Aldrich) were made from dry chemicals every other day while sodium orthophosphate (Na_2HPO_4, Fisher Scientific) stock solutions were prepared every few weeks.

Simulated Sequestration Tests.

A simulated sequestration test was used to determine the impact of phosphate type and other water quality parameters on iron particle size and visual discoloration. One half liter of DI water in Nalgene bottles (or a glass flask at elevated temperatures) was dosed with 10^{-3} M sodium bicarbonate, a target dose of phosphate and other chemicals as specified in text. When observing the effect of divalent cations (Ca^{+2}, Mg^{+2}), a constant ionic strength of 0.012 M was maintained by appropriately adjusting the amount of sodium chloride (NaCl) dosed.

The experiment began by dosing soluble Fe^{+2} dropwise in 20 seconds (from ferrous sulphate) while the target water was stirred with a 10 cm Teflon coated magnetic bar at 100 rpm. pH was adjusted to the target by dosing 0.5 M sodium hydroxide dropwise within 2 minutes. Subjective and objective measures of discoloration were made during the experiment.

Apparent color (hereafter referred to as 'color') was objectively determined using a HACH DR3900 spectrophotometer using the Platinum-Cobalt Standard Method (HACH Method 8025) (Hach, 2014). Turbidity was objectively measured using a LaMotte 2020we turbidity meter with a wavelength range of 400-600 nm. During the experiments it became obvious that neither color nor turbidity was completely effective in characterizing discoloration as subjectively detected by the eyes of the first author. Thus, each sample was also visually evaluated, after placing samples in clear 500 ml glass flasks for comparison to filtered deionized (DI) water under bright laboratory fluorescent lighting conditions with a white background.

Samples that were indistinguishable from DI water were classified as "visually clear" and deemed to have been successfully sequestered, whereas those exhibiting color or particles detectable by the human eye were classified as "visually discolored."

Apparent Particle Size Characterization

An attempt was made to create operational particle size distributions using two filters of different sizes: A 10 kDa (10K) NMWL Ultracel regenerated cellulose ultrafilter with an Amicon® stirred cell (pressurized to 30 psi using nitrogen gas), and a 0.45 μm nylon syringe filter.

Ferrous Iron

Ferrous iron levels were determined using the 1,10-Phenanthroline Method, as measured on a HACH DR3900 (HACH Method 8146) (Hach, 2019).

Other Analytes.

Total metal concentrations were determined using an Inductively Coupled Plasma Mass Spectrometer (ICP-MS), following Method 3030 D and 3125 B. Prior to analysis, samples underwent acidification and digestion for a minimum of 24 hours in 2% nitric acid. On a HACH DR3900, orthophosphate concentrations were measured using the USEPA PhosVer 3® (Ascorbic Acid) Method (HACH Method 8048) (Hach, 2017), and chlorine levels were assessed using the USEPA DPD Method (HACH Method 8167) (Hach, 2022). The pH was measured using a Fisher Scientific Accumet glass AgCl pH electrode. Calibration of the pH probe was performed once daily using pH 4, 7, and 10 standard calibration solutions.

Zeta Potential

Zeta potential was measured using a Zeta Meter 3.0. For each measurement, about 25 mL of sample was injected in the electrophoresis cell using disposable pipette tips. After the measurement was taken, the electrophoresis cell was rinsed 3 times using DI water.

Statistical Methods

Statistical comparisons between groups of samples were compared using two-tailed paired T-tests as indicated in the results sections. Linear best fit equations were determined in Excel while an exponential trend was fit using Solver fit in Figure 4-6.

Results and Discussion

A sequence of experiments and measurements was conducted to elucidate how the presence of orthophosphate and polyphosphate can hinder each of the steps leading to visible particle formation in waters with ferrous iron or ferric iron. Thereafter, the influence of water chemistry on the effectiveness of sequestration was examined, along with some novel discoveries of situations when phosphate (orthophosphate and polyphosphates) dosing can create discoloration. Hereafter, pyrophosphate is referred to as "pyro," tripolyphosphate as TPP, and hexametaphosphate as HMP. All doses of these phosphates are reported in mg/L as P.

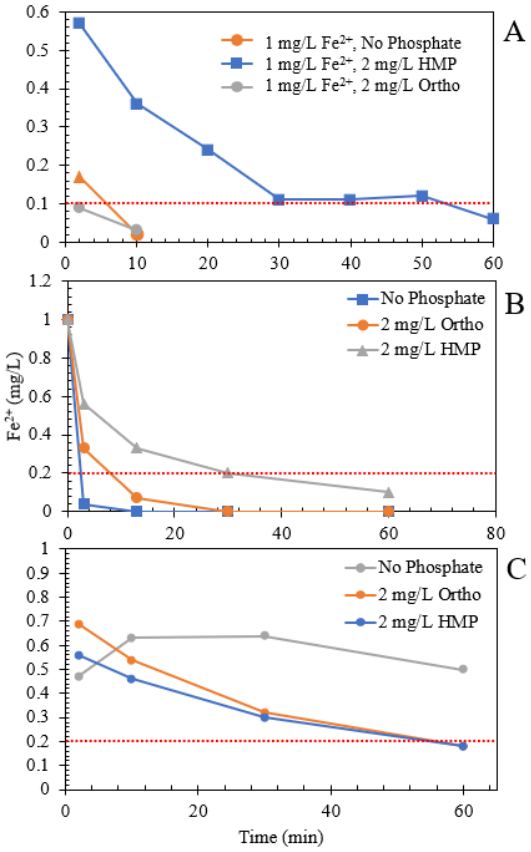

Figure 4-1. A) Polyphosphate decreases the rate of iron oxidation from Fe^{2+} to Fe^{3+} at pH 7, B) Polyphosphate and orthophosphate decrease the rate of iron oxidation from Fe^{2+} to Fe^{3+} at pH 8, and C) at pH 6.5, HMP and orthophosphate resulted in quicker oxidation. Red-dashed lines denote 80 or 90% oxidation.

Mechanisms of Sequestration

Step 1: Effect of Phosphate on Ferrous Oxidation

In oxygenated water at pH 7, 90% of 1 mg/L of initial Fe^{+2} was oxidized about 5 times (5X) more slowly when dosed with 2 mg/L HMP compared to a control without phosphate (i.e., 53 vs. 6 minutes in Figure 4-1A). However, with 2 mg/L orthophosphate, 0.1 mg/L Fe^{+2} was achieved in less than 3 minutes (Figure 4-1A), suggesting that orthophosphate may catalyze iron oxidation. The addition of 50 or 200 mg/L calcium had very little effect on ferrous oxidation rates in the presence of HMP (Figure A *1*).

HMP had a larger effect at pH 8, where 90% Fe^{+2} oxidation was achieved at least 20X slower with HMP compared to the control condition (60 vs < 3 minutes). At pH 8, orthophosphate slowed the oxidation rate by about 4X (12 vs < 3 minutes) (Figure 4-1B).

The unexpected increase in ferrous oxidation rates observed for orthophosphate at pH 7 prompted an additional experiment at pH 6.5. At this pH both orthophosphate and HMP increased ferrous oxidation relative to the control (Figure 4-1C). Another experiment confirmed the catalytic effect of HMP on ferric oxidation at pH 6.5 with 3 mg/L ferrous when dosed with 1, 3, and 10 mg/L of HMP (Figure A *2*). While there was faster oxidation in the presence of HMP, there was not a strong dependency on phosphate dose. For instance, after 1 hour, 70% of the Fe^{2+} was oxidized in the presence of 1 mg/L HMP compared to 77% at 10 mg/L. Catalysis of ferrous oxidation has previously been reported for orthophosphate at pH 6.6 - 7.1 (Mitra & Matthews, 1985), HMP below pH 7.2, and for pyro below pH 7.5 (D. A. Lytle, 2005).

Overall, these results confirm that phosphates can sometimes slow the rate of ferrous iron oxidation, using HMP above about pH 7 and orthophosphate above about pH 8. At lower pHs phosphates catalyze ferrous oxidation. But from a practical perspective, reducing Fe^{+2} oxidation rates from a few minutes to about an hour will have little effect on formation of color in water distribution systems, given that water transit times to homes are usually days to weeks (also see "Practical Implications of Sequestration Mechanisms on Visual Discoloration" in the Supplemental Information). Thus, Step 1, the inhibition of ferrous oxidation, is relatively unimportant to effective sequestration.

Combined Step 1+2: Effect of Phosphate on Fe^{2+} oxidation and precipitation of Fe^{3+}

Our plan to operationally monitor the formation of an iron precipitate during the above experiments was complicated by results of a control experiment. Whereas virtually 100% orthophosphate or TPP passed through the 10K ultrafilter (UF) membrane at pH 7 as expected, (Figure 4-2A), about 66% of 2 mg/L HMP was rejected by this membrane even when

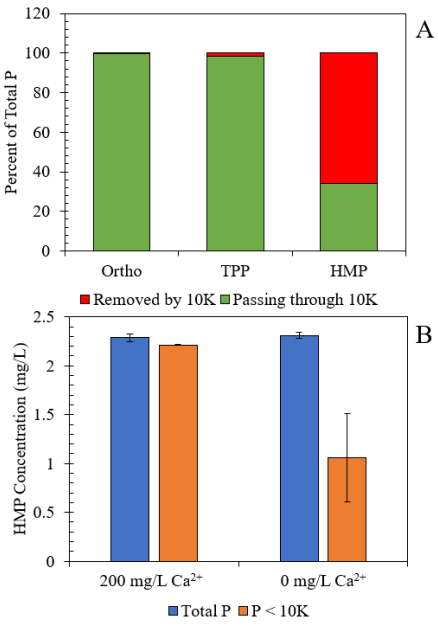

Figure 4-2. A) Nearly 100% of the 2 mg/L Orthophosphate and TPP passed through a 10K ultrafilter at pH 7, while 66% of the HMP was rejected. B) Almost all the HMP passed through the 10K filter when dosed with 200 mg/L $CaCO_3$.

no iron or calcium was present. Since it is believed that HMP is soluble, the rejection by the membrane is presumably by size or charge exclusion. Supporting this hypothesis, when 200 mg/L calcium as $CaCO_3$ was added to reduce the negative charge on HMP and its size (i.e., apparent molecular weight), there was no statistical rejection of the HMP ($p > 0.05$, two-tailed paired t-test on filter influent and effluent; Figure 4-2B). Likewise, dosing 1 mg/L of Fe^{2+} to a solution of 1.5 mg/L HMP at pH 7, increased the phosphate passing through a 10K filter from 0.77 to 1.12 mg/L (Figure A 4**Error! Reference source not found.**). On the basis of these results, rejection of iron by a 10K membrane in the presence of HMP, is not operational proof of insoluble iron, since it might result from formation of soluble polyphosphate complexes which are rejected by the membrane. Solutions with soluble ortho, pyro, and TPP were not rejected by the 10K filter, and in those cases, the traditional operational definition of 'dissolved' Fe^{2+} and Fe^{3+} by passage through this filter might be valid.

Both Pyro and TPP at 2 mg/L were able to maintain >80% of the dosed 1 mg/L Fe^{+2} as 'dissolved' or < 10K size, compared to 0% with no phosphates (Figure 4-3A, 3B, 3C). Orthophosphate was not able to maintain iron at below 10K in size to the extent of pyro and TPP, as evidenced by less than 8% of the 1 mg/L iron passing the 10K filter size (Figure 4-3A) even at a very high dose of 4 mg/L orthophosphate (Figure A *5*). Counterintuitively, the larger HMP, had more larger particles > 10K (Figure 4-3D), than did the pyro and TPP, and this may be an artifact of HMP rejection by the 10K membrane as mentioned earlier.

Combined Steps 1, 2, and 3: Formation of Visible Particles

Even when most iron particles could not be maintained at < 10K in size, phosphates still prevented formation of visible particles compared to conditions with no phosphates. Additions of as little as 0.1 ortho, TPP, pyro, and HMP resulted in a > 90% increase in particles passing through the 0.45 µm filter compared to the control (Figure 4-3A-D) although a faint orange color was still visible in all cases. Increasing the phosphate concentrations to 0.5 mg/L eliminated visual discoloration in all but the orthophosphate condition, despite more than 80% of the iron present at > 10K in size. At 2 mg/L visual color was eliminated even with ortho.

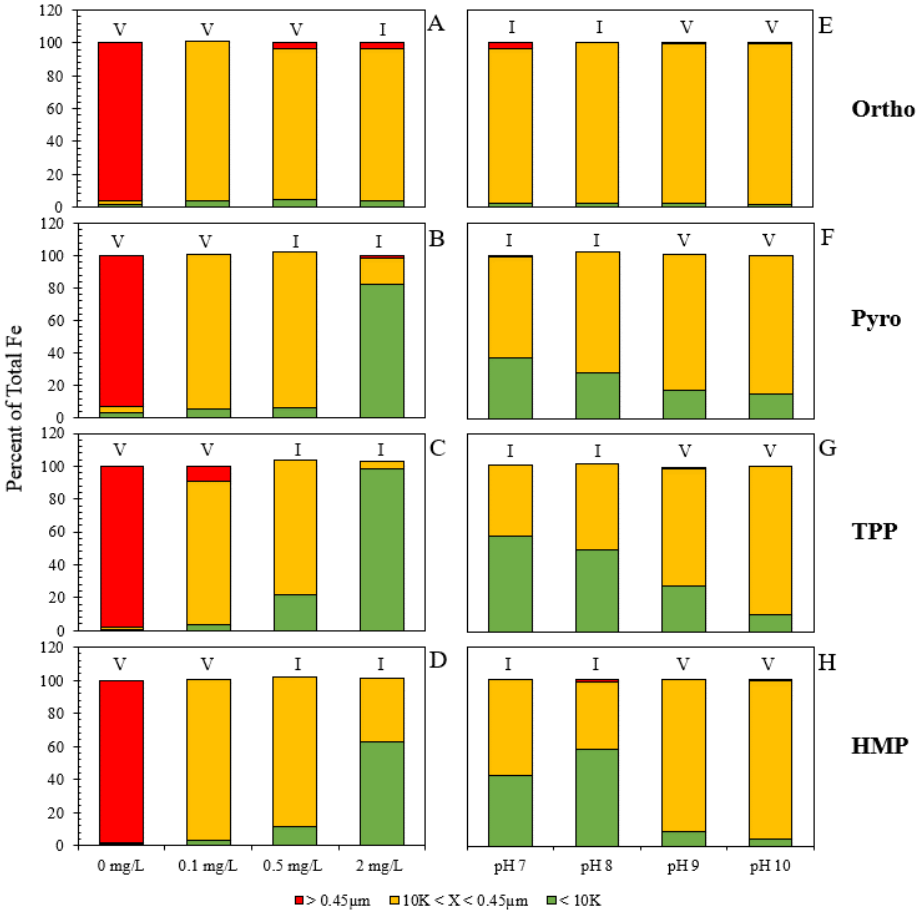

Figure 4-3. Increasing phosphate concentration and chain length reduced particle size of 1 mg/L iron (Left), and increasing pH resulted in increased iron between 10K and 0.45µm in size. A 'V' denotes visible iron and an 'I' denotes invisible iron.

Increasing the pH tended to produce a larger quantity of iron particles between 10K and 0.45 µm in size. At pH 7, the presence of 1 mg/L of ortho, pyro, TPP, or HMP resulted in visually clear water. But all of the polyphosphate conditions maintained a portion of iron particles < 10K in size whereas orthophosphate particles were larger (Figure 4-3E-H). The percent of iron < 10K in size decreased roughly linearly with each increment of higher pH for TPP and pyro. All conditions at pH 9 and 10 had visual discoloration.

If the TPP concentration was increased to 2 mg/L, the water was visually clear at pH 9, but not at pH 10 (Figure A 6). Compared to results of Figure 4-3G, at least four times more TPP is required to maintain visually clear water at pH 9 compared to pH 7 (0.5 mg/L compared to 2 mg/L).

Overall, while orthophosphate is not commonly considered a sequestrant, this work confirmed results of Lytle (2002) that it nonetheless behaves as one in some conditions (D. A. Lytle & Snoeyink, 2002). The effectiveness of phosphate sequestration in prevention of visible color always increased in the order orthophosphate ≤ pyro ≤ TPP ≤ HMP.

Effect of Phosphate, pH, and Calcium on Zeta Potential

It was not possible to measure zeta potential for most suspensions in the preceding section because the particles present were too small to track with an optical microscope. To explore the mechanistic basis for trends that were likely present in the preceding experiment, the effects of orthophosphate, polyphosphate, calcium, and pH on zeta potential were re-examined. In this case the experiment was conducted by titrating 10 mg/L ferric iron to various waters containing up to 2 times more phosphate, which always created particles detectable in the zeta-meter.

At pH 7, increasing the concentration of orthophosphate or HMP, at a constant iron concentration decreased the zeta potential from slightly positive to highly negative. HMP always resulted in lower zeta potential measurements compared to an equivalent dose of orthophosphate (Figure 4-4A). Importantly, both orthophosphate and HMP could decrease particle zeta potential to below the critical level of about -20 mV that is generally needed to stabilize very small particles. This result is consistent with the orthophosphate and polyphosphate suspensions at pH 7, that had virtually 100% of particles in the range of 10K to 0.45 μm, but were still invisible (Figure 4-3A-D, refer to conditions at 0.5 mg/L polyphosphate and 2 mg/L ortho).

Without phosphates, the zeta potential for ferric particles was ±15 mV between pH 7-9 (Figure 4-4B). Dosing an excess of HMP and orthophosphate (2 mg/L P per 1 mg/L Fe) again decreased the zeta potentials (< -25 mV) to a point sufficient to stabilize particles.

Nearly all of the zeta potential results are consistent with expectations and trends in data of the preceding section. But one experimental result from Figure 4-4A and Figure 4-4B, was inconsistent with trends based on trends in zeta potential. At pH 9 in the presence of orthophosphate and HMP, particles became visible and larger, whereas they were invisible at pH 7 and 8 (Figure 4-3E, 3H). The corresponding expectation was that the zeta potential for pH 9

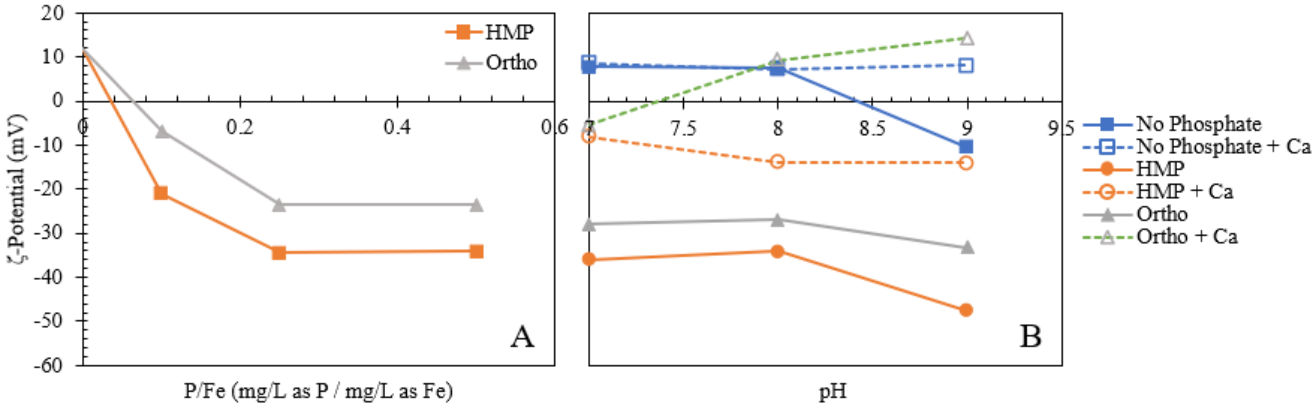

Figure 4-4. A) Increasing the concentration of orthophosphate and HMP resulted in more negative zeta potentials of ferric solids over a 1-day period (10 mg/L Fe^{3+}, 0, 2, 5, 10 mg/L P), and B) the addition of 200 mg/L $CaCO_3$ resulted in more neutral zeta potentials (after 10 minutes at 10 mg/L iron and 20 mg/L P).

would be more less negative than at pH 7 and 8, was contrary to the data (Figure 4-3E, 3H) suggesting that other factors are sometimes involved in sequestration.

Secondary Effects of Water Chemistry on Formation of Color

Further testing was conducted to elucidate the effect of other aspects of water chemistry on the formation of visible color from iron.

Chlorine

The presence of chlorine, a strong oxidant, should increase the rate of oxidation of Fe^{2+} to Fe^{3+}. But, a high dose of 4 mg/L of chlorine had no appreciable impact on iron size or visual observations when dosed with TPP or HMP at pH 7 (Figure A *7*). This is consistent with expectations, since the ferrous oxidation rate was previously identified as a minor mechanism for effective sequestration. It is possible, however, that the presence of chlorine could have a more

significant impact on iron particle size in systems with very low dissolved oxygen or at very low pH, where oxidation rate is much slower.

Temperature

Without phosphates, iron particles quickly formed at 60°C. The addition of 1 mg/L TPP effectively reduced all visual discoloration (Figure A *8*), consistent with results at room temperature. While there was no difference in visual observations, the 60°C condition did have an increased percentage of iron < 10K in size compared to 22°C (P=0.025, 2-tailed T-Test) (Figure A *8*). This could be a result of changes in iron solubility at different temperatures.

Silica

Prior studies have demonstrated that orthosilicate and polysilicate can effectively sequester iron (Robinson et al., 1992; Rushing et al., 2003; Schock et al., 2005). At pH 8.5 with 1 mg/L Fe^{2+}, the presence of 20 mg/L SiO_2 resulted in visually clear water, even though most of the iron was operationally between a10K and 0.45 µm pore size (Figure 4-5). However, the benefits of silica are greatly reduced at lower pHs, likely due to the shift of reactive $H_3SiO_4^{-1}$ to H_4SiO_4. At pH 7, more than 80% of the iron was > 0.45 µm in size when dosed with 20 mg/L SiO_2, and even a high dose of 100 mg/L did not result in visually clear water.

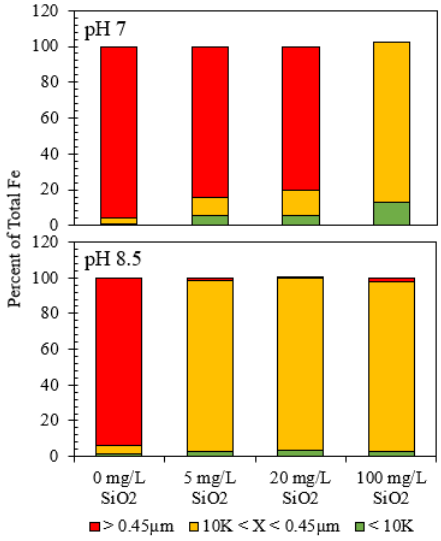

Figure 4-5. Effect of silica on 1 mg/L iron size characterization at pH 7 and 8.5.

Monovalent Ions and Ionic Strength

It is hypothetically possible that monovalent ions (i.e. Na^+ and Cl^-) could hinder sequestration of iron by (1) competing for phosphate complexation sites or (2) increasing particle agglomeration. But even extremely high NaCl concentrations (ionic strength of 0.15 I) had little impact on particle size and visual detection of color when dosing TPP (Figure A 9) or orthophosphate (Figure A 10). Thus, neither phosphate-monovalent ion complexes nor ionic strength seem to have significant impacts on sequestration.

Divalent Cations

Divalent cations (i.e. Zn, Cu, Pb, Ca, Mg, Mn) can form relatively strong complexes with phosphates. Moreover, calcium and magnesium are naturally present in water at orders of magnitude higher concentration than iron.

At 20 mg/L HMP and 10 mg/L ferric, the presence of 200 mg/L $CaCO_3$ increased the zeta potentials for conditions with orthophosphate and HMP from below -25 mV, to less than -6 mV for orthophosphate and less than -14 mV for HMP (Figure 4-4B). The less negative surface charge on the particles may be due to double layer compression from calcium, or competition between calcium and the iron surface for the available phosphate. In either case, the lower zeta potential is expected to cause increased particle formation, coagulation, and visual discoloration.

To test that hypothesis, 1 mg/L ferrous was dosed to water at pH 7 at a range of calcium concentrations. In conditions dosed with 2 mg/L Pyro or TPP as P, the % iron < 10K in size decreased linearly by about 10% for every 100 mg/L increase in $CaCO_3$ (Figure 4-6, Figure A 11). Furthermore, the % iron > 0.45 µm in size increased linearly by 0.086 for pyro, 0.045 for TPP, and 0.04 for HMP for each 1 mg/L $CaCO_3$. A roughly linear dependence between optimum phosphate dose and calcium level was also observed in prior sampling at nine groundwater utilities (C. J. Lytle & Edwards, 2023b).

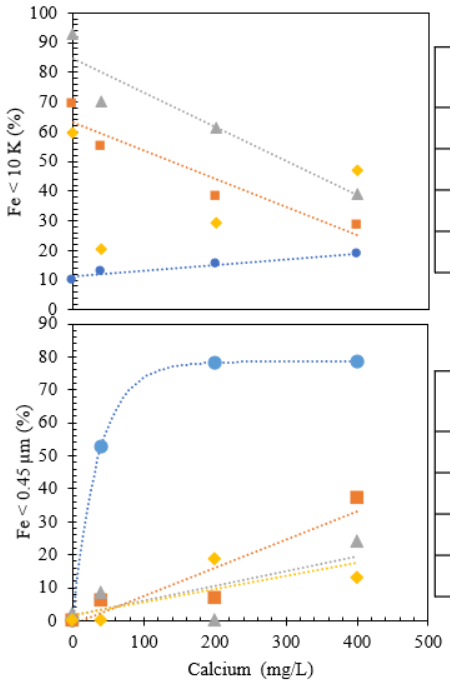

Phosphate Type	Best Fit Equation	R^2
Ortho	0.02x + 11.44	0.93
Pyro	-0.09x + 63.11	0.89
TPP	-0.12x + 84.68	0.88
HMP	NA	NA

Phosphate Type	Best Fit Equation	R^2
Ortho	$78.6 * (1-e^{-0.028 * x})$	1.0
Pyro	0.086x - 1.09	0.86
TPP	0.045x + 1.597	0.55
HMP	0.040x + 1.825	0.57

Figure 4-6. Effect of calcium on <10K iron concentration. Total iron = 1 mg/L, Total P = 2 mg/L. Note: trends for HMP have no simple interpretation, due to rejection of the polymers by 10 K ultrafilters.

Calcium was shown to have a larger impact on iron in the presence of orthophosphate than polyphosphate. Even a low dose of 50 mg/L of $CaCO_3$ increased the amount of iron > 0.45

µm from 0% to 59%. At a level of 200 mg/L $CaCO_3$, 2 mg/L orthophosphate no longer maintained any iron between 10K and 0.45µm in size. Total iron > 0.45 µm as a function of calcium could be fit by the exponential equation:

$$Percent\ of\ Fe > 0.45\ \mu m = 78.6 * (1 - e^{-0.028*(Ca)})$$

Without any Ca^2, 2 mg/L of ortho, pyro, TPP, and HMP effectively reduced visual discoloration of 1 mg/L of iron as before. However, visual discoloration occurred at 50 mg/L $CaCO_3$ and higher in the presence of ortho, and at 200 mg/L and higher with pyro, TPP, and HMP. The formation of visible particles was associated with a greater percentage of iron > 10K and > 0.45 µm in size. This is consistent with double layer compression by cations, or by competition between calcium and iron surfaces for polyphosphate. Magnesium was shown to have similar effects as Calcium (Figure A *12*).

Very High Doses of Phosphate Cannot Stop All Problems with Iron Discoloration, and Can Sometimes Make Them Worse

Water industry guidance suggests that iron sequestration by phosphates cannot be used in waters with above 1 mg/L iron (Great Lakes-Upper Mississippi River Board, 2012). We could find no scientific basis for this declaration. We conducted an experiment to determine if enough polyphosphate could be added to waters with iron above 1 mg/L to prevent all problems with discoloration.

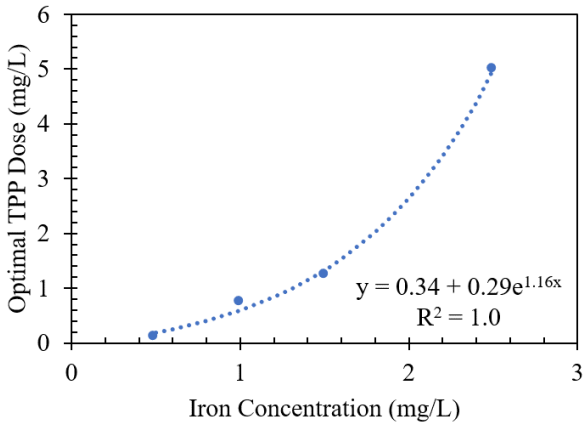

Figure 4-7. Optimal TPP phosphate dose trends for a synthetic water at pH 7 with 100 mg/L $CaCO_3$ and 40 mg/L magnesium as $CaCO_3$.

In a synthetic water with pH 7, 100 mg/L $CaCO_3$, and 40 mg/L magnesium as $CaCO_3$, the 'optimal dose,' or lowest dose needed to eliminate visual discoloration, of TPP was shown to increase exponentially with iron (Figure 4-7) and could be reasonably fit by the equation:

$$\text{Optimal TPP dose} = 0.34 + 0.29e^{1.16*[Fe]}$$

Clearly, a dose of 5 mg/L TPP, could effectively sequester 2.5 mg/L iron. But further assessments were conducted to determine if this was always the case, or if there is an upper threshold for the amount of iron that can be effectively sequestered by polyphosphate.

More Polyphosphate can Increase Turbidity and Color

As an extreme test of the ability of very high doses of phosphates to sequester iron, a high pH 9 water with 200 mg/L $CaCO_3$ was created with either 0.6, 1.2, or 2.5 mg/L ferrous. At or below 1.2 mg/L iron, sequestration could always be effective at reducing color below 4 mg/L TPP. But with 2.5 mg/L iron, the use of TPP could never reduce color below the 20 Pt-Co, but oddly turbidity and color increased with higher dose (Figure 4-8). A light orange/white solid began to form at higher TPP levels. High concentrations of iron, calcium, and phosphate unexpectedly precipitated and were removed by a 0.45 µm filter. The approximate stoichiometry of this solid was $Ca_{1.2}Fe_2P$.

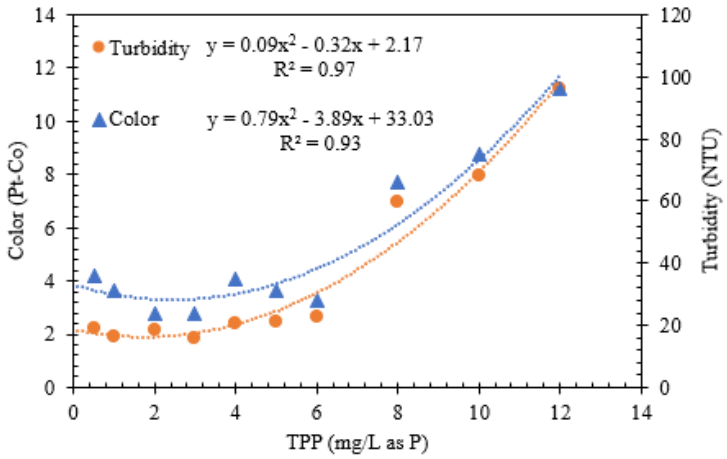

Figure 4-8. The use of TPP for sequestration caused an increase in color and turbidity in an extreme use case (200 mg/L $CaCO_3$, pH 9, 2.5 mg/L Fe^{2+}).

To confirm the existence and identity of possible Ca-P solids, the test was repeated without any iron or alkalinity, using waters at pH 7-9 with 200 mg/L Calcium as $CaCO_3$. In the control waters without phosphate, no color or turbidity formed over a 1-day period. However, at pH 9, the introduction of 10 mg/L orthophosphate, pyro, TPP, or HMP led to visual discoloration and increased color and turbidity. The solids had Ca:P molar ratios of 1.5 for orthophosphate, 0.8 for pyrophosphate, 0.9 for triphosphate, and 5.3 for hexametaphosphate Similar results were observed at pH 8, except no color and turbidity formed in the HMP condition (Figure A *13*). At pH 7, TPP did not form color and turbidity, whereas pyro did so. It seems Ca-pyro solubility is not a strong function of pH between pH 7-9.

The formation of solids with orthophosphate, including calcium orthophosphate (Devine, 2021), aluminum orthophosphate (City of Chicago - Department of Water Management, 2005), and iron orthophosphate has been reported, but we could find no prior research on formation of

calcium polyphosphate solids. This discovery puts an upper limit on the concentration of polyphosphate that can be added to water, especially at pH 9. It is possible that other limitations to phosphate sequestration of iron could arise from formation of ferric or ferrous phosphate solids.

References

1. AmeriWest Water Services Inc. (n.d.). *Frequently Asked Questions*. https://www.ameriwestwater.com/faq

2. Arnold, R. B., Rosenfeldt, B., Rhoades, J., Owen, C., & Becker, W. (2020). Evolving Utility Practices and Experiences With Corrosion Control. *Journal AWWA*, *112*(7), 26–40. https://doi.org/10.1002/awwa.1534

3. Bailey, R. A., Clark, H. M., Ferris, J. P., Krause, S., & Strong, R. L. (2002). *Chemistry of the Environment*. Elsevier Science & Technology Books.

4. City of Chicago - Department of Water Management. (2005). *Pipe Loop Testing Program-Pipe Loop and Full Scale Phosphoric Acid Testing Task*.

5. Davis, C. C., Chen, H. W., & Edwards, M. (2002). Modeling silica sorption to iron hydroxide. *Environmental Science and Technology*, *36*(4), 582–587. https://doi.org/10.1021/es010996t

6. Devine, C. (2021). *Effects of Scale Reduction Technologies and Chemical Inhibitors on Calcium Precipitation in Premise Plumbing Systems*. Virginia Polytechnic Institue and State University.

7. Dodrill, D. M., & Edwards, M. (1995). Corrosion control on the basis of utility experience. *Journal - American Water Works Association*, *87*(7), 74–85. https://doi.org/10.1002/j.1551-8833.1995.tb06395.x

8. Edwards, M., & McNeill, L. S. (2002). Effect of phosphate inhibitors on lead release from pipes. *Journal / American Water Works Association*, *94*(3), 79–90. https://doi.org/10.1002/j.1551-8833.2002.tb09383.x

9. Great Lakes-Upper Mississippi River Board. (2012). Recommended Standards for Water Works. *Health Education*, 89.

10. Hach. (2014). *Color , True and Apparent* (Issue 10).

11. Hach. (2017). *Phosphorus, Reactive (Orthophosphate). Method 8048.* (Vol. 10, pp. 1–8). https://www.hach.com/asset-get.download-en.jsa?id=7639983836

12. Hach. (2019). *Iron , Ferrous (1,10-Phenanthroline Method , Method 8146)* (pp. 2–5).

13. Hach. (2022). *Chlorine , Total (USEPA DPD Method, Method 8167)*.

14. Holm, T. R., & Edwards, M. (2003). Metaphosphate reversion in laboratory and pipe-rig experiments. *Journal / American Water Works Association*, *95*(4), 172–178. https://doi.org/10.1002/j.1551-8833.2003.tb10343.x

15. Holm, T. R., & Schock, M. R. (1991). Potential effects of polyphosphate products on lead solubility in plumbing systems. *Journal / American Water Works Association*, *83*(7), 76–82. https://doi.org/10.1002/j.1551-8833.1991.tb07182.x

16. Huber, E., & Frost, M. (1998). Light scattering by small particles. *Journal of Water Supply: Research and Technology - AQUA*, *47*(2), 87–94. https://doi.org/10.1046/j.1365-2087.1998.00086.x

17. Irani, R. R., & Morgenthaler, W. W. (1963). Iron sequestration by polyphosphates. *Journal of the American Oil Chemists' Society*, *40*(7), 283–285. https://doi.org/10.1007/BF02633692

18. *Iron in Drinking Water*. (n.d.).

19. Klueh, K. G., & Robinson, R. B. (1988). Sequestration of iron in ground water by polyphosphates. In *Journal of Environmental Engineering (United States)* (Vol. 116, Issue 5, p. 1002). https://doi.org/10.1061/(ASCE)0733-9372(1990)116:5(1002.2)

20. Locsin, J. A., Trueman, B. F., Doré, E., Bleasdale-Pollowy, A., & Gagnon, G. A. (2022). Impacts of orthophosphate–polyphosphate blends on the dissolution and transformation of lead (II) carbonate. *Scientific Reports*, *12*(1), 17885. https://doi.org/10.1038/s41598-022-22683-2

21. Lytle, C. J., & Edwards, M. A. (2023a). Phosphate Chemical Use for Sequestration, Scale Inhibition, and Corrosion Control. *ACS ES&T Water*, *3*(4), 893–907. https://doi.org/10.1021/acsestwater.2c00570

22. Lytle, C. J., & Edwards, M. A. (2023b). Simultaneous Use of Polyphosphate for Sequestration and Antiscaling. *ACS ES&T Water*. https://doi.org/10.1021/acsestwater.3c00553

23. Lytle, D. A. (2005). *The Effect of Water Chemistry on the Properties of Iron Particles and Aqueous Suspensions Derived from the Oxidation of Fe(II)*. University of Illinois at Urbana-Champaign.

24. Lytle, D. A., & Snoeyink, V. L. (2002). Effect of ortho- and polyphosphates on the properties of iron particles and suspensions. *Journal / American Water Works Association*, *94*(10), 87–99. https://doi.org/10.1002/j.1551-8833.2002.tb09560.x

25. Mitra, A. K., & Matthews, M. L. (1985). Effects of pH and phosphate on the oxidation of iron in aqueous solution. *International Journal of Pharmaceutics*, *23*(2), 185–193. https://doi.org/10.1016/0378-5173(85)90008-0

26. Rashchi, F., & Finch, J. A. (2000). Polyphosphates: A review. Their chemistry and application with particular reference to mineral processing. *Minerals Engineering*, *13*(10), 1019–1035. https://doi.org/10.1016/S0892-6875(00)00087-X

27. Robinson, R. B., Reed, G. D., Christodos, D., Frazier, B., & Chidamarish, V. (1990). *Sequestering Methods of Iron and Manganese Treatment* (A. R. Foundation & A. W. W. Association (Eds.)).

28. Robinson, R. B., Reed, G. D., & Frazier, B. (1992). Iron and manganese sequestration facilities using sodium silicate. *Journal / American Water Works Association*, *84*(2), 77–82. https://doi.org/10.1002/j.1551-8833.1992.tb07307.x

29. Rushing, J. C., McNeill, L. S., & Edwards, M. (2003). Some effects of aqueous silica on the corrosion of iron. *Water Research*, *37*(5), 1080–1090. https://doi.org/10.1016/S0043-1354(02)00136-7

30. Schock, M. R., Lytle, D. A., Sandvig, A. M., Clement, J., & Harmon, S. M. (2005). Replacing polyphosphate with silicate to solve lead, copper, and source water iron problems. *Journal - American Water Works Association*, *97*(11), 84–93. https://doi.org/10.1002/j.1551-8833.2005.tb07521.x

31. US EPA, O. (2015, September). *Secondary Drinking Water Standards: Guidance for Nuisance Chemicals* [Overviews and Factsheets].

32. Van Wazer, J. R., & Callis, C. F. (1958). Metal Complexing by Phosphates. *Chemical*

Reviews, *58*(6), 1011–1046. https://doi.org/10.1021/cr50024a001

33. Volpe, D. (2012). Assessment of iron and manganese sequestration. In *American Water Works Association Annual Conference and Exposition 2012, ACE 2012*. https://doi.org/10.7275/HA5A-GG93

34. Zeta-Meter, I. (1993). *Everything you want to know about Coagulation & Flocculation ....* Zeta-Meter, Inc.

APPENDIX A

Supporting Information

A MECHANISTIC STUDY OF IRON SEQUESTRATION BY PHOSPHATES

Christian Lytle and Marc Edwards

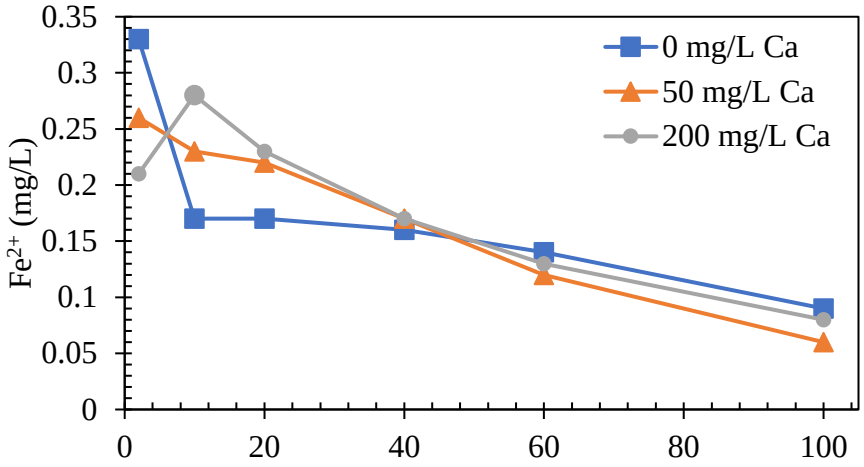

Figure A 1. the addition of calcium had little influence on 0.5 mg/L iron at pH 7 when dosed with 2 mg/L HMP

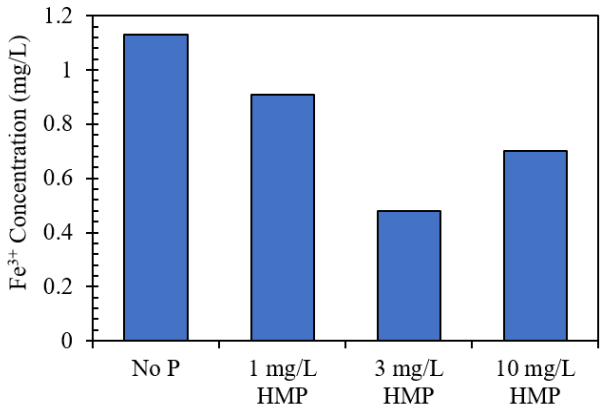

	Color	Turbidity	Percent of Fe > 0.1µm	Visual Observation
No P	158	9.2	70.9	Orange
1 mg/L HMP	12	0.12	0	Light Orange
3 mg/L HMP	20	0	0	Light Orange
10 mg/L HMP	1	0.1	0	Clear

Figure A 2. After 1 hour at pH 6.5 with 3 mg/L total ferrous, the condition with no HMP had a higher concentration of Fe^{2+} remaining. Interestingly, 3 mg/L of HMP resulted in lower Fe^{2+} than 1 or 10 mg/L. In practice however, higher HMP concentrations resulted lower color, turbidity, and particle size.

Practical Implications of Sequestration Mechanisms on Visual Discoloration.

Despite an increase in oxidation rate at lower pHs, increasing the HMP dose decreased color, turbidity, and particle size in all reasonable cases. To determine if there was any situation where HMP increased the color compared to no phosphates due to increased oxidation, a 'worst case' water at pH 6 with 200 mg/L $CaCO_3$ was contrived. Under these conditions, it took only 3 hours for 90% of the 1.1 mg/L of iron to oxidize in the presence of 2 mg/L HMP, compared to about 20 hours with orthophosphate and no phosphate. Nonetheless, the color and turbidity were significantly lower in the presence of HMP after 20 hours (23 Pt-Co, 2.36 NTU) compared to orthophosphate (54 Pt-Co, 7.93 NTU), which formed some iron phosphate particles, and no phosphate (74 Pt-Co, 3.44 NTU) (**Error! Reference source not found.**).

Figure A 3. An increase in oxidation rate of ferrous to ferric due to HMP did not result in higher turbidity or color compared to orthophosphate or no phosphates. 90% of iron oxidation occurred in about 3 hours with HMP compared to around 20 hours for orthophosphate and no phosphates. Note, the formation of white/tan-colored solids and high ratio of 1.74 moles iron per mole P indicated the formation of some iron phosphate in the orthophosphate condition.

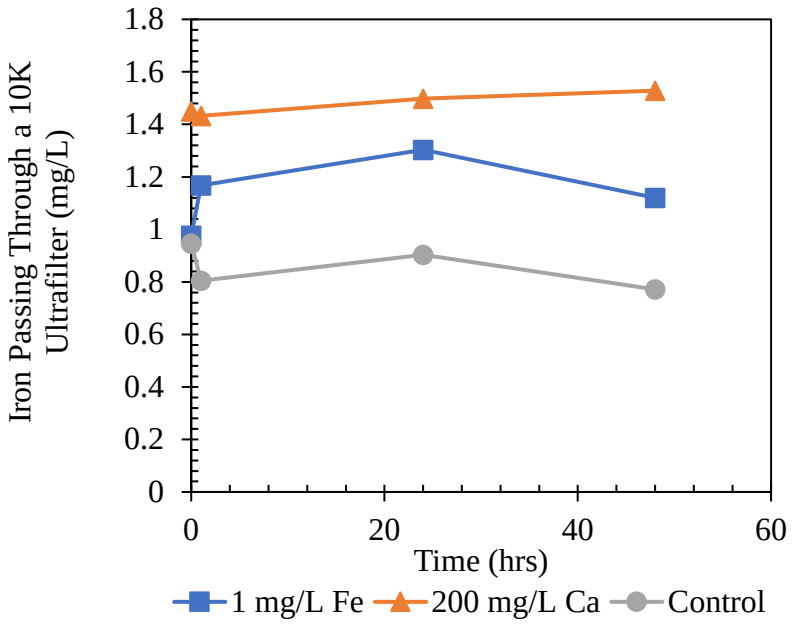

Figure A 4. The introduction of 1 mg/L iron or 200 mg/L $CaCO_3$ cause more HMP to pass through a 10K filter. Total HMP = 1.5 mg/L as P.

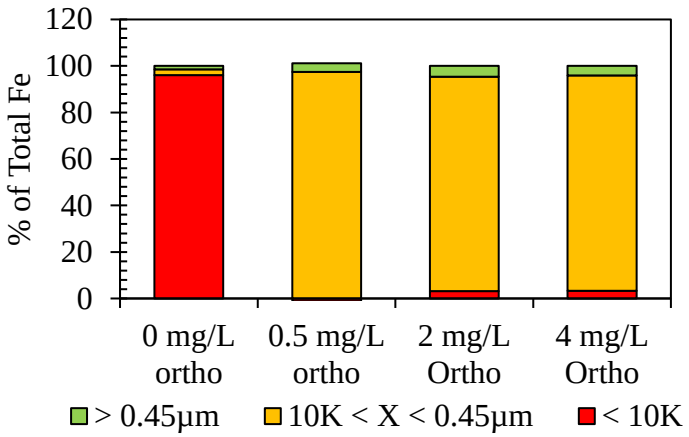

Figure A 5. Increasing the orthophosphate concentration to 4 mg/L did not result in any of the 1 mg/L of iron to remain <10K in size.

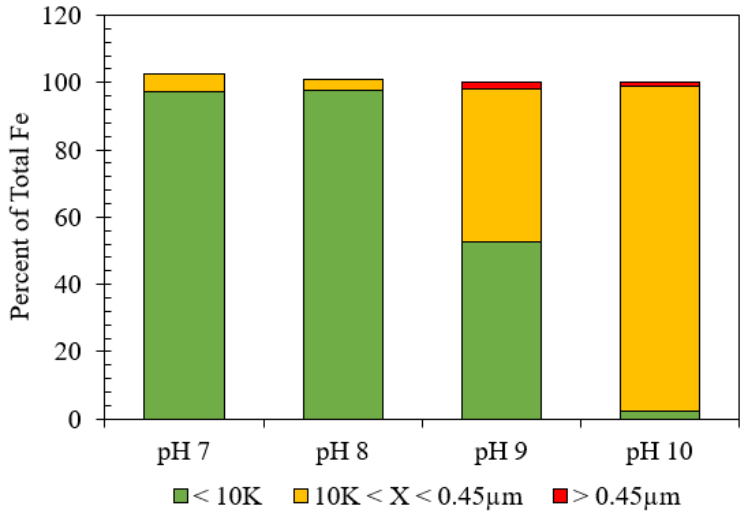

Figure A 6. Increasing the TPP dose to 2 mg/L caused a shift to iron < 10K in size in pH 7, 8, and 9, but all iron was still between 10K and 0.45µm in size at pH 10.

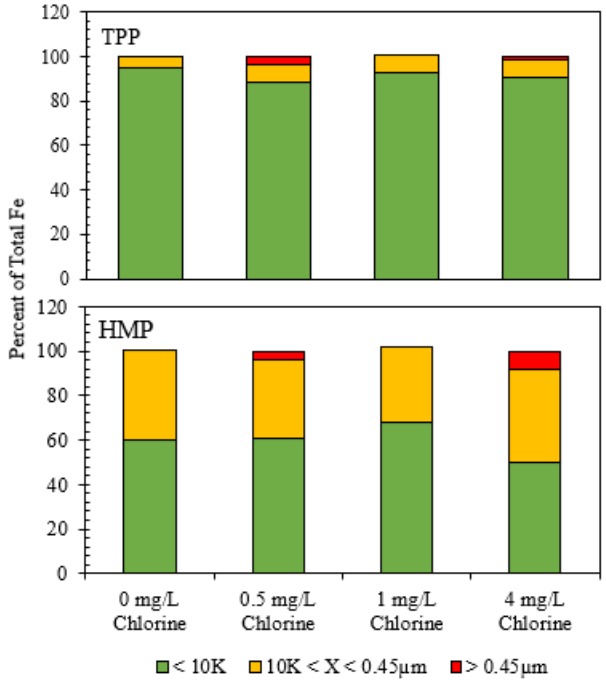

Figure A 7. Impact of chlorine on iron particle size characterization when dosed with 2 mg/L HP and TPP.

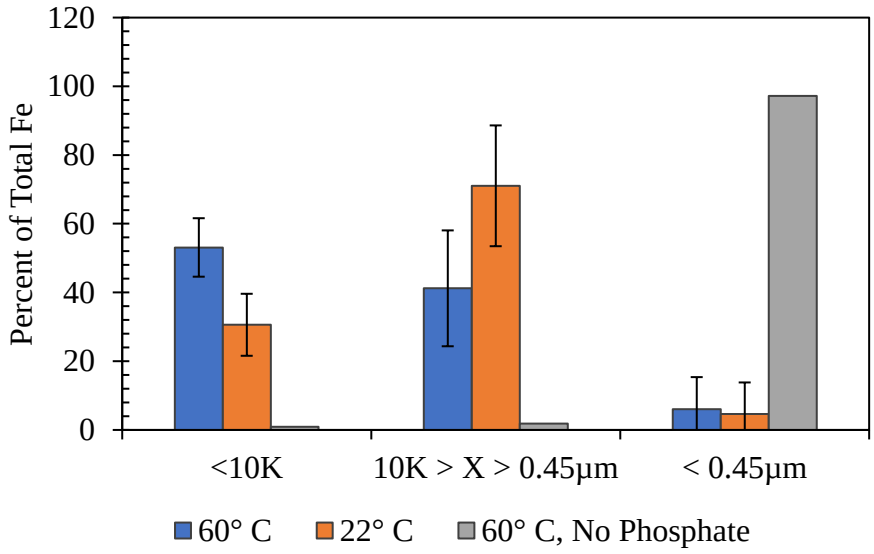

Figure A 8. Impact of temperature on iron particle size in the presence of 1 mg/L TPP. Total iron = 1 mg/L.

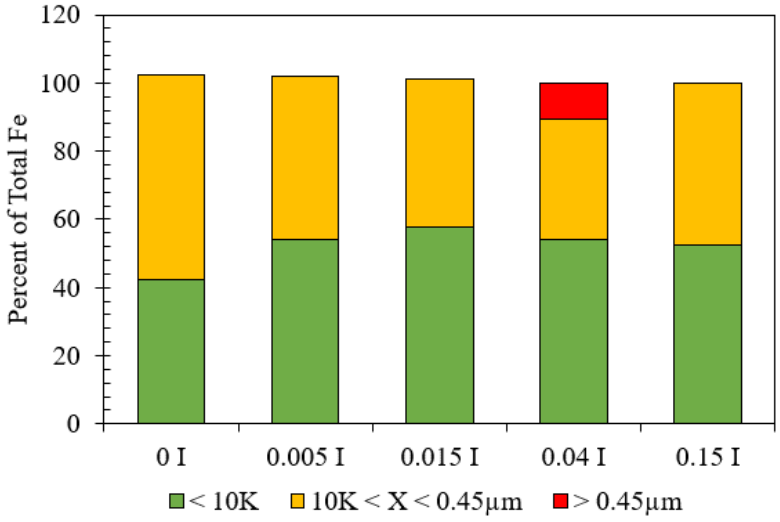

Figure A 9. Increasing ionic strength (using NaCl) had a minimal impact on the particle size of 1 mg/L iron when dosed with 1 mg/L TPP.

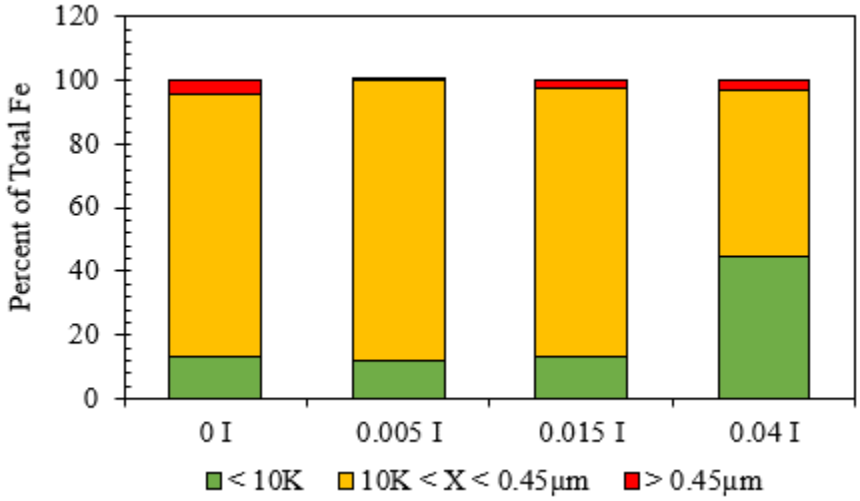

Figure A 10. Increasing ionic strength (using NaCl) had a minimal impact on iron particle size in 2 mg/L of orthophosphate.

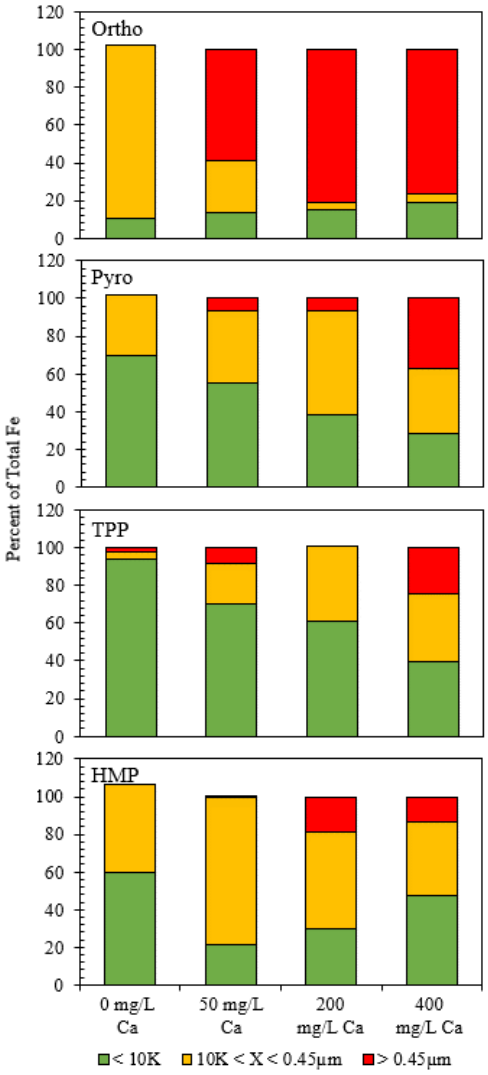

Figure A 11. Effect of increasing $CaCO_3$ on particle size distribution of 1 mg/L iron for 2 mg/L of different phosphate inhibitors.

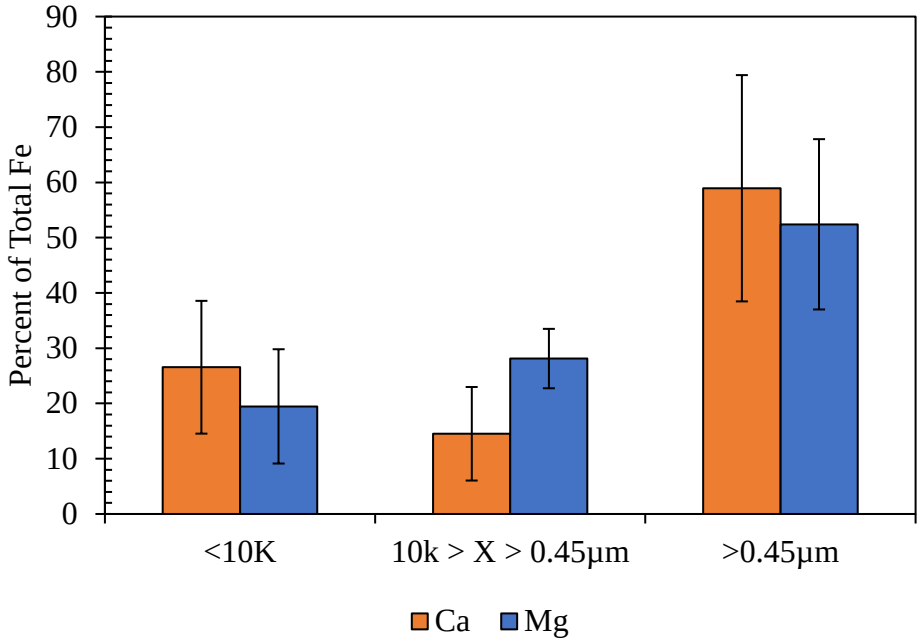

Figure A 12. Effect of 400 mg/L of calcium and magnesium (as $CaCO_3$) on particle size for 1 mg/L iron and 2 mg/L TPP. The results for magnesium and calcium were very similar.

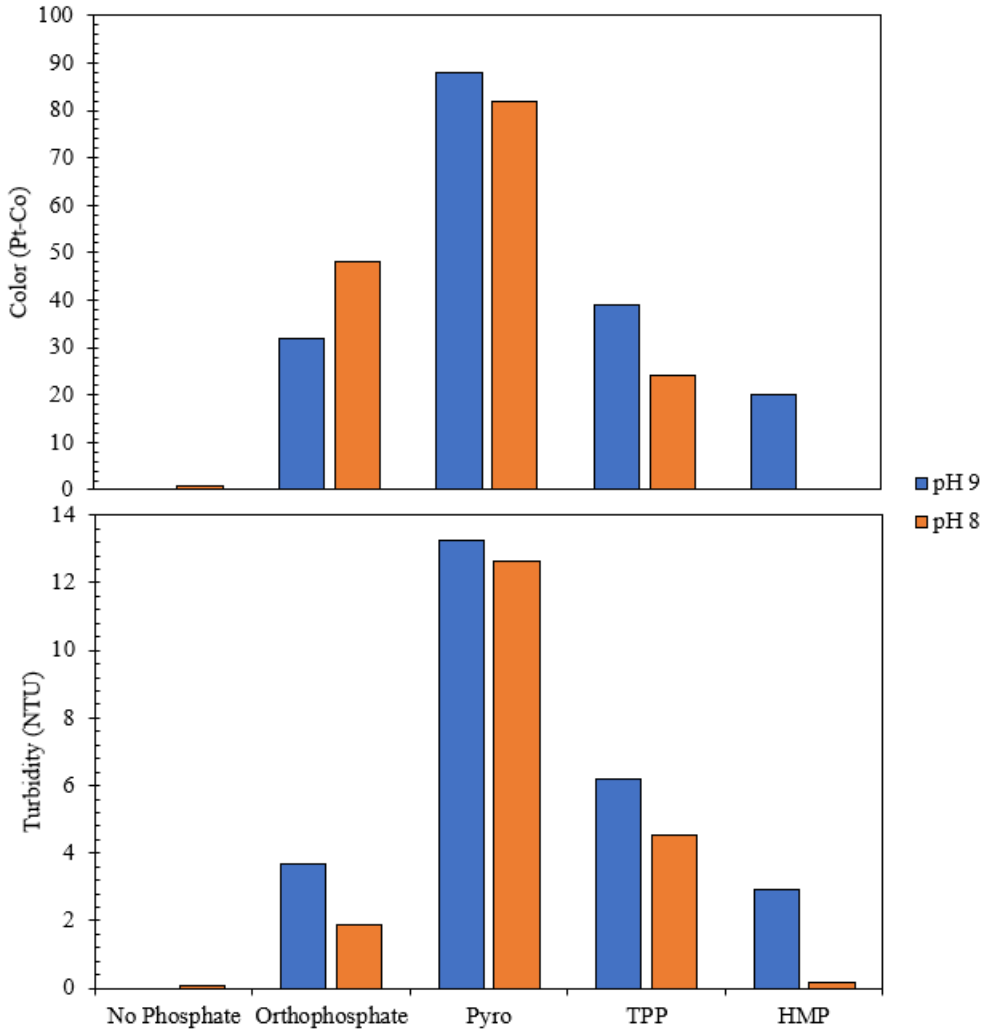

Figure A 13. Color and turbidity measurements after 24 hours when 200 mg/L $CaCO_3$ and 0 mg/L sodium bicarbonate was dosed with no phosphate or 10 mg/L of orthophosphate, pyro, TPP, or HMP.

CHAPTER 5 : STABILIZATION OF A MAGNESIUM SILICATE SCALE PROVIDING CORROSION CONTROL IN A POTABLE WATER DISTRIBUTION SYSTEM

Christian Lytle, Luke Snell, Rebecca Poole, Marc Edwards

Abstract

Analysis of harvested pipes from the Oklahoma City Water Utility Trust distribution system revealed a thick (~1 mm) magnesium silicate (MgSi) scale covering surfaces in service prior to the 1960s. Due to historically low lead levels in homes (≤ 1.2 ppb), this glassy MgSi lining is hypothesized to be an extremely effective and novel means of corrosion control. To mitigate the risk of destabilizing the scale, we aim to (1) characterize the MgSi solid, (2) examine its solubility, (3) investigate the impact of phosphate inhibitors, and (4) consider an operational strategy for maintaining the coating. Experimental results indicated that MgSi did not precipitate below pH 10 without the presence of a pre-existing seed. However, with a seed, MgSi formed at pH levels as low as 8.5-9 in one water source and 7.5-8 in another. Scale dissolved below these pHs and precipitated above it. Phosphate inhibitors had little effect on MgSi solubility at pH 8.5 and 10,

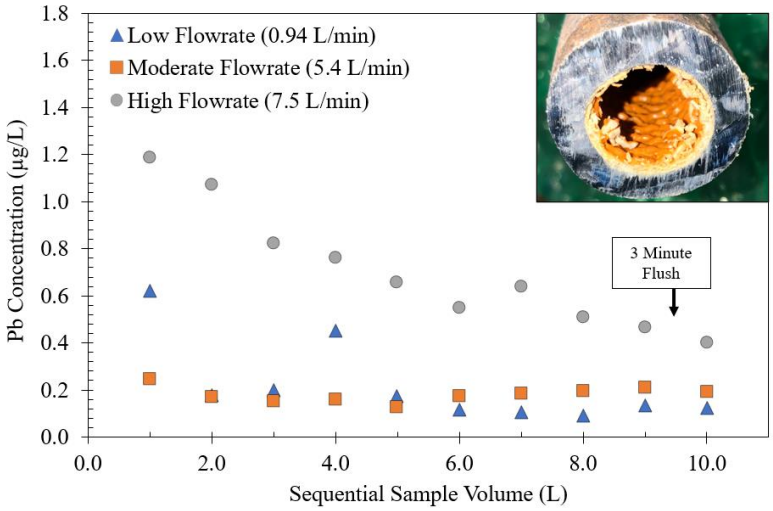

Figure 5-1. Exemplary sequential Pb profile samples from a residential customer with a LSL on the utility side of the meter using an escalating flow rate protocol (Clark et al., 2014). Low flowrate sampling from the LSL (0.94 L/min) was conducted after a minimum 6-hour stagnation, followed immediately by a set of samples at a moderate flowrate (5.4 L/min), and then an atypical high scouring flow rate (7.5 L/min) with the faucet aerator removed. Pipes were lined with an approximately 1 mm thick coating, as shown by a harvested lead pipe.

although HMP and Zn-ortho slightly reduced dissolution rate at pH 7. Chemical equilibrium models could not accurately predict dissolution or precipitation of the solid, so the practical testing with a seed was the only way to predict the optimal pH to maintain the coating.

Introduction

The City of Oklahoma City owns a large drinking water utility which is operated by the Oklahoma City Water Utility Trust (OCWUT). The utility currently serves a population of approximately 1.4 million within central Oklahoma through more than 4,300 miles of water distribution system lines in an area exceeding 621 square miles. As required by recent Environmental Protection Agency (EPA) Lead and Copper Rule Revisions (LCRR), OCWUT has been working to inventory lead service lines (LSL) remaining within their water distribution pipe network. Similar to many water utilities, OCWUT has been routinely removing and replacing any LSLs found through normal leak repairs or water main upgrades. The utility has had no history of problems with elevated lead (Pb) as revealed by previous compliance water sampling conducted since EPA's original Lead and Copper Rule was enacted in 1991. Recent intensive sequential sampling of homes with known LSLs was conducted at escalating flow rates, which confirmed extremely low levels of Pb concentration in the water from taps with known LSLs (≤1.2 ppb) even at high flow rates with aerator removal (Figure 5-1).

Copper (N=3), Cast Iron (CI) (N=4), Ductile Iron (DI) (N=1), and LSL (N=9) pipes were harvested from the distribution system. Visual inspection of some of these pipes [(1) copper, (4) CI, (9) LSL] revealed a thick (≈ 1 mm) scale covering their surfaces. Preliminary elemental analysis of the scale on one copper and four cast iron pipes indicated it was comprised of glassy magnesium silicate (MgSi) solids (LSL samples are awaiting analysis). Two harvested copper pipes, which were placed into service after 1964, did not exhibit this scale. A working hypothesis is that the current MgSi pipe coating formed before the 1960s.

Dissolved magnesium (Mg) and silica (Si) are naturally occurring in ground- and surface-waters. SiO_2 concentrations in water range from 7-60 mg/L as SiO_2, but can occasionally be as high as 100 mg/L. Magnesium concentrations tend to range from 1-50 mg/L as Mg but can be higher than 150 mg/L (Center for Watershed Science and Education, 2020; Langmuir et al., 2004; NC Department of Health and Human Services, 2019; Nerbrand et al., 2003).

Although not as widespread as calcium carbonate ($CaCO_3$), magnesium scales are known to cause issues with scale build-up in water heaters, pipes, membranes, and other equipment, and can also contribute to soap scum accumulation on appliances, dishes, and bathtubs (Mehta et al., 2015). Magnesium can precipitate as magnesium hydroxide [$Mg(OH)_2$] at higher pH and magnesium carbonate [$MgCO_3$]) in some circumstances (Larson et al., 1959; MacAdam & Jarvis, 2015). Formation of amorphous silica scales is a known problem in geothermal waters, cooling waters, and reverse osmosis membranes (Gallup & von Hirtz, 2015).

Our review revealed only one prior report of solids containing magnesium silicate (MgSi) in a potable water system (Roalson et al., 2003). More commonly, they have been reported in desalination plants, cooling water systems, and geothermal waters (Amjad & Zuhl, 2008; Gallup & von Hirtz, 2015; Gunnarsson et al., 2002; Gunnlaugsson et al., 2014; Gunnlaugsson & Einarsson, 1989; Haidari et al., 2022; Morita et al., 2021; Spinthaki et al., 2018; Stapleton & Weres, 2011). Increases in temperature and pH appear to reduce the solubility of these solids (Demadis, 2010; Hauksson et al., 1995). Industry "rules of thumb" have been developed to minimize the formation of MgSi. For instance, these guidelines indicate that below pH 7.5, the product of soluble Mg (ppm as $CaCO_3$) times soluble Si (ppm as SiO_2) should be below a threshold of 40,000 to reduce MgSi precipitation (Demadis, 2010).

At drinking water treatment plants, MgSi solid formation during high pH softening has been reported (Latour et al., 2014; Parks & Edwards, 2007; Rioyo et al., 2018). In one study, silica was precipitated from hard waters at pH 10.8 if the soluble Mg:Si molar ratio was less than 6:1 (Parks & Edwards, 2007). In that study, the formed solid had an Mg:Si ratio of 2:1 and a solubility product constant (K_{sp}) of about $10^{-25.66}$, but lower-solubility MgSi solids also formed with aging (Parks & Edwards, 2007). Some representative MgSi crystalline compounds that might hypothetically form in water include talc ($Mg_3Si_4O_{10}$), chrysotile ($Mg_3Si_2O_5(OH)_4$), Forsterite (Mg_2SiO_4), and sepiolite ($Mg_4Si_6O_{15}(OH)_26H_2O$) (Demadis, 2010; Kent & Kastner, 1985; Parks & Edwards, 2007).

For this study, it was hypothesized that the widely distributed MgSi scale was serving as an unconventional, but very effective, form of corrosion control. This is analogous to the classic theory of protective $CaCO_3$ lining of distribution systems as embodied in the Langelier Index approach to controlling corrosion. The general assumption is that maintaining a thin lining of

MgSi (or $CaCO_3$) could protect the distribution system pipes, but if the linings become too thick there could be unacceptable problems with head loss, pipe clogging and consumer complaints. In an ideal situation, the goal is to operate at or near the solubility saturation point for the precipitate, so that the protective lining on the pipe does not become too thick or thin.

In the OCWUT distribution system, it is possible that some consumer complaints of localized discolored water occurred due to water quality (WQ) shifts related to mixing zones and nitrification. It is suspected that these events might arise from dissolution, and then detachment, of the MgSi coating on pipes at lower pHs. While the presence of MgSi scale throughout the distribution system may pose a unique benefit for corrosion control, given the pervasiveness of the scale, its dissolution and detachment could pose aesthetic problems and higher lead.

With these challenges and implications in mind we conducted experiments to: (1) characterize the MgSi solid, (2) examine its solubility, (3) investigate the impact of corrosion control inhibitors on MgSi formation and dissolution, and 4) consider an operational strategy that could stabilize the coating, to maintain its benefits for corrosion control while minimizing possible problems if it were to destabilize.

Materials and Methods

OKC Source Water and Analysis of MgSi Solids

Historically, the OCWUT water system utilized three treatment plants with two different water sources and finished water qualities, but only two plants are currently operational. Water from the existing plants are refered to as Water A and B. Each water was collected at the treatment plant as filtered effluent with no phosphate or chlorine additions, shipped to Virginia Tech, and stored at 6˚C. Before the first water shipment, a few gallons of each finished water were filtered though 0.45 μm pore size filters. Digestion of these filters with 20% nitric acid indicated that insignificant amounts of MgSi solids were present in the effluent water.

Table 5-1. Representative water quality of the two source waters, and SEM analysis of harvested MgSi solids (refered to as "seeds") from different locations in the distribution system.

	Source Water A (mg/L)	Source Water B (mg/L)	Seed A (% of total Moles)	Seed B (% of total Moles)	Seed C (% of total Moles)
Mg	3	32.5	15.9	14.6	17.5
Al	0.02	0.002	1.0	1.1	1.5
Si	1.5	3.5	11.1	10.0	12.6
P	0.03	0.012	0.1	-	-
Ca	12.5	47	0.4	3.2	1.1
Fe	-	-	0.3	0.2	0.2
Mn	-	-	-	-	-
C	NA	NA	8.0	-	-
O	NA	NA	62.3	69.2	66.2
Zn	0.02	0.037	0.9	1.7	1.4

NA: Not Applicable

Harvested Magnesium Silicate Seed

Samples of solids flushed from the main distribution system at different sites were collected to characterize the MgSi solids and for later use as "seeds" for dissolution and precipitation experiments (Figure 5-2). The source water at each collection point was an unknown blend of Water A and Water B that is assumed to have varied throughout the history of the water system. Upon arrival at Virginia Tech, the wet seed samples were first dried and characterized using a Scanning Electron Microscope and ICP-MS analysis (after dissolution of the solid) (Table 5-1).

Figure 5-2. Image of Seed A, Seed B, and Seed C after drying.

In some experiments, it was desirable to have pre-existing MgSi solids from the distribution system present to avoid the need for spontaneous crystalization. This seed stock solution was prepared prior to each experiment, using an equal mixture of Seed A, Seed B, and Seed C by mass. Initial experiments dosed the seed at low, medium, and high concentrations as defined below (

Table *5-2*).

Table 5-2. Approximate solid metal concentrations found in each seed level, as measured by ICP-MS.

Seed Addition	Mg (mg/L)	Si (mg/L)	Al (mg/L)	Ca (mg/L)	Zn (mg/L)
Low	1.8	0.8	0.2	0.3	0.3
Medium	5.6	2.4	0.5	0.3	1.1
High	14.7	6.4	1.2	0.1	2.8

Analytical Methods

Turbidity measurements were taken using a LaMotte 2020we turbidity meter. pH was measured using a Fisher Scientific Accumet glass AgCl pH electrode calibrated daily using pH 4, 7, and 10 standards. Particle size was characterized using 0.45 μm syringe filters or vacuum filters, with dissolved being operationally defined as < 0.45μm and particulate as > 0.45 μm. An inductively coupled plasma mass spectrometer (ICP-MS) was used to measure total metal concentrations (Method 3030 D and 3125 B). Samples were acidified using 2% nitric acid and digested for a minimum of 24 hours. Scanning Electron Microscopy (SEM) was conducted using a FEI Quanta 600 FEG. Equilibrium models for Mg were generated using MINEQL+ (version 4.62.3) software.

Chemicals

Fresh stock solutions of sodium hexametaphosphate, sodium orthophosphate, a proprietary zinc-orthophosphate chemical, magnesium chloride, and sodium metasilicate pentahydrate were made prior to experimentation. Chemical concentrations were confirmed by ICP-MS.

Precipitation and Dissolution Experiments

For initial experiment, large nalgene bottles were filled with their respective water and dosed with seed and/or another chemicals. Aliquots from these large bottles were poured into smaller bottles, covered with plastic wrap to reduce mixing with air, placed on a shaker table at 60 rpm (except for 6°C samples), and opened once to obtain samples. pH was adjusted to its target (between pH 7-10.5) at time 0 and then recorded at the time of sampling. Some experiments used one large bottle from which multiple aliquots were collected over time. In that case, pH was recorded before samples were taken and re-adjusted back to the target value in anticipation of subsequent sampling. In a few cases, synthetic waters were created to mimic Water A and Water B. For these conditions, deionized (DI) water was dosed with Mg, Si, and alkalinity to replicate the composition of the source water.

In addition to tests at 22˚C, some testing was conducted at 6°C, 12.8°C, and 60°C. The samples at 60°C were heated in a water bath on the shaker table. Those at 6°C were placed in a refrigerated cold room and were not shaken. 12.8°C (55°F) samples were cooled in a small lab fridge on a shaker table. Details of experimental conditions can be found in the Results and Discussion Section.

Statistical Methods

All p-values were calculated using one-tailed t-tests at 95% confidence unless otherwise stated. Furthermore, error values were determined at 95th percentile confidence intervals.

Results and Discussion

The conditions under which the MgSi solid may have formed were explored. Thereafter, we examined precipitation, dissolution, and stabilization of the solid under a range of practically relevant circumstances.

Examining the Possible Origins of the MgSi Solids

Spontaneous Formation of MgSi Solids

At 22˚C and pH 8.3, results indicated that spontaneous precipitation of MgSi in Water A, B, and a 50:50 mixture of the two was negligible. All three water conditions displayed no significant losses in soluble magnesium or silica ($p > 0.05$, 2-tailed t-Test) over the 13-day period (Figure B 1**Error! Reference source not found.**). There were also no statistical changes in dissolved Al,

Ca, Fe, or Zn. Testing at other pHs from 8.7-9.1 and temperatures up to 60˚C also did not cause spontaneous precipitation (Figure B 2, Figure B 3).

When pH was increased to above 10, a level which has not occurred in this distribution system during recent recorded history at this utility, MgSi solids did spontaneously precipitate in synthetic experiments (Figure 5-3). It is possible that before 1960, previous operational conditions of the treatment plants could have allowed spontaneous formation of MgSi, such as a finished water pH above 10 and solids carryover through softening processes.

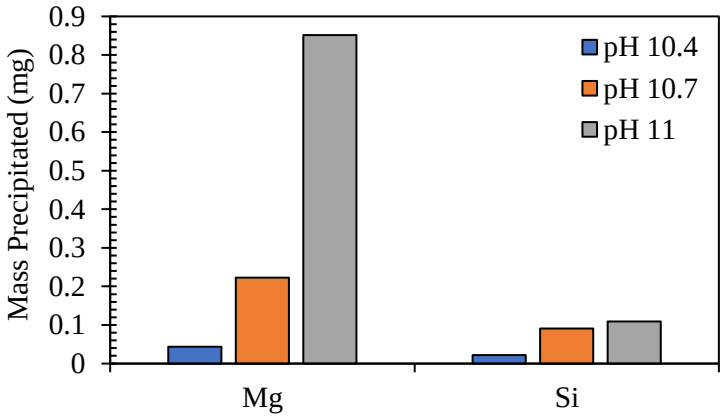

Figure 5-3. A MgSi solid can precipitate at elevated pH in a synthetic water comprised of 32 mg/L Mg and 3.5 mg/L Si to simulate water B.

Magnesium Silicate Precipitation in the Presence of Pre-Existing Seed

It was expected that a lower degree of supersaturation would be required for precipitation in the presence of a pre-existing seed. This was confirmed for Water A, Water B, and a 50:50 mixture of the two at pH 9.1 over a 1-week period. With a medium seed level, at 6˚C, 22˚C, and 60˚C (Figure B *4*), soluble magnesium decreased in every case for Water A and B (one-Tailed T-Test, $p = 0.003$-$0{,}011$), and at 22˚C in the 50:50 mixture ($p = 0.037$). Similarly, there was a corresponding decrease ($p < 0.05$) for soluble Si in all conditions, with the exception of Water B at 22˚C.

To further explore these results, experiments were conducted with a medium seed level in Water A and B at 22˚C in a range of pHs from 7-10.5. After a 1-week period, Mg and Si dissolution was observed at low pH while precipitation occurred at higher pH's (Figure 5-4). In Water A, 28.1% of total soluble magnesium (0.84 mg/L) and 11.0% of total soluble silica (0.17 mg/L) precipitated at pH 10.5, while 7.0% of the magnesium in the seed (0.52 mg/L) and 13.1% of the silica in seed (0.33 mg/L) dissolved at pH 7. In Water B, 19.9% of total soluble magnesium (6.5 mg/L) and 71.6% of total soluble silica (2.5 mg/L) precipitated at pH 10.5, while 2.5 % of the magnesium in the seed (0.19 mg/L) and 8.7% of the silica in seed (0.22 mg/L) dissolved at pH 7. At pH 8.5-9.0 for Water A and 7.5-8.0 for Water B, the water was at equilibrium, with no net dissolution or precipitation.

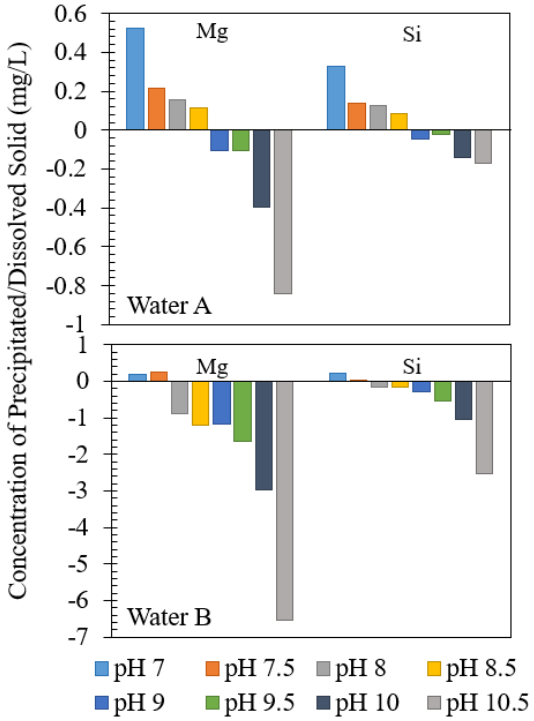

Figure 5-4. Magnesium and silica tended to dissolve from the seed at lower pHs and precipitate from the bulk water at higher pHs. These samples were taken after 1-week to represent a reasonably old water age in the distribution system. Similar trends, but at lower magnitudes, were observed at 1, 8, and 72 hours.

Zn and Ca precipitation and dissolution also displayed some dependency on pH similar to Mg and Si (Figure B *5*, Figure B *6*), although their role in the formation of the solid is less clear given their trace amount (< 3.2% based on moles) found in the solid. Al was also present in the seed (1-1.5 % of the total moles), and it precipitated in the solid for all pH conditions.

The ratio of Mg:Si, that was lost to precipitation or gained due to dissolution, varied slightly between the two waters and as a function of pH. For instance, at pH 7, the seed dissolved at ratios roughly similar to its composition in the solid, of 1.66 Mg:Si by weight in for Water A and 0.99 for Water B (the seeds averaged 1.43). But at pH 10.5, precipitation of the solid in Water A occurred at an approximate Mg:Si ratio of 5.7 and in Water B at a ratio of 3.0. The

results at higher pH could be skewed by formation of some solids like $Mg(OH)_2$ [e.g., brucite], which is expected to be supersaturated above pH 10.7 in Water A and 9.6 in Water B based on solubility calculations.

Influence of Seed Surface Area

As MgSi formation in the modern-day OCWUT water distribution system is likely dependent upon the pre-existing solids coating the pipes rather than spontaneous precipitation in the bulk water not in contact with the MgSi Scale, increases in the surface area of the seed should increase kinetics of precipitation and dissolution.

When Water A was dosed with a low, medium, and high seed level at pH 7.0 and 10.5, expected changes in the precipitation and dissolution rates were observed (Figure 5-5). Increasing the seed concentration and surface area by 10x from 'low' to 'high,' level, increased the rate of magnesium precipitation by 3.7x (291 to 1090 mg/L) and magnesium dissolution by 6.4x (272 to 1750 mg/L) after 336 hours. Similarly, the 10X increase in seed increased silica precipitation by 23x (14 to 340 mg/L) and dissolution by 3.75x (318 to 1200 mg/L) after 336 hours.

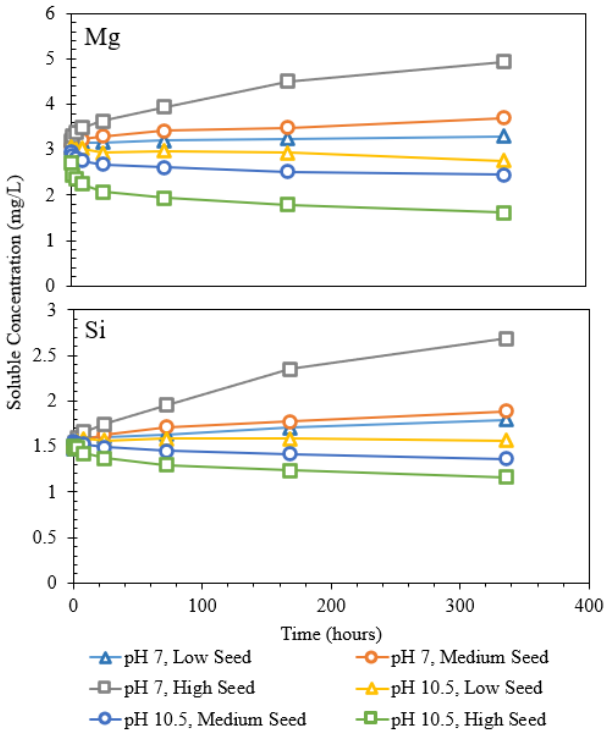

Figure 5-5. Increased seed surface area increased the rate of precipitation and dissolution of magnesium and silica.

During these experiments, no clear plateauing, or equilibrium point was ever reached even after as long as 120 days (Figure B *7*). Additional solubility experiments using the same methods in DI water at pH 7 with a medium seed level displayed similar trends (Figure B *8*). Thus, even in the presence of a seed, the precipitation or dissolution of the MgSi solid is a slow process, in which equilibrium is expected to be approached over a period of months to years.

Influencing MgSi Solubility by Silica Additions

If the OKC MgSi solids follow prediction of classical precipitation and dissolution chemistry, it may be possible to adjust the soluble Mg or Si leaving the plant to control the kinetics of precipitation or dissolution and the equilibrium stability of the solid coating the pipe.

When 5 mg/L of silica was added to the water, the MgSi solid released magnesium more slowly at pH 7 (between 1.3 and 6.2x less dissolution) and sped up the rate of magnesium precipitation at pH 10.5 (between 3.9 and 5.6x more precipitation) at low, medium and high seed levels in Water B when compared to the control (Figure 5-6). Similarly, increased silica resulted in increased magnesium precipitation at pH 10.5 (between 1.9 and 2.9x); however unexpected results occurred at the lower pH; Mg dissolution inexplicably increased at pH 7 (between 1.2 and 1.91x) (Figure 5-6).

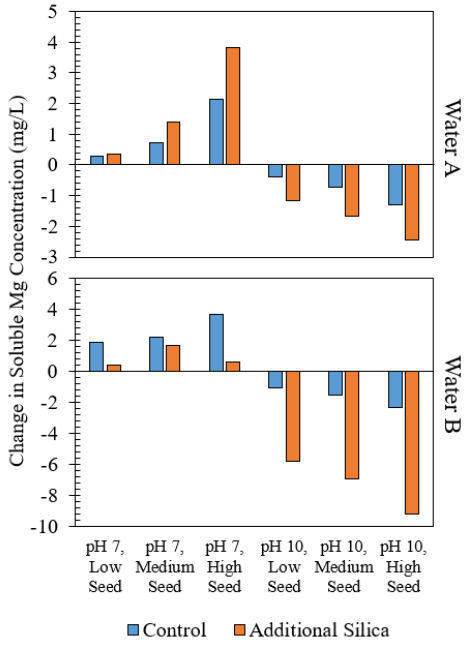

Figure 5-6. Effect of spiking 5 mg/L of silica on MgSi equilibrium in Water A and Water B.

Impact of Phosphate Inhibitors

The question arose as to how dosing of corrosion control chemicals might impact the Mg:Si solid. It was considered possible that the use of traditional phosphates might inhibit formation of the MgSi, as occurs via crystal poisoning in the case of $CaCO_3$ precipitation, or that dosing of Zn^{+2} might somehow enhance formation of the solid. Testing was conducted with orthophosphate (ortho) at 0.6 mg/L as P, Zinc-orthophosphate (Zn-Ortho) at 0.6 mg/L of ortho as P and 0.1 mg/L of Zinc, and hexametaphosphate (HMP) at 1 mg/L as P.

At pH 7, Zn-ortho and HMP inhibited the dissolution of magnesium and silica in Water A compared to the no inhibitor (control) condition ($p < 0.05$), whereas orthophosphate alone had no impact (Figure 5-7). Addition of Zn-ortho resulted in 50% less dissolution of Mg than the control (from 0.6 to 0.3 mg/L-Mg) and completely inhibited Si dissolution. Similarly, HMP decreased

dissolution of Mg by 32% (from 0.6 to 0.4 mg/L-Mg) and Si by 63% (from 0.17 to 0.06 mg/L-Si). Interestingly, these phosphates did not have any impact on dissolution in Water B (Figure B *9*). It is possible that the 10 times higher level of Mg and 4 times higher level of Ca in Water B compared to Water A limited the impact of Zn or HMP.

At pH 8.5, Mg dissolution and Si precipitation occurred with all three types of phosphates, and changes over 168-hours were relatively marginal. At pH 10, the inhibitors had no statistical impact on soluble Si and Mg concentrations compared to the control.

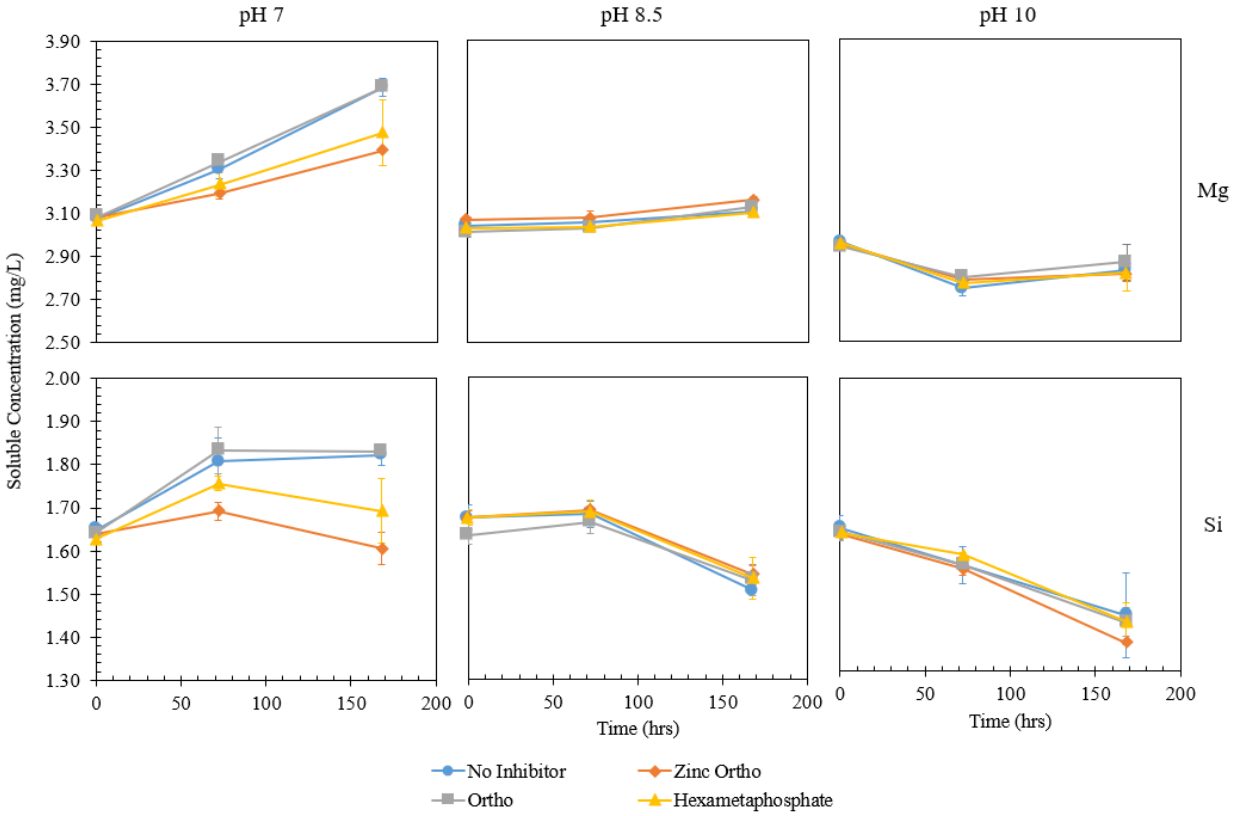

Figure 5-7. Impact of phosphate inhibitors on MgSi precipitation and dissolution in Water A when dosed with a medium seed concentration.

Impact of Temperature on MgSi Solubility

While changes in temperature did not result in spontaneous precipitation of MgSi, they could have an impact on solubility of preformed solids. In such a scenario, MgSi may be unexpectedly dissolving or precipitating in areas of hotter or colder water, such as water heaters

or water mains. A solubility test was conducted at 6, 23, or 50°C using a synthetic water at pH 8.75 with 0.6 mg/L of soluble Si and 2.6 mg/L of soluble Mg. Each water sample was dosed with a high seed level, sealed in plastic wrap to minimize mixing with air, and tested for dissolved metals concentrations after a 1-week period.

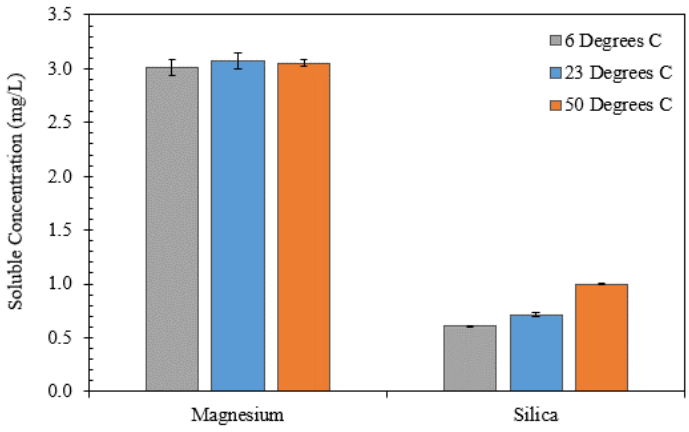

Figure 5-8. Impact of temperature on dissolved Mg and Si concentrations in a synthetic water at pH 8.75 with 0.6 mg/L of soluble Si and 2.6 mg/L of soluble Mg.

Results indicated temperature only had a minor impact on MgSi solubility (Figure 5-8). About 0.4 mg/L of Mg dissolved from the seed at 6, 23, and 50°C over the 1-week period, while no silica dissolved from the seed at 6°C, 0.1 mg/L at 25°C, and 0.4 mg/L at 50°C.

Considering Approaches for Stabilizing MgSi Scales

We explored whether analogies to calcium carbonate corrosion control theories, presently used to guide targeting of suitable operating pHs and alkalinities at many utilities, could be developed to control precipitation and dissolution of the MgSi solids coating pipes in the OCWUT water distribution system. These included models to predict the kinetics of MgSi precipitation and dissolution under various scenarios, and to predict the equilibrium pH for MgSi as in the case of the Langelier Index (Langelier, 1936).

A modified Noyes-Whitney mass transfer dissolution and precipitation equation was fit to the experimental data (Table 5-3; detailed in the supporting information):

$$C = Xe^{C_{solid,\ inital} * k * t} + C_{eq}$$

where C_{eq} is the analyte equilibrium concentration, C is the concentration at time t, k is the rate constant, and X is equal to C(0)-C_{eq}, and $C_{solid,\ inital}$ is the mg/L of solid added at time 0 .

Table 5-3. Best fit X, equilibrium concentration, and rate constants over the 53-day period.

	Seed Concentration	$Ceq_{,Mg}$ (µg/L)	k_{Mg} [L/(µg*days)]	X_{Mg} (µg/L)	R^2_{Mg}	Ceq_{Si} (µg/L)	k_{Si} [L/(µg*days)]	X_{Si} (µg/L)	R^2_{Si}
Water A, pH 7	Low	3325	1.5E-01	-522	0.88	1720	9.0E-01	-522	0.80
	Medium	3850	2.1E-02	-1413	0.95	2000	4.7E-02	-1102	0.95
	High	5800	6.9E-03	-3559	0.97	3200	1.6E-02	-2708	0.98
Water A, pH 10.5	Low	2640	4.6E-02	355	0.95	1450	3.1E-02	99	0.23
	Medium	2290	2.7E-02	644	0.90	1190	3.1E-02	351	0.98
	High	1445	2.1E-02	1248	0.88	950	1.4E-02	505	0.96
Di Water, pH 7	Medium	1550	2.8E-02	-1748	0.97	1550	2.8E-02	-396	0.98

The experimental data was reasonably well fit by the model. There were obvious and noteworthy discrepancies. For instance, increasing the seed concentration should not affect the equilibrium value as long as solid remained, but the best fit equilibrium concentration nonetheless varied (Table 5-3). It is possible that a longer experimental time frame would reconcile this and other problems, but if so, the duration would likely have to be on the order of years.

MgSi Solubility

Solubility models, including the Langelier or Ryznar Index (Langelier, 1936; Ryznar, 1944), have been used in attempts to maintain acceptable $CaCO_3$ supersaturation or undersaturation in practice. Development of analogous MgSi models could allow OCWUT to use a similar index for MgSi to maintain their pipe scale. Data from two conditions did allow the pH range of equilibrium to be determined: between pH 8.5-9 in Water A and between 7.5-8 in Water B (Figure 5-4).

This pH range was used to determine a range of apparent Ksp values for candidate MgSi solids. Although the precise molar ratios or identity of the solid formed in the OCWUT

distribution system was not known, molar ratios of Mg:Si for the provided seed were about 1:0.7 and for those formed through experimentation were 1:0.4. Ksp values were determined for $MgSi_{0.4}(OH)_2$ and $MgSi_{0.7}(OH)_2$ (Table 5-4). The hope was that one Ksp value would fit data for both waters. But the range of possible Ksps for $MgSi_{0.4}(OH)_2$ or $MgSi_{0.7}(OH)_2$ did not overlap in the two different waters (Table 5-4), indicating that no single Ksp could apply.

Table 5-4. Experimentally determined Ksp values for a hypothesized $MgSi_{0.4}(OH)_2$ and $MgSi_{0.7}(OH)_2$ solid in Water A and Water B.

	pH	**$MgSi_{0.4}(OH)_2$**	**$MgSi_{0.7}(OH)_2$**
Water A	8.5	2.56E-17	1.32E-18
	9	2.28E-16	1.10E-17
Water B	7.5	3.67E-18	2.47E-19
	8	3.52E-17	2.33E-18

A MgSi "Marble Test"

When it is not possible to use chemical models to predict trends in calcium carbonate solubility as a function of pH and temperature, practical testing can still be conducted via the "marble test." By adding a "marble" seed of calcium carbonate to a water in question, and adjusting pH as in Figure 5-4, the pH of equilibration with the solid can be determined (see marble test protocol in Standard Methods for the Examination of Water and Wastewater (22nd ed), American public health association et al., 2012). The identified pH is considered optimal for stabilization of $CaCO_3$ scales. The practical approach outlined in Figure 5-4 could therefore be used to determine the optimal operating pH of equilibrium in water A and B, and in these waters as they change seasonally, or with addition of corrosion control or extra Mg or Silica to the plant effluent.

Conclusion

Analysis of water from the two OCWUT treatment plants revealed spontaneous precipitation of MgSi is unlikely to be occurring in the distribution system under current

conditions. It is considered likely that the solids formed throughout the system when the plant effluent rose above pH 10, and has continued to grow at higher pHs over a period of decades.

The corrosion inhibitors included in the testing had little effect on MgSi solubility at pH 8.5 and 10, but HMP and Zn-ortho reduce Mg and Si dissolution rates at pH 7. Zn-ortho reduced Mg dissolution by 50% and completely inhibited silica dissolution, while HMP decreased dissolution of Mg by 32% and Si by 63%.

With pre-existing seed scale, equilibration of MgSi began at a pH 8.5-9 in Water A and 7.5-8 in Water B. Below these equilibrium points, scale dissolution was shown to occur. The rate of precipitation and dissolution of MgSi was shown to be a function of seed surface area, but the rate of MgSi precipitation, dissolution or equilibrium did not fit simple rate models. Nonetheless, a practical “MgSi Marble Test” could be conducted, to predict pH conditions at which no net precipitation or dissolution occurs, to maintain the stability of the existing scale in the system in a range of influent water chemistries.

References

1. American public health association, American water works association, & Water environment federation (Eds.). (2012). *Standard methods for the examination of water and wastewater* (22nd ed). American public health association.

2. Amjad, Z., & Zuhl, R. W. (2008). An Evaluation of Silica Scale Control Additives. In *Nace. COrrosion* (Issue 08368).

3. Center for Watershed Science and Education. (2020). *Interpreting Well Water Quality Results for common metals and minerals*.

4. Demadis, K. (2010). Recent Developments in Controlling Silica and Magnesium Silicate Foulants in Industrial Water Systems. In *The Science and Technology of Industrial Water Treatment* (pp. 179–203). CRC Press. https://doi.org/10.1201/9781420071450-c10

5. Gallup, D. L., & von Hirtz, P. (2015). Control of Silica-Based Scales in Cooling and Geothermal Systems. In *Mineral Scales and Deposits* (pp. 573–582). Elsevier. https://doi.org/10.1016/B978-0-444-63228-9.00022-X

6. Gunnarsson, I., Arnórsson, S., & Jakobsson, S. (2002). *Magnesium-silicate scales in geothermal utilization. An experimental study*. 67.

7. Gunnlaugsson, E., Ármannsson, H., Thorhallsson, S., & Steingrímsson, B. (2014). Problems in geothermal operation-scaling and corrosion. *Short Course VI on Utilization of Low-and Medium-Enthalpy Geothermal Resources and Financial Aspects of Utilization*, 1–18.

8. Gunnlaugsson, E., & Einarsson, A. x. r. (1989). Magnesium-silicate scaling in mixture of geothermal water and deaerated fresh water in a district heating system. *Geothermics*, *18*(1–2), 113–120. https://doi.org/10.1016/0375-6505(89)90017-5

9. Haidari, A. H., Witkamp, G. J., & Heijman, S. G. J. (2022). High silica concentration in RO concentrate. *Water Resources and Industry*, *27*, 100171. https://doi.org/10.1016/j.wri.2022.100171

10. Hauksson, T., Pórhallsson, S., Gunnlaugsson, E., & Albertsson, A. (1995). Control of Magnesium Silicate Scaling in District Heating Systems. *World Geothermal Congress*, *May 1995*, 2487–2490.

11. Kent, D. B., & Kastner, M. (1985). Mg2+ removal in the system Mg2+—amorphous SiO2—H2O by adsorption and Mg-hydroxysilicate precipitation. *Geochimica et Cosmochimica Acta*, *49*(5), 1123–1136. https://doi.org/10.1016/0016-7037(85)90003-1

12. Langelier, W. F. (1936). *The Analytical Control of Anti-Corrosion Water Treatment*. *28*(10), 1500–1521.

13. Langmuir, D., Chrostowski, P., Vigneault, B., & Chaney, R. (2004). *Issue Paper on the Environmental Chemistry of Metals*. https://doi.org/10.4135/9781446216187.n12

14. Larson, T. E., Lane, R. W., & Neff, C. H. (1959). Stabilization of Magnesium Hydroxide in the Solid-Contact Process. *American Water Works Association*, *51*(12), 1551–1559.

15. Latour, I., Miranda, R., & Blanco, A. (2014). Silica removal in industrial effluents with high silica content and low hardness. *Environmental Science and Pollution Research*, *21*(16), 9832–9842. https://doi.org/10.1007/s11356-014-2906-8

16. MacAdam, J., & Jarvis, P. (2015). Water-Formed Scales and Deposits. In Z. Amjad & K. D. Demadis (Eds.), *Mineral Scales and Deposits* (pp. 3–23). Elsevier. https://doi.org/10.1016/B978-0-444-63228-9.00001-2

17. Mehta, S., Shulman, J., & Dufour, A. (2015). Scaling Problems in Home Care Applications. In *Mineral scales and deposits: An overview. The Science and Technology of Industrial Water Treatment.* (pp. 323–352).

18. Morita, M., Yamaguchi, A., Koyama, S., & Motoda, S. (2021). Method for imitating magnesium silicate scale formed at the geothermal power plant in Obama Hot Spring, Japan. *Geothermics*, *96*, 102203. https://doi.org/10.1016/j.geothermics.2021.102203

19. NC Department of Health and Human Services. (2019). *Total Hardness , Calcium , Magnesium & Private Wells*.

20. Nerbrand, C., Agréus, L., Lenner, R. A., Nyberg, P., & Svärdsudd, K. (2003). The influence of calcium and magnesium in drinking water and diet on cardiovascular risk factors in individuals living in hard and soft water areas with differences in cardiovascular mortality. *BMC Public Health*, *3*(1), 21. https://doi.org/10.1186/1471-2458-3-21

21. Parks, J. L., & Edwards, M. (2007). Boron Removal via Formation of Magnesium Silicate Solids during Precipitative Softening. *Journal of Environmental Engineering*, *133*(2), 149–156. https://doi.org/10.1061/(asce)0733-9372(2007)133:2(149)

22. Rioyo, J., Aravinthan, V., Bundschuh, J., & Lynch, M. (2018). 'High-pH softening pretreatment' for boron removal in inland desalination systems. *Separation and Purification Technology*, *205*(May), 308–316. https://doi.org/10.1016/j.seppur.2018.05.030

23. Roalson, S. R., Kweon, J., Lawler, D. F., & Speitel, G. E. (2003). Enhanced softening: Effects of lime dose and chemical additions. *Journal / American Water Works Association*, *95*(11), 97–109. https://doi.org/10.1002/j.1551-8833.2003.tb10496.x

24. Ryznar, J. W. (1944). A New Index for Determining Amount of Calcium Carbonate Scale Formed by a Water. *AWWA*, *36*(4), 472–483.

25. Spinthaki, A., Matheis, J., Hater, W., & Demadis, K. D. (2018). Antiscalant-Driven Inhibition and Stabilization of "magnesium Silicate" under Geothermal Stresses: The Role of Magnesium-Phosphonate Coordination Chemistry. *Energy and Fuels*, *32*(11), 11749–11760. https://doi.org/10.1021/acs.energyfuels.8b02704

26. Stapleton, M., & Weres, O. (2011). Recent developments in oilfield scale control. *International Workshop on Mineral Scaling*, *May*, 69–76. https://doi.org/10.1016/b978-0-12-822896-8.00005-4

APPENDIX B

Supporting Information

STABILIZATION OF A MAGNESIUM SILICATE SCALE PROVIDING CORROSION CONTROL IN A POTABLE WATER DISTRIBUTION SYSTEM

Christian Lytle, Luke Snell, Rebecca Poole, Marc Edwards

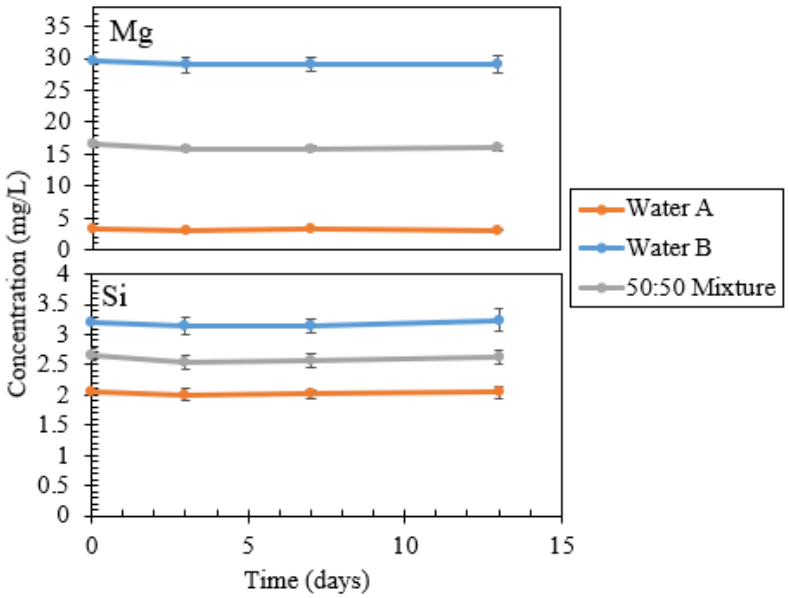

Figure B 1. No statistical difference in Mg or Si concentration after 13 days at pH 8.3 at 22˚C.

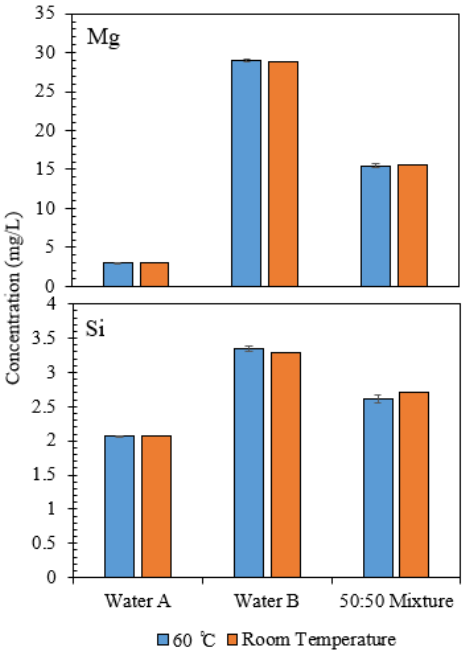

Figure B 2. Increasing Temperature to 60˚C did not increase spontaneous precipitation of MgSi in Water A, Water B, or the 50:50 Mixture at pH 8.3.

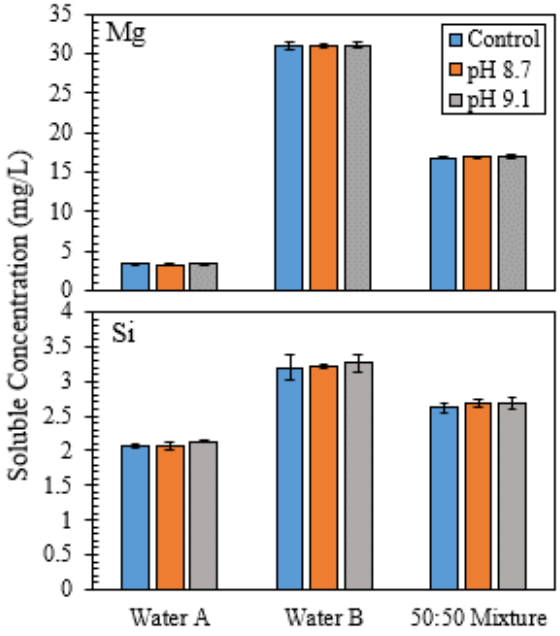

Figure B 3. There was no statistical precipitation of magnesium and silica over a 4-hr period at 60˚C.

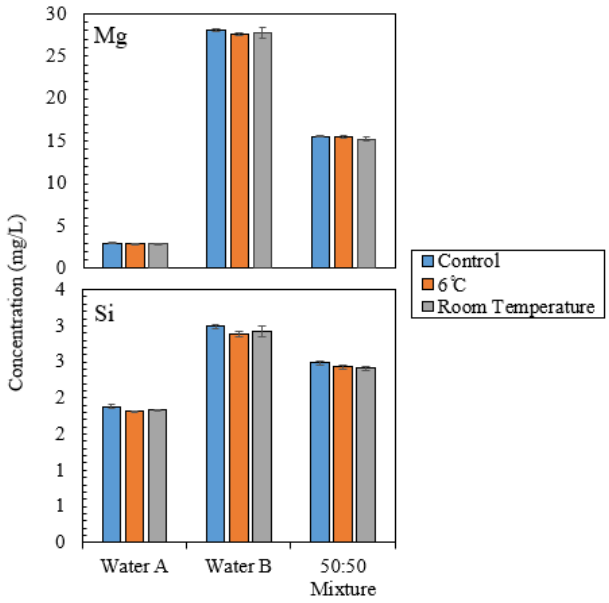

Figure B 4. At pH 9.1, with a medium seed level, and at 22˚C, 60˚C, and 6˚C, there was a statistical loss in soluble magnesium at 6˚C in Water A ($p = 0.003$) and Water B ($p = 0.011$), and at room temperate in the 50:50 mixture condition ($p = 0.037$). Furthermore, soluble Si was lower in all conditions except for Water B at 22˚C ($p < 0.05$).

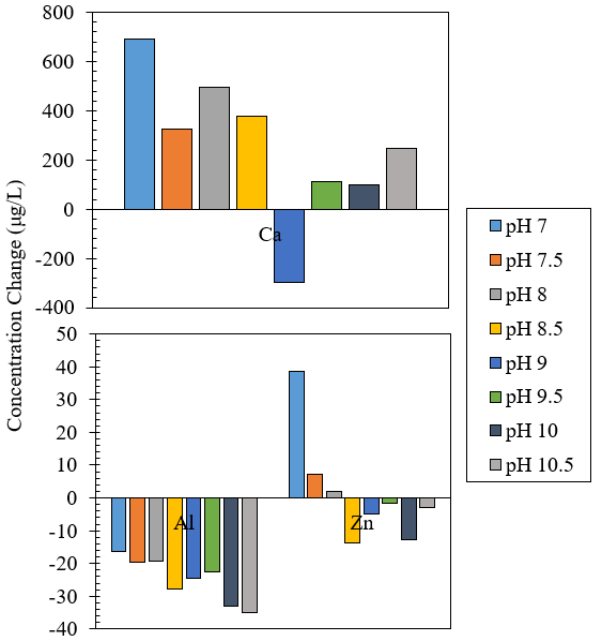

Figure B 5. Change of aluminum, calcium, and zinc concentration over a 1-week period in Water A with a medium seed concentration.

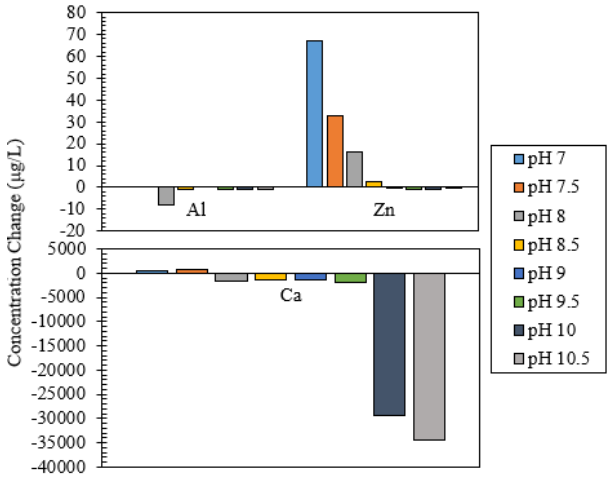

Figure B 6. Change of aluminum, zinc, and calcium concentration over a 1-week period in Water B water with a medium seed concentration.

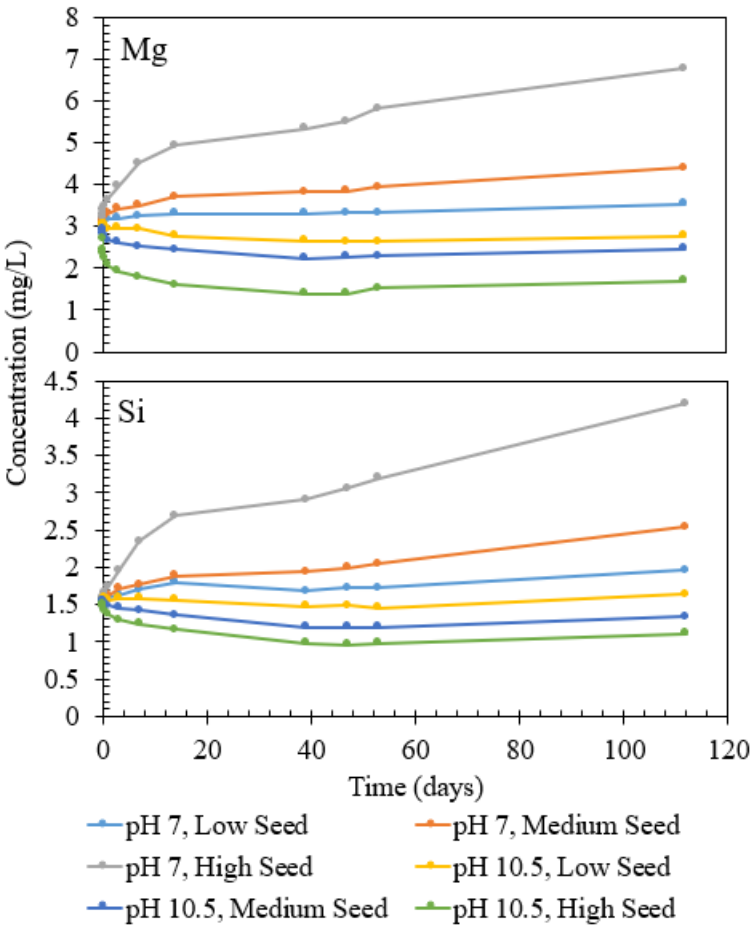

Figure B 7. Long term dissolution/precipitation trends of Water A.

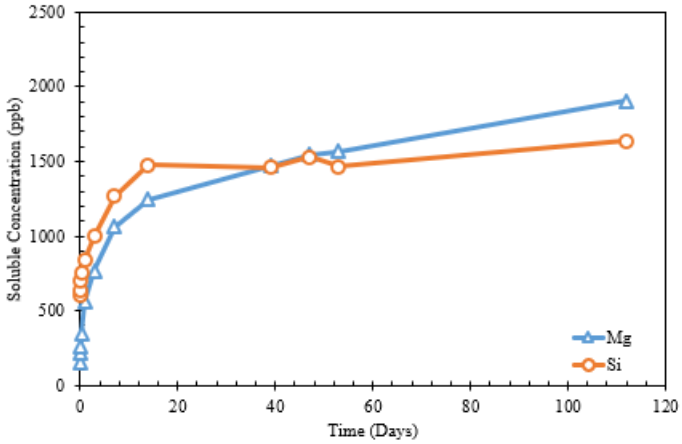

Figure B 8. Long term dissolution/precipitation trends of a medium level of seed in DI water at pH 7.

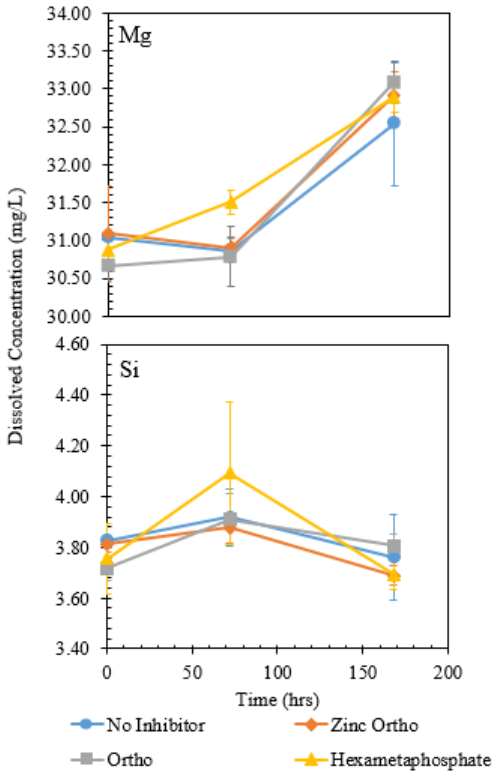

Figure B 9. Impact of phosphate inhibitors on Water B when dosed with a medium seed concentration.

Modeling MgSi Precipitation/Dissolution

Data from Figure 5-4 and Figure B 8. Long term dissolution/precipitation trends of a medium level of seed in DI water at pH 7.were examined to determine if a modified Noyes-Whitney equation would explain the rates of precipitation or dissolution as follows:

$$\frac{dC}{dt} = k[C_{solid,\ inital} - C_{Solid,\ dissolved}][C_{eq} - C]$$

This equation was integrated to get:

$$C = Xe^{(C_{solid,\ inital} - C_{Solid,\ dissolved}) * k * t} + C_{eq}$$

Where C_{eq} is the equilibrium concentration, C is the concentration at time t, and k is the rate constant, X is a equal to C(0)-C_{eq}, $C_{solid,\ inital}$ is the concentration of added solid at time 0, and $C_{Solid,dissolved}$ is the change in solid concentration at each time point. Considering only less

than 20% of the solid disappeared in most cases and was roughly constant as a first approximation, the equation simplifies to the following:

$$C = Xe^{C_{solid,\ inital} * k * t} + C_{eq}$$

CHAPTER 6 : SIMULTANEOUS USE OF POLYPHOSPHATE FOR SEQUESTRATION AND ANTI-SCALING

Christian J. Lytle, Marc A. Edwards

Reprinted (adapted) with permission from Lytle, C. J., & Edwards, M. A. (2023). Simultaneous Use of Polyphosphate for Sequestration and Antiscaling. *ACS ES&T Water*, *4*(1), 227-236.

Abstract

Bench-scale testing methods examined polyphosphate dose response relationships for sequestration and anti-scaling. Tests in water from 9 utilities with two different phosphate chemicals indicated that the minimum dose for effective sequestration was a linear function of iron, manganese, magnesium, and calcium concentration. Chemical A had an optimal polyphosphate dose (in mg/L as P) equal to 58.5[Fe] + 59.7[Mn] + 0.041[Ca + Mg] + 0.4669 (units mM). Chemical B was similar, but had about 33% more dependency on calcium and magnesium hardness, and tended to sequester manganese more effectively on a mole Mn/mole P basis (P = 0.001). Chemical B also reverted to orthophosphate at about 3 times the rate of Chemical A. Color in samples was strongly correlated with particulate manganese ($R^2 = 0.79$) while turbidity was mostly correlated with particulate iron ($R^2 = 0.601$), and neither color nor turbidity measurements perfectly agreed with visual observations of discoloration. Bench-top scaling tests indicate a significantly higher dose was needed for sequestration than scale inhibition in all systems tested. At three utilities tested, at least 3.6X more phosphate was needed for sequestration than scale inhibition, but lab tests indicated that anti-scaling could sometimes control the minimum dose at extremely high levels of calcium.

Introduction

Drinking water systems with elevated iron (Fe), manganese (Mn), and calcium (Ca) hardness can experience problems with discoloration and scale buildup. High Fe/Mn can cause unpleasant taste and odor issues, staining of appliances and clothes, and red or black water. The Environmental Protection Agency (EPA) has set secondary maximum contaminant levels (SMCLs) of 0.3 mg/L for Fe and 0.05 mg/L for Mn (United States Environmental Protection

Agency, 2022b), but utilities and communities can use judgment to deal with the problem as they see fit.

Calcium carbonate scaling is another serious concern in many communities and industries due to pipe clogging, decreased heat transfer and water heater life, pressure losses and unsightly deposits on appliances and glassware (Devine, 2021). In 2000 alone, the total annual cost of scaling for all industries was estimated between $8-10 billion (Müller-Steinhagen, 2000; Richards et al., 2018). As no EPA regulations exist on hardness or scaling problems, if and how to treat potable water to reduce scaling is another judgment call.

Many utilities decide to install centralized treatment including Fe/Mn removal, lime softening or membrane treatments to eliminate these problems. But dosing of polyphosphate is often used to reduce the severity of Fe/Mn discoloration issues (sequestration) and calcium scale formation (scale inhibition) due its very low-cost. For instance, a small Fe/Mn removal plant serving 200 people can cost about $500,000, compared to only about $1,400 per well for polyphosphate (AmeriWest Water Services Inc, n.d.). Similar cost efficiencies can be achieved for anti-scaling from polyphosphate dosing versus centralized treatment. Even greater cost efficiencies may be achieved by dosing polyphosphate at a utility with both Fe/Mn and scaling problems, when compared to the costs of installing centralized treatment(s).

The potential adverse consequences of dosing polyphosphate to increase lead and copper release to drinking water is increasingly scrutinized. Groundbreaking research in the 1990s demonstrated a tendency of polyphosphate to sometimes increase lead in water (Boffardi et al., 1991; Dodrill & Edwards, 1995; Holm & Schock, 1991). More recent research confirmed these problems can still be significant (Locsin et al., 2022; Trueman et al., 2018). After high profile concerns with elevated lead in Washington, DC, Flint, MI in 2014, and Newark, NJ there is greater concern about levels of lead in drinking water that were once considered to be trace (i.e., ≈ 1-5 ppb) (Roy & Edwards, 2019). Moreover, a new Lead and Copper Rule will require many systems to optimize their phosphate chemical use by October, 2024 (United States Environmental Protection Agency, 2022a). The net result is that utilities are increasingly interested in optimizing dosing of polyphosphate to achieve control of Fe/Mn or scaling, while also minimizing adverse consequences to lead release. Here we review prior literature and develop a protocol to achieve that objective.

Background

Understanding Sequestration and Scale Inhibition

Fe and Mn sequestration occurs through the formation of strong polyphosphate-metal complexes. These complexes can slow or inhibit each step in the sequence that affects formation of visible particles including: 1) oxidation of soluble Fe^{+2} to Fe^{+3}, or soluble Mn^{+2} to Mn^{+4}, 2) precipitation of Fe^{+3} and Mn^{+4} solids, 3) particle growth (coagulation) to a visible size, and 4) hypothesized deagglomeration (i.e., growth reversal or dispersion) of large visible particles to invisible sizes (C. J. Lytle & Edwards, 2023). Sequestration effectiveness is dependent on water quality and type of phosphate (Coelho et al., 2008; Klueh & Robinson, 1988; D. A. Lytle & Snoeyink, 2002; Robinson et al., 1990; Volpe, 2012). Factors thought to be influential include Fe/Mn concentration, pH, hardness, natural organic matter (NOM), disinfectant type and concentration, alkalinity, and water age (i.e., reaction time). A lack of research and practical understanding makes it impossible to predict a required chemical dose; consequently, trial and error experimentation at full-scale is the industry standard for optimization.

Phosphates can also inhibit calcium carbonate scale formation by preventing nucleation of calcium carbonate (threshold inhibition), disturbing the growth of crystals (crystal distortion), and dispersion of particles (Amjad & Koutsoukos, 2015; Mpelwa & Tang, 2019; Vidic et al., 2015). Dispersion is considered a minor contributor compared to threshold inhibition and crystal distortion which can be achieved using sub-stoichiometric concentrations of phosphate. In fact, little as 0.1 mg/L polyphosphate-P can inhibit 75-95% of scaling (Devine, 2021; Y. P. Lin & Singer, 2005; F. Wang et al., 2017). Orthophosphate (ortho) is less effective than polyphosphate but it can still markedly reduce scaling in some circumstances. Other factors such as increasing temperature and pH can strongly influence calcium scale formation with or without polyphosphate.

It is often desirable to inhibit scale and sequester Fe/Mn at the same time. An important possible conceptual simplification, is based on literature indicating that more polyphosphate will result in better control of both sequestration and scale inhibition, but for both objectives there is a dose beyond which there is a point of diminishing return. Therefore, optimization is the determination of the lowest dose that effectively achieves all objectives.

Literature Guidance for Dose Selection.

The required polyphosphate dose for scale inhibition and sequestration differs as would be expected based on their differing mechanisms. Reductions in visual discoloration of Fe/Mn occur predominantly through sequestration (i.e., complexation) and dispersion, which requires a molar excess of phosphate ligands per mole of Fe/Mn metal. In contrast, scale inhibition occurs through threshold inhibition and crystal distortion, which can occur even if the molar ratio of P:Ca is less than 1:10000. The net result, is that more polyphosphate is often required for effective sequestration than for scale inhibition, even though there is often 1000 times more calcium in water than Fe/Mn.

This dosing discrepancy is apparent in "rule of thumb" guidance provided by manufacturers. Doses of 0.65 – 1.3 mg/L of polyphosphate as P are often recommended for effective Fe/Mn sequestration (Pure water Products, n.d.; The phosphate Forum of the Americas, n.d.; Water Guard, n.d.). That guidance might include a safety factor (i.e., overdosing) to make sure the product is successful, which also increases product sales and costs to the utility, this dose is much higher than the 0.1 mg/L polyphosphate-P or orthophosphate-P dose range that can significantly reduce scaling even in waters exceeding 300 mg/L as $CaCO_3$ (Devine, 2021). Other organizations have recommended against use of polyphosphate sequestration if the combined Fe/Mn concentrations are above 1 mg/L, because the required doses of polyphosphate may be too high and the approach might not be completely successful (Great Lakes-Upper Mississippi River Board, 2012). More research is needed to confirm, if and when, polyphosphate dosing to control sequestration will also exceed the minimum dose needed to control anti-scaling. Under such circumstances, optimization of the dose for sequestration will also control anti-scaling.

Competition between Hardness and Fe/Mn for Polyphosphate.

Even though polyphosphate controls scaling by crystal poisoning, it can still bind significantly with Ca^{+2} and Mg^{+2} in water (Klueh & Robinson, 1988; Schock et al., 2005; Spon, 2008; Volpe, 2012). Given the high molar ratio of hardness ions relative to polyphosphate ligands, only a small fraction of the hardness is usually bound by polyphosphate, but that still results in a significant competition between hardness and Fe/Mn for the available polyphosphate. The presence of high levels of calcium and magnesium (Mg) are therefore expected to increase the required polyphosphate dose for effective Fe/Mn sequestration.

pH

Lower pH is associated with decreased incidence of Fe/Mn discoloration and calcium scale formation. This is due to lower rates of oxidation and higher solubility for Fe/Mn, and lower degrees of calcium carbonate supersaturation for scaling as per conventional Langelier Saturation Index (LSI) calculations. But the pH dependency of sequestrant effectiveness is uncertain. Available complexation constants suggest that competition with higher H^+ at lower pH might make polyphosphate less effective (Smith & Martell, 1976), and that longer polyphosphate chains may be more sensitive to this effect (Irani & Callis, 1962), but it is unclear if this is always the case.

Groundwater systems with lower pH and/or redox potential often tend to have higher Fe/Mn due to the formation of soluble Fe^{2+} and Mn^{2+} (Smedley, 2003). Drinking water at pHs lower than about 7.5 will likely have fewer issues with calcium carbonate precipitation (Richards et al., 2018; University of California, n.d.). More work is required to better understand the interplay between scale inhibition and sequestration as a function of pH.

Simulated Distribution System Testing

Simulated distribution tests are proposed herein as a useful tool for estimating the impact of phosphates on discoloration as a function of water age in pipe systems without running the risks of full-scale experimentation. Previous studies have demonstrated the effectiveness of simulated distribution tests in evaluating scale formation in a water heater (Devine et al., 2021), chlorine decay in distribution systems (Masters et al., 2015) and TTHM formation (Sfynia et al., 2022). All of these simulations have limitations but their results are nonetheless considered useful for system optimization.

Here, we develop and apply bench-scale testing methods to elucidate polyphosphate dose response relationships for Fe/Mn sequestration and anti-scaling. We then compile experiences from field case studies at 9 water utilities to vet the methods, and develop a preliminary framework to guide rational decisions. Specific objectives include (1) evaluate the impact of two different polyphosphate products on Fe/Mn sequestration to predict optimal doses and avoid overdosing, (2) conduct parallel experiments investigating the impact of various polyphosphate levels on $CaCO_3$ scale formation in simulated electric water heaters, and (3) examine the relationship between dose requirements for scale inhibition and sequestration.

Experimental/Methods

System Selection

Nine groundwater systems in North Carolina were selected for testing Fe/Mn sequestration (

Table 6-1). These systems were chosen based on several criteria, including their availability, their current use of polyphosphate for Fe/Mn sequestration, their relatively high Fe/Mn concentrations, past consumer complaints related to Fe, Mn, or hardness, and their geographic distribution.

Table 6-1. Water quality parameters for each water tested. Those labeled with a 1 and 2 represent systems which were resampled

System	Fe (mg/L)	Mn (mg/L)	Ca (mg/L as $CaCO_3$)	Mg (mg/L)	Si (mg/L)	Alkalinity (mg/L as $CaCO_3$)	pH, 0 Days	pH, 7 Days	Total Chlorine, 0 Days (mg/L)	Total Chlorine, 7 Days (mg/L)	Max Chemical A Dose (mg/L as P)	Max Chemical B Dose (mg/L as P)
A1	*0.991*	*0.481*	*83.8*	*5.8*	*15.6*	*110.8*	*7.60*	*7.35*	*1.78*	*1.09*	1.95	1.90
A2	0.302	0.293	87.9	5.7	16.9	NM	7.35	7.00	1.51	1.06	3.66	3.63
B	0.68	0.046	23.8	2.8	13.3	NM	7.30	7.10	1.48	1.26	2.73	2.61
C	0.02	0.074	58.5	4.4	10.7	NM	7.80	7.65	0.63	0.31	1.42	1.64
D	0.224	0.077	179.7	10.7	9.8	260.4	7.70	7.28	1.87	1.39	1.84	1.88
E	0.611	0.064	53.9	6.2	15.8	NM	6.70	6.62	1.13	0.86	2.20	1.98
F	0.445	0.153	82.1	5.9	11.3	NM	7.50	7.49	1.76	1.54	1.75	1.88
G1	0.571	0.1	150	8.3	22.5	154.4	7.90	7.62	5.43	2.45	2.06	2.08
H1	0.978	0.364	102.5	5.3	18.5	54.9	8.20	7.42	1.54	0.81	2.17	2.14
H2	0.061	0.001	23.2	5	19.9	NM	NM	6.50	NM	0.48	3.81	3.85

NM: No Measurements

Systems Excluded from Data Analysis

During the first set of tests, the highest dose tested at systems A, G, and H did not achieve complete sequestration. These utilities were then resampled in order to test higher

phosphate doses (tests labeled as A2, G2, and H2) (Table C 1). Upon retesting test A2 achieved an optimal polyphosphate dose and is included in the data analysis and results. However, sample G2 and H2 were not included in the optimal dosing trend due to unusual data. Specifically, G2 had abnormally high total and particulate Fe/Mn concentration directly out of the well, possibly due to a lack of flushing before sample collection. Inexplicably, sample H2 had very low Fe/Mn compared to H1, and did not exhibit any visual discoloration.

Furthermore, sample J1 had large variations in Fe directly from the well and was resampled. However, the resampled J2, showed no visual discoloration over the 1-week period despite relatively high Fe/Mn. All these samples (A1, G2, H2, J1, J2) were excluded from data analysis, with the exception that H2 was included in the turbidity and color analysis of Figure 6-4Figure 6-5Figure 6-6.

Simulated Sequestration Test

A simulated sequestration test was conducted to replicate the effects of phosphate on Fe/Mn in distribution systems, and to estimate the optimal dose for each system. The experiment involved pre-dosing 1-L Nalgene bottles with a target dose of phosphates, filling them with raw water directly from the well, and shaking them briefly to enhance Fe/Mn complexation. Each bottle was filled to the top during this process and tightly closed to minimize air/water transfer. Two proprietary chemical products (A and B) were used at 0, 25, 50, 75, and 100% of the "Maximum Phosphate Dose" creating a total of 10 bottles for utility test site. This maximum dose was calculated as the 95th percentile of reported phosphate concentrations from utility operating data. Two of the systems did not have recorded doses so a relatively high dose of 2 mg/L as P was chosen as the maximum dose. Chlorine was dosed at each site to achieve a residual of about 1 mg/L. The water was tested as collected for initial pH, chlorine and soluble metals using a 0.45 μm pore size filter. The samples were shipped to Virginia Tech and placed on a shaker table in the dark to simulate travel time through a distribution system.

One week thereafter, each bottle was tested for multiple parameters including apparent color, turbidity, pH, total chlorine residual, total phosphate, orthophosphate residual, and particle size. Each bottle was determined to be 'visually clear' or 'visually colored' as determined by eyesight of the first author using two observing two samples (a large 1-L Nalgene bottle and a 150 mL glass jar) under light with a white background. Any discoloration or visual particles were noted as "visually discolored" in comparison to clear water samples identified as "visually clear" (Figure C 1). Using this data, the minimum amount of polyphosphate needed to reduce visual discoloration, or the "optimal dose" was determined.

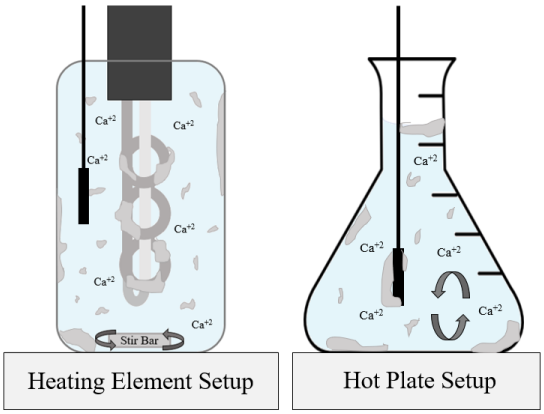

Figure 6-1. Simulated (left) and synthetic (right) scaling test setups.

Simulated Scaling Tests

A modified version of scaling tests developed by Devine et al., was tested. At each sampling site, a 5-gallon container was filled with raw water that contained no added phosphates or chlorine, to be used in the synthetic scaling tests. Each container was filled to the top and tightly closed to minimize contact with air. To preserve the dissolved calcium, the pH of the water was reduced by exhaling bubbles into the water via a straw for 3 minutes, which reduced pH to about 5.5-6. The containers were then shipped to Virginia Tech, where the pH was further lowered using tanks of CO_2, and each container was stored at 6°C until the synthetic scaling tests were to be conducted.

Prior to conducting any tests, the water pH was adjusted back to its original value by stripping some CO_2 by bubbling air through each water sample. Two separate setups were used to test scaling potential: a heating element setup was used to test scaling potential of raw water from three systems, and an improved hot plate setup was used for synthesized scaling tests (Figure 6-1). The heating element setup included a Heatiac 1500W heating element connected to an Inkbird 1100W thermostat. Each condition was treated with the respective phosphate concentration of only Chemical A (0, 25, 50, 75, and 100% of the maximum phosphate dose). A 1.5-L bottle containing each desired condition was placed on a stir plate and stirred at 100 rpm. The bottles were covered with plastic wrap to minimize air flow, and the water was heated to 83 degrees Celsius for a 3-hour period to simulate temperatures near the heating element of a

household water heater. Thereafter the bulk water pH was tested, and the water was filtered using a 0.45 μm pore size nylon membrane vacuum filter. Any calcium scale that precipitated on the heating element, bottle, and temperature probe was dissolved in vinegar over a 24-hour period. This allowed for determination of total scale without damaging the heating element or temperature probe. Changes in bulk water concentrations and the mass of calcium on the heating element, bottle, temperature probe, and filter were measured using inductively coupled plasma mass spectrometry (ICP-MS).

An improved hot plate setup was later utilized for the synthetic scaling tests (Figure 6-1). The original heating element setup resulted in significant bubble formation at the heating element surface resulting in a pH increase in some waters, so the hot plate setup was used to minimize degassing. For this test, the hot plate was used to heat 1-L of water to 75 degrees Celsius for three hours, and the water was mixed by convection. Upon completion, the bulk water pH was tested and scale was dissolved similar to the heating element setup.

Chemicals.

Phosphate Chemicals

Two proprietary phosphate chemicals (Chemical A or B) used at these utilities were dosed during the experiments. The structure and length of the polyphosphates are unknown and they slowly revert to orthophosphate with age (C. J. Lytle & Edwards, 2023). Each phosphate chemical was stored at 6˚C and fresh stock solution was prepared before experimentation to reduce the chance for reversion. Total P was measured using ICP-MS and orthophosphate was measured using HACH DR 3900 Spectrophotometer using Method 8048 (Hach, 2017).

Chemical A had a manufacturer reported 27% orthophosphate and 73% polyphosphate, whereas lab testing confirmed values closer to 32% ± 0.9 ortho consistent with some reversion. One mg/L of this product is reported by the manufacturer to be sufficient to sequester 1 mg/L of either Fe-Mn' or inhibit scaling of 200 mg/L total $CaCO_3$ hardness. Chemical B was reported to be 30:70 ortho:poly but testing showed ortho was about 41% ± 1.0 consistent with some reversion. The manufacturer estimated 1 mg/L of this product would sequester 0.25 mg/L of Fe and 0.13 mg/L of Mn.

Chlorine

A fresh stock solution of laboratory grade Fisher Scientific sodium hypochlorite was prepared before experimentation and stored in the dark at 6˚C.

Other Chemicals

Additional Fe, Mn and Ca were added to the synthetic scaling test to replace precipitated metals. Fresh Fe^{+2} and Mn^{+2} stock solutions were created using Fisher Scientific ferrous sulfate and manganese chloride chemicals in a low pH DI water solution. Calcium was replaced directly in the test waters using a Fisher Scientific $CaCO_3$ chemical.

Particle Size Characterization

Metals in the simulated sequestration test were operationally categorized as dissolved, colloidal, and particulate using two different filters. First, a 10 kDa NMWL Ultracel regenerated cellulose ulotrafilter with an Amicon® stirred cell (pressurized to 30 psi using nitrogen gas) was used to filter out colloidal and particulate particles. Metals passing through this filter were operationally defined as dissolved. Metals removed by a 0.45 μm nylon syringe were operationally defined as particulate. Colloidal metal concentrations were calculated by subtracting the soluble and particulate concentrations from the total metal.

Statistical Methods

Model fitting utilized a least-squares method. Statistical comparisons between data sets used one- or two-tailed paired T-tests as indicated in the results sections. Uncertainties in model parameters were given as 95^{th} percentile confidence intervals.

Analytical Methods

Total Metals Analysis

Total metal concentrations were measured using an ICP-MS (Method 3030 D and 3125 B). All were acidified with 2% nitric acid and digested for a minimum of 24 hours before ICP-MS analysis.

Color and Turbidity

Apparent color (hereby referred to as 'color') and turbidity measurements were taken for each sample in the simulated sequestration tests. Color was measured on a HACH DR3900 spectrophotometer using the Platinum-Cobalt Standard Method (HACH Method 8025) (Hach, 2014). Turbidity was measured using a LaMotte 2020we turbidity meter at a wavelength of 400-600 nm.

Phosphates

Orthophosphate was measured using USEPA PhosVer 3® (Ascorbic Acid) Method (HACH Method 8048) (Hach, 2017) using a HACH DR3900. Total phosphates were measured using

ICP-MS. Polyphosphate concentration was determined using the difference between the two measurements.

pH

The pH was measured using a Fisher Scientific Accumet glass AgCl pH electrode. The probe was calibrated daily using pH 4, 7, and 10 calibration standards.

Results and Discussion

Effectiveness of Sequestration at Each Utility

The bench scale simulated distribution system color formation test revealed that visible discoloration formed in 8 of the 9 utilities without addition of polyphosphate. More than 90% of the Fe/Mn was in particulate or colloidal form at the end of the test. This Fe/Mn eventually formed large flocs that would settle after about a minute of stagnation. Addition of polyphosphate was an effective solution for completely eliminating perceived visual discoloration in 6 out of these 8 cases. Success of using polyphosphate in these systems can be attributed to a decrease in particle size and an increase in dissolved Fe/Mn (Figure 6-2). For instance, in system B, nearly 0% of the Fe and Mn remained in the dissolved form without polyphosphate compared to about 85% when dosed with 2.6 mg/L as P of Chemical A.

The maximum experimental dose of polyphosphate tested did not eliminate visual discoloration in 2 out of 8 systems and sample A1. These samples also had a combination of high concentrations of Fe, Mn, and hardness. For instance, sample H1 (0.98 mg/L Fe, 0.36 mg/L Mn) and sample A1 (0.99 mg/L Fe, 0.48 mg/L Mn) had the highest Fe and Mn concentrations, while calcium was elevated in sample G1 (0.57 mg/L Fe, 0.1 mg/L Mn, 150 mg/L $CaCO_3$). Without the addition of polyphosphate, virtually all Fe/Mn was particulate and large, discernable particles were present in the water. Increasing the

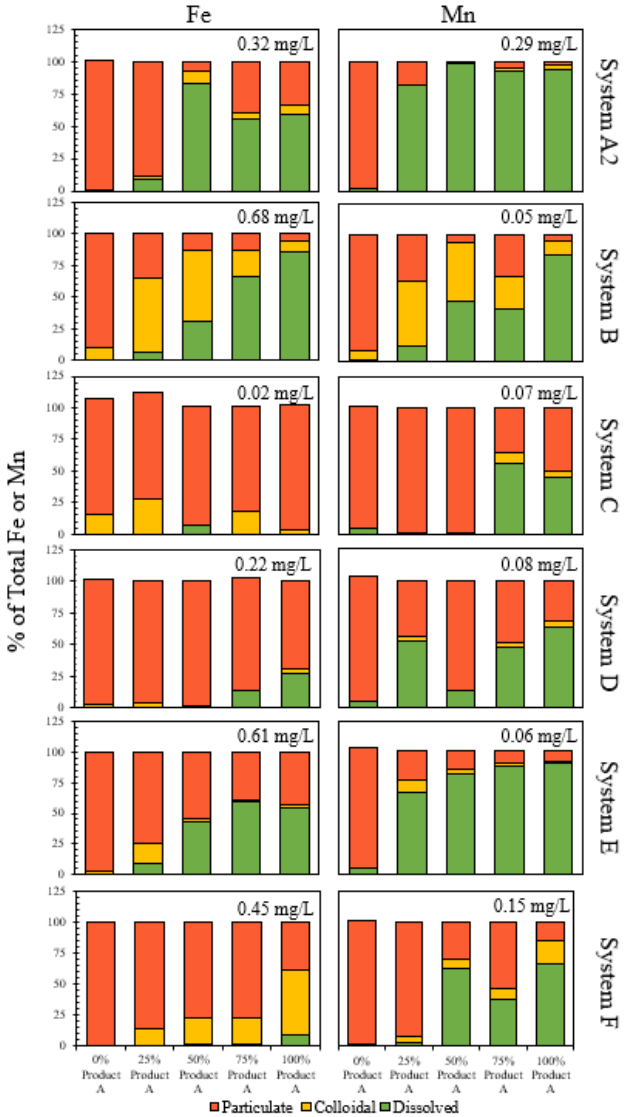

Figure 6-2. Size distribution of iron and manganese after 1 week using Chemical A. The 0, 25, 50, 75, and 100% represent the percentage of the max dose used.

polyphosphate dose produced less obvious visual discoloration, but the particle size characterization indicated that virtually all Fe and much of the Mn was particulate (Figure 6-3). Polyphosphate was partially successful in that 11% of Mn in sample G1, 43% in sample H1, and 63% in sample A1 was dissolved at the highest polyphosphate dose. It is possible that an optimum dose that prevented all color formation, could have been achieved if higher doses of polyphosphate were tested in these samples.

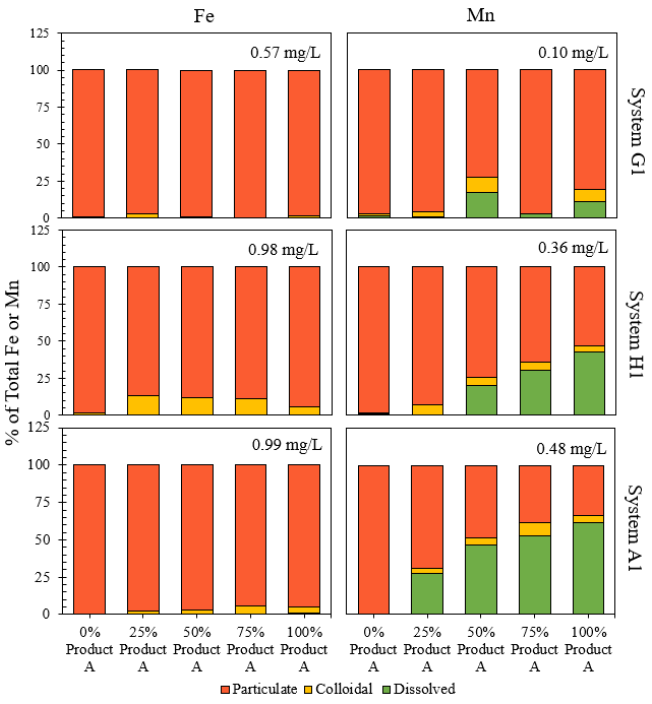

Figure 6-3. Samples which did not completely eliminate color at the highest phosphate dose had high concentrations of particulates (only Chemical A shown). The 0, 25, 50, 75, and 100% represent the percentage of the max dose used.

Overall, these simulated sequestration tests showed good agreement with the dosing experience of the utilities. For the systems in which polyphosphate completely prevented visual discoloration, the simulated tests predicted lower phosphate doses than the utility experience in 5/6 cases. This represents either a safety factor or over-dosing of polyphosphate (depending on perspective), that ranges from 20% to 46%.

Difference between Iron and Manganese.

Fe and Mn levels varied considerably among the utilities. All but system C had higher Fe concentrations than Mn. Seven of the systems exceeded the 0.30 mg/L SMCL for Fe, with concentrations ranging from 0.02 to 0.991 mg/L, a mean of 0.54 mg/L, and a standard deviation of 0.32 mg/L. Eight systems exceeded the 0.05 mg/L SMCL for Mn, with concentrations ranging from 0.046 to 0.481 mg/L, a mean of 0.18 mg/L, and a standard deviation of 0.16 mg/L.

In the absence of polyphosphate, most of the Fe/Mn precipitated during the 7-day test period. At the highest phosphate dose tested for each system (100% of Product A or B), a greater percentage of total Mn remained in the dissolved phase compared to total Fe ($p = 1.8E-8$). The only exception was Chemical A in sample B1, where 85.8% of Fe and 84.9% of Mn remained dissolved. Interestingly, even in systems where almost no Fe was dissolved, such as samples C,

F, G1, H1, and A1, a relatively high percentage of Mn remained dissolved. Consequently, there was no statistically significant difference ($p = 0.69$, two tailed t-test) in the concentration of dissolved Fe/Mn after the 1-week period, despite differences in their total concentrations.

This difference in the effectiveness of polyphosphate to sequester Fe versus Mn might be due to a higher oxidation rate of Fe compared to Mn (Stumm & Morgan, 1995). Another possibility is that Mn is more strongly complexed by polyphosphate than Fe.

Chemical A vs Chemical B

As measured by increases in orthophosphate, both proprietary phosphate chemicals had some reversion over the course the week. Chemical A had an initial ortho: poly ratio of 32: 68 but averaged 36: 64 at the completion of the experiment. Similarly, Chemical B had an initial ortho: poly ratio of 40: 60, was an average of 52: 48 at the end of the test. This indicates that about 3 times more polyphosphate reverted to orthophosphate for Chemical B compared to Chemical A. There were no correlations with water chemistry that could be identified between the extent of reversion for both chemicals. It is unclear why this discrepancy exists, but differences in polyphosphate chain length and shape play a role.

The two chemicals had differences in effectiveness. Chemical B, which had less polyphosphate, sequestered Mn more effectively compared to Chemical A on a mole dissolved Mn/mole poly as P basis (average of 0.173 compared to 0.108) ($P = 0.001$, one tailed paired t-test). Chemical A resulted in a higher concentration of dissolved Fe remaining at the end of the one-week period (average of 40.2 vs 68.5 μg/L) ($P = 0.004$), but this can likely be attributed to more polyphosphate as there was no difference in dissolved Fe per polyphosphate as P ($P = 0.25$, two tailed-paired t-test).

Color and Turbidity

At the end of the 1-week period, measurements were taken for turbidity and apparent color in each condition. Turbidity, which is a measure of light scattering and absorption caused by particles in a solution, can vary depending on the size of particles and the wavelength of the light used. For instance, Rayleigh and Mie scattering can cause particles of different sizes to scatter light differently. In this research, a turbidimeter of wavelength 400-600 nm was used. Apparent color is a measurement of light absorbance and scattering at a specific wavelength (measured at 455 nm for this research).

Relationships between color, turbidity, particle size/shape, and consumer perception have described in other industries (i.e. food sciences) (Carrasco & Siebert, 1999; Lawless & Heymann, 2010) seem to be relevant to our experiences with drinking water. The measurement of turbidity does tend to increase with larger and more numerous particles present in the solution, but factors such as shape and refractive index also contribute. Color measurements are also influenced by light absorption from dissolved substances, and the effect of number, shape, size, and refractive index of particles are less influential than for turbidity.

On this basis it was expected that color would be a function of the mg/L of particulate and colloidal iron and manganese that was present. But a multi-linear regression curve fit to the data indicated that the inclusion of colloidal Fe and Mn did not significantly improve the correlation. The following simple equation:

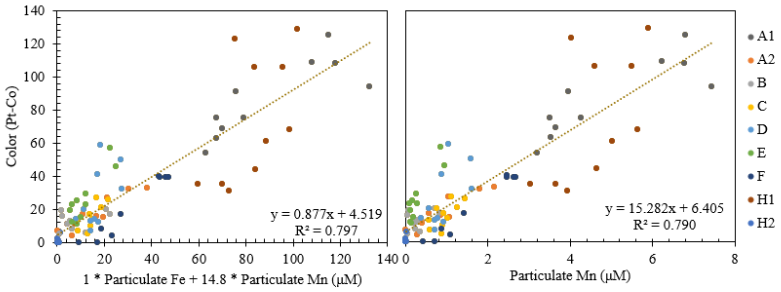

Figure 6-4. Simple relationships provided strong correlations between color and particulate Fe/Mn. Slope = 0.877 ± 0.047, y-int = 4.52 ± 2.11 (left); Slope = 15.28 ± 0.084, y-int = 6.40 ± 2.08 (right).

$$\text{Color} = 0.877\,[\text{Fe}] + 13.1\,[\text{Mn}] + 4.52$$

where the concentration of Fe and Mn was in µM of particulates provided a good correlation (R^2 = 0.797). An even simpler equation of color = 15.282 [Mn] + 6.40 had nearly as good a correlation (R^2 = 0.790) (Figure 6-4).

Turbidity was also expected to be some function of particulate and colloidal iron and manganese. But inclusion of colloidal Fe and particulate Mn did not lead to any enhancement in the

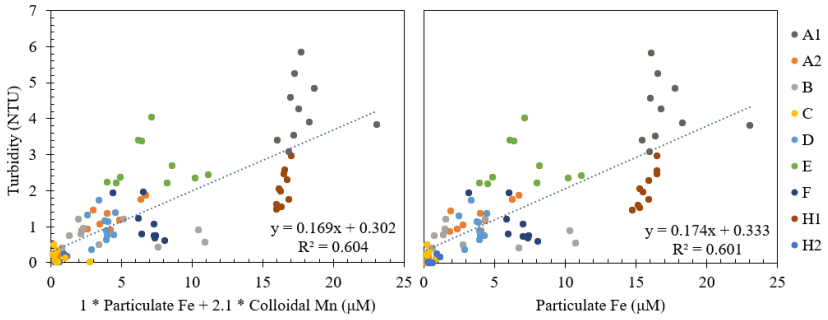

Figure 6-5. Simple relationships between turbidity and Fe/Mn. Slope = 0.169 ± 0.015, y-int = 0.302 ± 0.135 (left); Slope = 0.174 ± 0.015, y-int = 0.302 ± 0.134 (right).

performance of the regression model. The best-fit simplified multi-linear regression:

$$\text{Turbidity} = 0.169\,[\text{Fe}] + 0.355\,[\text{Mn}] + 0.302$$

where the concentration of Fe is expressed in µM of particulates and Mn was in µM of colloids (Figure 6-5) provided an R^2 of 0.604. A simplified equation of turbidity = 0.174 * [Fe] + 0.333 was nearly as good with an $R^2 = 0.601$ (Figure 6-5). Thus, turbidity was primary controlled by the particulate iron level, whereas color in the same sample was primarily controlled by particulate manganese.

Neither color or turbidity measurements were perfect predictors of perceived discoloration by the visual observations of the first author. That said, there were still some trends. First, all visually clear samples had color less than 27 Pt-Co and turbidity less than 2.4 NTU, with only one exceptional sample that had 3.4 NTU (Figure 6-6). But 19% of the samples below this 27 Pt-Co color threshold and 39% of the samples below the 3.4 NTU turbidity threshold were still visually discolored. All of these observations indicate, that visual observations of the human eye reflect some combination of turbidity (light scattering), color (light absorption) and other factors including room lighting, path length, background color and the nature of the particles.

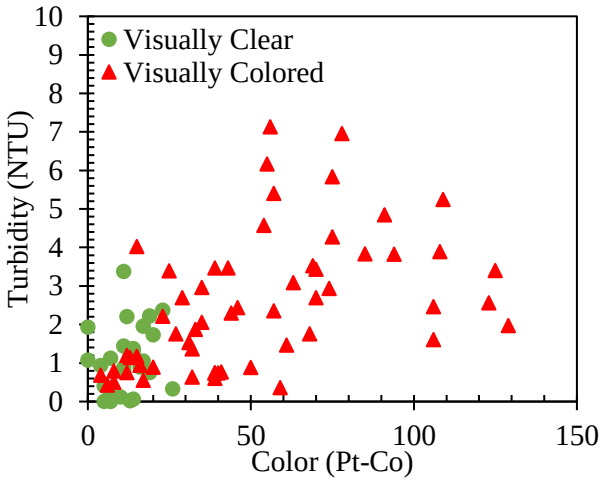

Figure 6-6. Relationship between the color and turbidity in systems A1, A2, B, C, D, E, F, G1, H1.

Understanding the relationship between phosphates and sequestration

There are many factors that play a role in sequestration effectiveness. Calcium and magnesium are expected to complex a significant amount of polyphosphate, which would cause systems with high hardness to require more polyphosphate to have the same effect on Fe/Mn sequestration. To test this, a best fit equation was derived to predict visual discoloration in the six systems that identified an optimal phosphate dose. A strong correlation between the phosphate dose and a combination of Fe, Mn, Ca, and Mg (Figure C 2) was obtained for each chemical:

$$\text{Chemical A: Optimal Dose} = 58.5[\text{Fe}] + 59.7[\text{Mn}] + 0.041[\text{Ca} + \text{Mg}] + 0.467$$

$$\text{Chemical B: Optimal Dose} = 49.6[\text{Fe}] + 59.5[\text{Mn}] + 0.060[\text{Ca} + \text{Mg}] + 0.37$$

where the optimal polyphosphate concentration in mg/L as P and Fe, Mn, Ca, and Mg are in mM. Error bars indicate the range in which the true optimal dose may fall (i.e. somewhere between the experimentally highest dose that did not eliminate visual discoloration and the lowest dose that did.) These models were shown to accurately predict optimal polyphosphate doses for the experimental data (Figure 6-7).

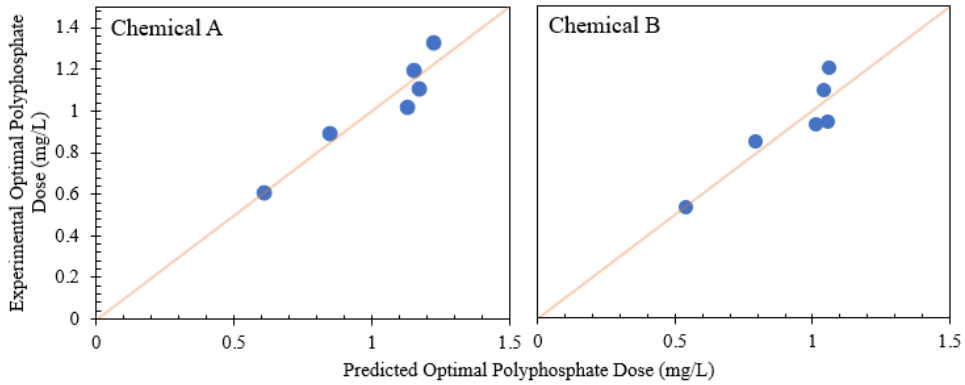

Figure 6-7. This model accurately predicts the polyphosphate doses determined by experimentation. The orange line represents y = x.

Future work would should vet and refine this preliminary relationship for an independent dataset for wider range of waters. In particular, systems with higher Fe/Mn may be more difficult to sequester than predicted, and the presence of other factors such as NOM, pH, and silicate might also affect the sequestration process, even though considering pH and silicate had little influence for the waters tested. Furthermore, different polyphosphate chemical structures and sizes are likely to have different trends, and the efficacy of different phosphate products can vary as well.

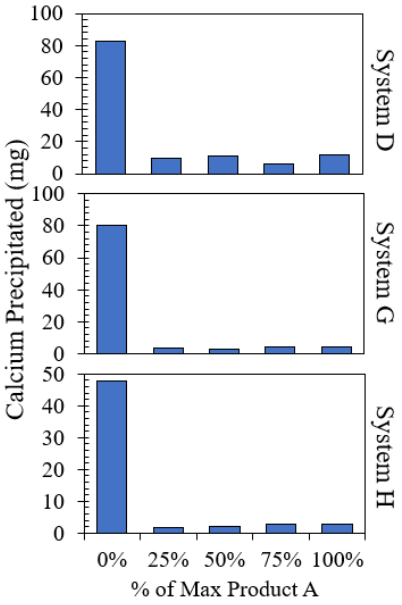

Figure 6-8. Mass of calcium precipitated in 1.5 L bottles in the three systems with > 100 mg/L $CaCO_3$.

<u>Simultaneous Scale Inhibition and Sequestration</u>

Three of the sampled systems had calcium concentrations exceeding 100 mg/L as $CaCO_3$. Although it was uncertain if these systems had scaling problems, their high hardness levels could make them vulnerable to calcium carbonate buildup at high temperatures in water heaters.

Furthermore, the relationship between the dose of phosphate and scaling is not well-established. To determine the scaling potential of each water was tested as described in the materials and methods. Phosphate Chemical A was tested at the same concentration range used in the sequestration tests.

The results indicated that all three systems produced significant amounts of scale without the presence of any polyphosphate (Figure 6-8). However, the addition of even the lowest dose of polyphosphate significantly reduced scaling. In all three sites, 25% of the total added Chemical A, inhibited scaling to the same extent as the highest tested dose. It is unclear how low a polyphosphate dose could have inhibited scaling, but these results confirm expectations that the concentration of phosphates required to reduce scaling is much lower than that needed for sequestration in these systems. Another point of this analysis, is that many systems that have optimized polyphosphate for sequestration, are also inhibiting scaling whether they know it or not. This is a possible unintended benefit of dosing polyphosphate that is often overlooked.

Anti-Scaling Can Control Optimal Polyphosphate Dose

It was hypothesized that there would be some situations in which control of anti-scaling will require more polyphosphate than Fe/Mn sequestration. Since no such condition was tested in our study with hardness over 180 mg/L as $CaCO_3$, and calcium exceeded a level of 250 mg/L as $CaCO_3$ in nearly 10% of surface waters in one survey, we contrived a reasonable sample to attempt and prove this point (Langmuir et al., 2004). A sample stored from System D was filtered and the original level of Fe^{2+} [0.224 mg/L] and Mn^{+2} [0.077 mg/L] were restored, and Ca^{+2} was adjusted to a final concentration of 180, 400 or 600 mg/L by dosing from a $CaCO_3$ solutions in contact with high CO_2 at the same initial pH. A sequestration test and hot plate scaling test were then conducted.

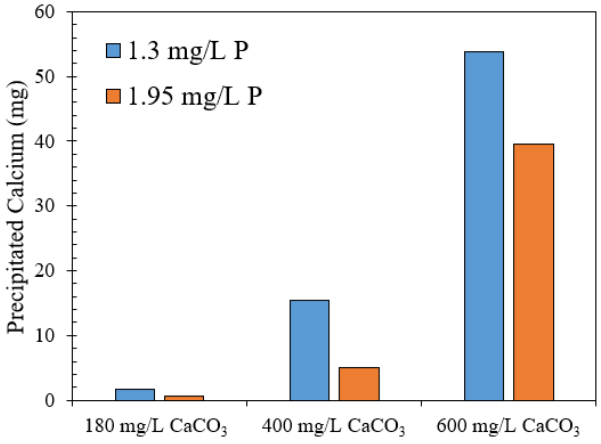

Figure 6-9. Mass of calcium precipitated in 1 L of water at 75˚C for 3 hours. Without phosphate, 136 mg/L $CaCO_3$ precipitation in the heating element setup.

At the calcium concentration present in the original sample of 180 mg/L, only 1.6 mg/L of $CaCO_3$ precipitated at the optimal Chemical A dose of 1.3 mg/L phosphate for sequestration (Figure 6-9). Assuming that up to 5 mg/L $CaCO_3$ precipitation is acceptable for anti-scaling control, in this sample more polyphosphate was required to maintain effective Fe/Mn sequestration (1.3 mg/L) than to inhibit scale.

But at 400 mg/L of $CaCO_3$, 1.3 mg/L of Chemical A did not effectively inhibit Ca scale formation, even though Fe/Mn visual discoloration was controlled. Increasing the dose to 1.95 mg/L did reduce scaling to below 5 mg/L. When the hardness was further increased to 600 mg/L $CaCO_3$; about 54 mg of $CaCO_3$ precipitated at 1.3 mg/L and 40 mg precipitated at 1.95 mg/L of phosphate Product A. We ran out of water and could not investigate if much higher polyphosphate doses would have been effective in controlling scaling in this water. In any case, that are some unusual situations in which scale inhibition would require more polyphosphate than sequestration. We estimate that this would occur at about 300 mg/L $CaCO_3$ in this water (Figure 6-10). While relatively high, this calcium concentration was reported to occur in about 1-3% of predominantly surface waters reported in one survey (Langmuir et al., 2004).

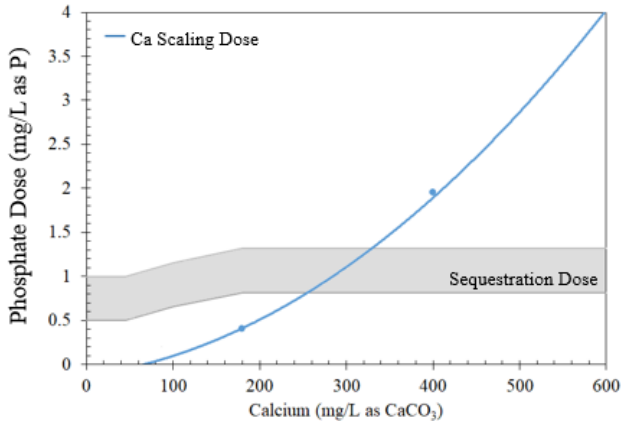

Figure 6-10. Conceptual phosphate dose and response for Ca scale inhibition and sequestration in system D. More polyphosphate is needed for sequestration than scale inhibition near 300 mg/L $CaCO_3$.

Conclusion

Two different proprietary phosphate chemicals effectively eliminated visual discoloration in bench testing of 6 of 8 different groundwater utilities with high iron and manganese. The minimum chemical dose achieving effective sequestration for these systems were a function of the Fe, Mn, Mg, and Ca concentration. Sequestration was unsuccessful in 2 of 8 conditions due to a combination of high Fe, Mn, and/or hardness, but it could have been successful if higher doses of polyphosphate were tested. In all systems, increasing polyphosphate doses tended to decrease visual discoloration and particle size while often maintaining higher dissolved Fe/Mn

over a 1-week period. Color measurements were mostly correlated to particulate Mn ($R^2 = 0.790$) while turbidity was mostly correlated with particulate Fe ($R^2 = 0.601$).

Scaling tests for three systems with high hardness indicated significantly more polyphosphate was generally needed for effective sequestration than anti-scaling. In these systems, the phosphate dose can be selected based on control of Fe/Mn visual discoloration, as that dose effectively controls scaling as well. It is expected that in very, very hard waters, the polyphosphate dose to control scaling may sometimes be higher than that required for effective sequestration.

References

1. AmeriWest Water Services Inc. (n.d.). *Frequently Asked Questions*. https://www.ameriwestwater.com/faq

2. Amjad, Z., & Koutsoukos, P. G. (2015). Mineral Scales and Deposits. In *The Science and Technology of Industrial Water Treatment*. Elsevier. https://doi.org/10.1016/C2012-0-07278-X

3. Boffardi, B. P., Holm, T. R., & Schock, M. R. (1991). Polyphosphate Debate. *American Water Works Association*, *83*(12), 18–20.

4. Carrasco, A., & Siebert, K. J. (1999). Human visual perception of haze and relationships with instrumental measurements of turbidity. Thresholds, magnitude estimation and sensory descriptive analysis of haze in model systems. *Food Quality and Preference*, *10*(6), 421–436. https://doi.org/10.1016/S0950-3293(99)00029-4

5. Coelho, J., Kucher, K., & Ting, A. (2008). *Optimizing Sequestration of Manganese (II) with Sodium Triphosphate*. Worcester Polytechnic Institute.

6. Devine, C. (2021). *Effects of Scale Reduction Technologies and Chemical Inhibitors on Calcium Precipitation in Premise Plumbing Systems*. Virginia Polytechnic Institue and State University.

7. Devine, C., Wang, F., & Edwards, M. (2021). A Standardized Test Protocol for Evaluation of Scale Reduction Technologies. *Environmental Engineering Science*, *38*(12), 1109–1119. https://doi.org/10.1089/ees.2021.0047

8. Dodrill, D. M., & Edwards, M. (1995). Corrosion control on the basis of utility experience. *Journal - American Water Works Association*, *87*(7), 74–85. https://doi.org/10.1002/j.1551-8833.1995.tb06395.x

9. Great Lakes-Upper Mississippi River Board. (2012). Recommended Standards for Water Works. *Health Education*, 89.

10. Hach. (2014). *Color , True and Apparent* (Issue 10).

11. Hach. (2017). *Phosphorus, Reactive (Orthophosphate). Method 8048.* (Vol. 10, pp. 1–8). https://www.hach.com/asset-get.download-en.jsa?id=7639983836

12. Holm, T. R., & Schock, M. R. (1991). Potential effects of polyphosphate products on lead solubility in plumbing systems. *Journal / American Water Works Association*, *83*(7), 76–82. https://doi.org/10.1002/j.1551-8833.1991.tb07182.x

13. Irani, R. D., & Callis, C. F. (1962). Calcium and magnesium sequestration by sodium and potassium polyphosphates. *Journal of the American Oil Chemists Society*, *39*(3), 156–159. https://doi.org/10.1007/BF02632750

14. Klueh, K. G., & Robinson, R. B. (1988). Sequestration of iron in ground water by polyphosphates. In *Journal of Environmental Engineering (United States)* (Vol. 116, Issue 5, p. 1002). https://doi.org/10.1061/(ASCE)0733-9372(1990)116:5(1002.2)

15. Langmuir, D., Chrostowski, P., Vigneault, B., & Chaney, R. (2004). *Issue Paper on the Environmental Chemistry of Metals*. https://doi.org/10.4135/9781446216187.n12

16. Lawless, H. T., & Heymann, H. (2010). *Color and Appearance* (pp. 283–301). https://doi.org/10.1007/978-1-4419-6488-5_12

17. Lin, Y. P., & Singer, P. C. (2005). Inhibition of calcite crystal growth by polyphosphates. *Water Research*, *39*(19), 4835–4843. https://doi.org/10.1016/j.watres.2005.10.003

18. Locsin, J. A., Trueman, B. F., Doré, E., Bleasdale-Pollowy, A., & Gagnon, G. A. (2022). Impacts of orthophosphate–polyphosphate blends on the dissolution and transformation of lead (II) carbonate. *Scientific Reports*, *12*(1), 17885. https://doi.org/10.1038/s41598-022-22683-2

19. Lytle, C. J., & Edwards, M. A. (2023). Phosphate Chemical Use for Sequestration, Scale Inhibition, and Corrosion Control. *ACS ES&T Water*, *3*(4), 893–907. https://doi.org/10.1021/acsestwater.2c00570

20. Lytle, D. A., & Snoeyink, V. L. (2002). Effect of ortho- and polyphosphates on the properties of iron particles and suspensions. *Journal / American Water Works Association*, *94*(10), 87–99. https://doi.org/10.1002/j.1551-8833.2002.tb09560.x

21. Masters, S., Wang, H., Pruden, A., & Edwards, M. A. (2015). Redox gradients in distribution systems influence water quality, corrosion, and microbial ecology. *Water Research*, *68*, 140–149. https://doi.org/10.1016/j.watres.2014.09.048

22. Mpelwa, M., & Tang, S. F. (2019). State of the art of synthetic threshold scale inhibitors for mineral scaling in the petroleum industry: a review. *Petroleum Science*, *16*(4), 830–849. https://doi.org/10.1007/s12182-019-0299-5

23. Müller-Steinhagen, H. (2000). *Heat Exchanger Fouling: Mitigation and Cleaning Technologies*. IChemE.

24. Pure water Products, L. (n.d.). *Feeding Polyphosphate to Sequester Iron and Manganese*. Retrieved November 1, 2022, from https://www.purewaterproducts.com/articles/feeding-polyphosphate

25. Richards, C. S., Wang, F., Becker, W. C., & Edwards, M. (2018). A 21st-Century Perspective on Calcium Carbonate Formation in Potable Water Systems. *Environmental Engineering Science*, *35*(3), 143–158. https://doi.org/10.1089/ees.2017.0115

26. Robinson, R. B., Reed, G. D., Christodos, D., Frazier, B., & Chidamarish, V. (1990). *Sequestering Methods of Iron and Manganese Treatment* (A. R. Foundation & A. W. W. Association (eds.)).

27. Roy, S., & Edwards, M. A. (2019). Preventing another lead (Pb) in drinking water crisis: Lessons from the Washington D.C. and Flint MI contamination events. *Current Opinion in Environmental Science & Health*, *7*, 34–44. https://doi.org/10.1016/j.coesh.2018.10.002

28. Schock, M. R., Lytle, D. A., Sandvig, A. M., Clement, J., & Harmon, S. M. (2005). Replacing polyphosphate with silicate to solve lead, copper, and source water iron problems. *Journal / American Water Works Association*, *97*(11), 84–93. https://doi.org/10.1002/j.1551-8833.2005.tb07521.x

29. Sfynia, C., Bond, T., Kanda, R., & Templeton, M. R. (2022). Simultaneous prediction of trihalomethanes, haloacetic acids, haloacetonitriles and haloacetamides using simulated distribution system tests. *Environmental Science: Water Research & Technology*, *8*(4), 742–756. https://doi.org/10.1039/D1EW00824B

30. Smedley, P. (2003). *Water Quality Fact Sheet : Manganese*. British Geological Survey. https://nora.nerc.ac.uk/516303/1/Manganese.pdf

31. Smith, R. M., & Martell, A. E. (1976). Critical Stability Constants. In *Critical Stability Constants: Vol. 4: Inorgan*. Springer US. https://doi.org/10.1007/978-1-4757-5506-0

32. Spon, R. (2008). Polyphosphate Chemicals: Dosing Rates and Recipes. *Opflow*, *34*(12), 8–9. https://doi.org/10.1002/j.1551-8701.2008.tb02010.x

33. Stumm, W., & Morgan, J. J. (1995). *Aquatic Chemistry: Chemical Equilbria and Rates in Natural Waters* (Issue 1). John Wiley & Sons, INC. https://doi.org/10.16309/j.cnki.issn.1007-1776.2003.03.004

34. The phosphate Forum of the Americas. (n.d.). *The Use of Phosphates For Potable Water Treatment*. 1–6.

35. Trueman, B. F., Krkošek, W. H., & Gagnon, G. A. (2018). Effects of ortho- and polyphosphates on lead speciation in drinking water. *Environmental Science: Water Research and Technology*, *4*(4), 505–512. https://doi.org/10.1039/c7ew00521k

36. United States Environmental Protection Agency. (2022a). *Revised Lead and Copper Rule*. https://www.epa.gov/ground-water-and-drinking-water/revised-lead-and-copper-rule

37. United States Environmental Protection Agency. (2022b). *Secondary Drinking Water Standards: Guidance for Nuisance Chemicals*. https://www.epa.gov/sdwa/secondary-drinking-water-standards-guidance-nuisance-chemicals

38. University of California. (n.d.). *Maintenance of Microirrigation Systems; Lime (calcium carbonate)*. Division of Agriculture and Natural Resources. https://micromaintain.ucanr.edu/Solutions/know/Chemical_precipitation/Treatments_to_Mi

nimize_Clogging_182/Lime_calcium_carbonate/

39. Vidic, R. D., Liu, W., Li, H., & He, C. (2015). Water Treatment Chemicals: Types, Solution Chemistry, and Applications. In *Mineral scales and deposits: An overview. The Science and Technology of Industrial Water Treatment.* (pp. 169–192).

40. Volpe, D. (2012). Assessment of iron and manganese sequestration. In *American Water Works Association Annual Conference and Exposition 2012, ACE 2012*. https://doi.org/10.7275/HA5A-GG93

41. Wang, F., Devine, C., & Edwards, M. A. (2017). Effect of Corrosion Inhibitors on in Situ Leak Repair by Precipitation of Calcium Carbonate in Potable Water Pipelines. *Environmental Science and Technology*, *51*(15), 8561–8568. https://doi.org/10.1021/acs.est.7b01380

42. Water Guard, I. (n.d.). *TECHNICAL BULLETIN ~ FERRO-QUEST*.

APPENDIX C

Supporting Information

SIMULTANEOUS USE OF POLYPHOSPHATE FOR SEQUESTRATION AND ANTI-SCALING

Christian J. Lytle, Marc A. Edwards

Table C 1. Water quality parameters for each water tested. Those labeled with a 1 and 2 represent systems which were resampled

System	Fe (mg/L)	Mn (mg/L)	Ca (mg/L as $CaCO_3$)	Mg (mg/L)	Si (mg/L)	Alkalinity (mg/L as $CaCO_3$)	pH, 0 Days	pH, 7 Days	Total Chlorine, 0 Days (mg/L)	Total Chlorine, 7 Days (mg/L)	Max Chemical A Dose (mg/L as P)	Max Chemical B Dose (mg/L as P)
A1	*0.991*	*0.481*	*83.8*	*5.8*	*15.6*	*110.8*	*7.60*	*7.35*	*1.78*	*1.09*	1.95	1.90
A2	0.302	0.293	87.9	5.7	16.9	NM	7.35	7.00	1.51	1.06	3.66	3.63
B	0.68	0.046	23.8	2.8	13.3	NM	7.30	7.10	1.48	1.26	2.73	2.61
C	0.02	0.074	58.5	4.4	10.7	NM	7.80	7.65	0.63	0.31	1.42	1.64
D	0.224	0.077	179.7	10.7	9.8	260.4	7.70	7.28	1.87	1.39	1.84	1.88
E	0.611	0.064	53.9	6.2	15.8	NM	6.70	6.62	1.13	0.86	2.20	1.98
F	0.445	0.153	82.1	5.9	11.3	NM	7.50	7.49	1.76	1.54	1.75	1.88
G1	0.571	0.1	150	8.3	22.5	154.4	7.90	7.62	5.43	2.45	2.06	2.08
G2	3.70 [1]	0.213	150.6	8.3	24.8	NM	NM	7.45	NM	0.2	3.64	3.68
H1	0.978	0.364	102.5	5.3	18.5	54.9	8.20	7.42	1.54	0.81	2.17	2.14
H2	0.061	0.001	23.2	5	19.9	NM	NM	6.50	NM	0.48	3.81	3.85
J1	1.36 [1]	0.44	34	4.7	14.9	NM	7.5	7.29	1.13	1.1	1.63	1.89
J2	0.76	0.042	36.8	5.2	15.5	NM	7.4	7.31	1.26	1.19	1.71	1.59

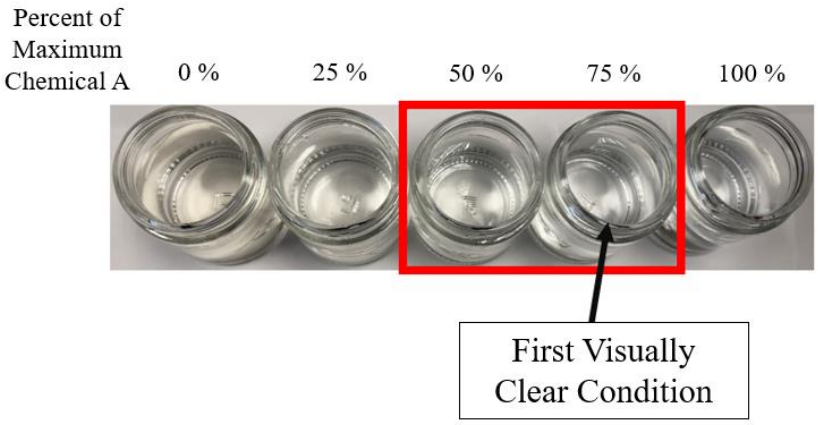

Figure C 1. Example of the visual discolored vs visually clear water conditions in Water D.

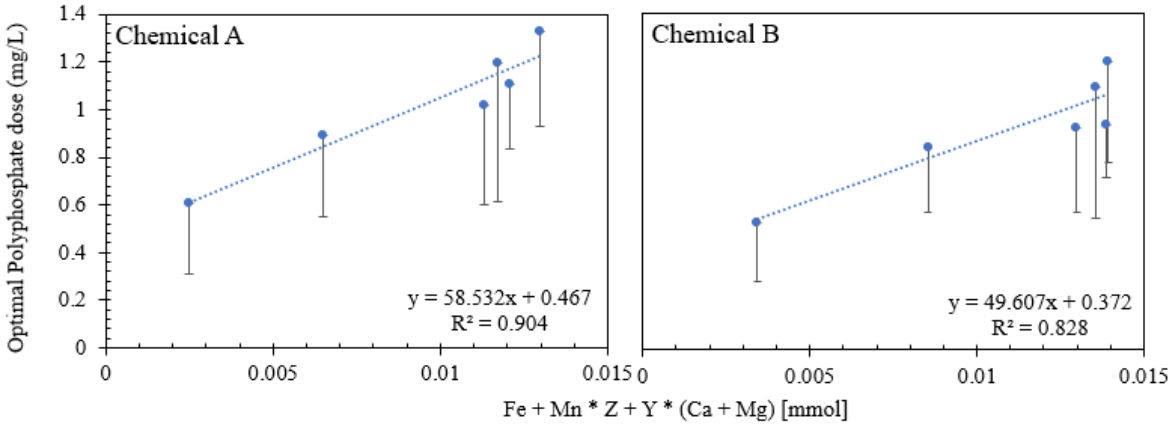

Figure C 2. Optimal dosing trends for systems that did reach an optimal dose. For Chemical A, Z = 1.02 and X = 0.0007, slope = 58.5 ± 9.5, y-int = 0.47 ± 0.10. For Chemical B, Z = 1.2 and X = 0.0012, slope = 49.61 ± 11.31, y-int = 0.37 ± 0.13.

CHAPTER 7 : CONCLUSIONS AND FUTURE WORK

Conclusions

1. Due to the proprietary nature of polyphosphate chemicals, limited funding, and some negative perceptions regarding polyphosphate chemical use, there are significant gaps in understanding optimization of orthophosphate and polyphosphate type and dose in potable water systems. Further research is needed to enable water systems to make holistically sound decisions.
2. Objective color and turbidity measurements occasionally have little or no correlation to what consumers see by eye and therefore may not always be the best measure of visual discoloration and cloudiness.
3. Phosphates can sequester iron by 1) slowing the rate of ferrous oxidation to ferric, 2) preventing the precipitation of $Fe(OH)_3$, and 3) stabilizing very small, less visible particles. In oxygenated waters above about pH 7, a combination of Steps 2 and 3 dominate, whereas impacts on ferrous oxidation rates plays less important role.
4. Increased phosphate chain length, phosphate concentration, and silica concentration improved iron sequestration, whereas calcium, magnesium, and increased pH interfered with its effectiveness.
5. Magnesium silicate solubility decreases with pH, and the solid was at equilibrium been pH 7.5-8 in one water and 8.5-9 in another. Maintaining this scale is important, as dissolution could cause problems with scale release to water and expose underlying pipe materials to corrosion, whereas continued precipitation could clog pipes.
6. The rate of magnesium silicate precipitation and dissolution is a function of seed surface area, pH and other factors. Without a seed, no precipitation occurred.
7. Phosphate corrosion inhibitors had little effect on the rate of magnesium silicate precipitation at pH 8.5 and 10, but zinc orthophosphate and hexametaphosphate decreased the rate of magnesium and silica dissolution at pH 7.
8. A new bench scale test methodology was developed to evaluation phosphate use for sequestration and anti-scaling. Application of the method to water from nine small groundwater utilities revealed that the optimal polyphosphate dose was a strong function of the concentrations of magnesium, calcium, manganese and iron.

9. Much more polyphosphate is often needed to sequester iron and manganese than to inhibit scale formation. However, in certain waters with very high hardness, more polyphosphate will be required to control scaling than to effectively sequester metals.

Future Work

There is a growing interest in the use of phosphates due to the (1) increasing focus on the consequences of sequestering iron/manganese, from proposed maximum contaminant levels for manganese (USEPA, 2022), (2) increased problems with calcium carbonate scaling concerns in drinking water (Richards et al., 2018), (3) revisions to the lead and copper rule that emphasize higher dosing of phosphate for corrosion control (USEPA, 2021), and (4) concerns about sustainability and costs of phosphates (Scholz et al., 2013). Some utilities, who have never used phosphates before, will soon be required to consider doing so. Other utilities who have been using phosphates for a long time will be considering alternative approaches and strategies, to reduce or eliminate costs of phosphate use, and to improve environmental sustainability. Such changes should consider the wide-ranging benefits, detriments and implications of phosphate dosing.

Future work, should extend the mechanistic studies described herein for ferrous iron, to sequestration of manganese. Manganese oxidation rates tend to be slower than iron. Manganese is also known to cause severe discoloration at much lower concentrations than iron, and is expected to show markedly different dependencies with pH, phosphate type and dose, as well as secondary impacts from chlorine, silica and hardness.

The simulated sequestration and anti-scaling tests utilized throughout this work could be further used to determine optimal dosing conditions in other systems with different water qualities. The nine groundwater utilities sampled in this work all had pHs below 7.8 and only three had calcium hardness above 100 mg/L as $CaCO_3$. Testing on a broader set of data might show limitations to the empirical relationship discovered in this research.

While the simultaneous optimization of polyphosphate dose for sequestration and anti-scaling was addressed in this dissertation, addressing the third dimension of corrosion control will be more difficult due to the range of pipe materials of interest, and the diversity of corrosion mechanisms (e.g., uniform, non-uniform, galvanic, concentration cell). Very little is known about the possible benefits and detriments of polyphosphate on corrosion control. While such research

requires years of testing (e.g., McNeill & Edwards, 2000), the profound economic and public health consequences justify an serious investment in improved understanding.

References

1. McNeill, L. S., & Edwards, M. (2000). Phosphate Inhibitors and Red Water in Stagnant Iron Pipes. *Journal of Environmental Engineering*, *126*(12), 1096–1102. https://doi.org/10.1061/(ASCE)0733-9372(2000)126:12(1096)

2. Richards, C. S., Wang, F., Becker, W. C., & Edwards, M. (2018). A 21st-Century Perspective on Calcium Carbonate Formation in Potable Water Systems. *Environmental Engineering Science*, *35*(3), 143–158. https://doi.org/10.1089/ees.2017.0115

3. Scholz, R. W., Ulrich, A. E., Eilittä, M., & Roy, A. (2013). Sustainable use of phosphorus: A finite resource. *Science of The Total Environment*, *461–462*, 799–803. https://doi.org/10.1016/j.scitotenv.2013.05.043

4. USEPA. (2021). *Lead and Copper Rule Revisions*.

5. USEPA. (2022). *Contaminant Candidate List (CCL) and Regulatory Determination*. https://www.epa.gov/ccl/ccl-5-chemical-contaminants